T2K Near Detector Constraints for Oscillation Results

Leïla Haegel
University of Geneva
on behalf of the T2K collaboration

NuFact 2016
Quy Nhon, Vietnam

The T2K experiment

production of ν flux : horn current sign selects neutrino and antineutrino mode beam

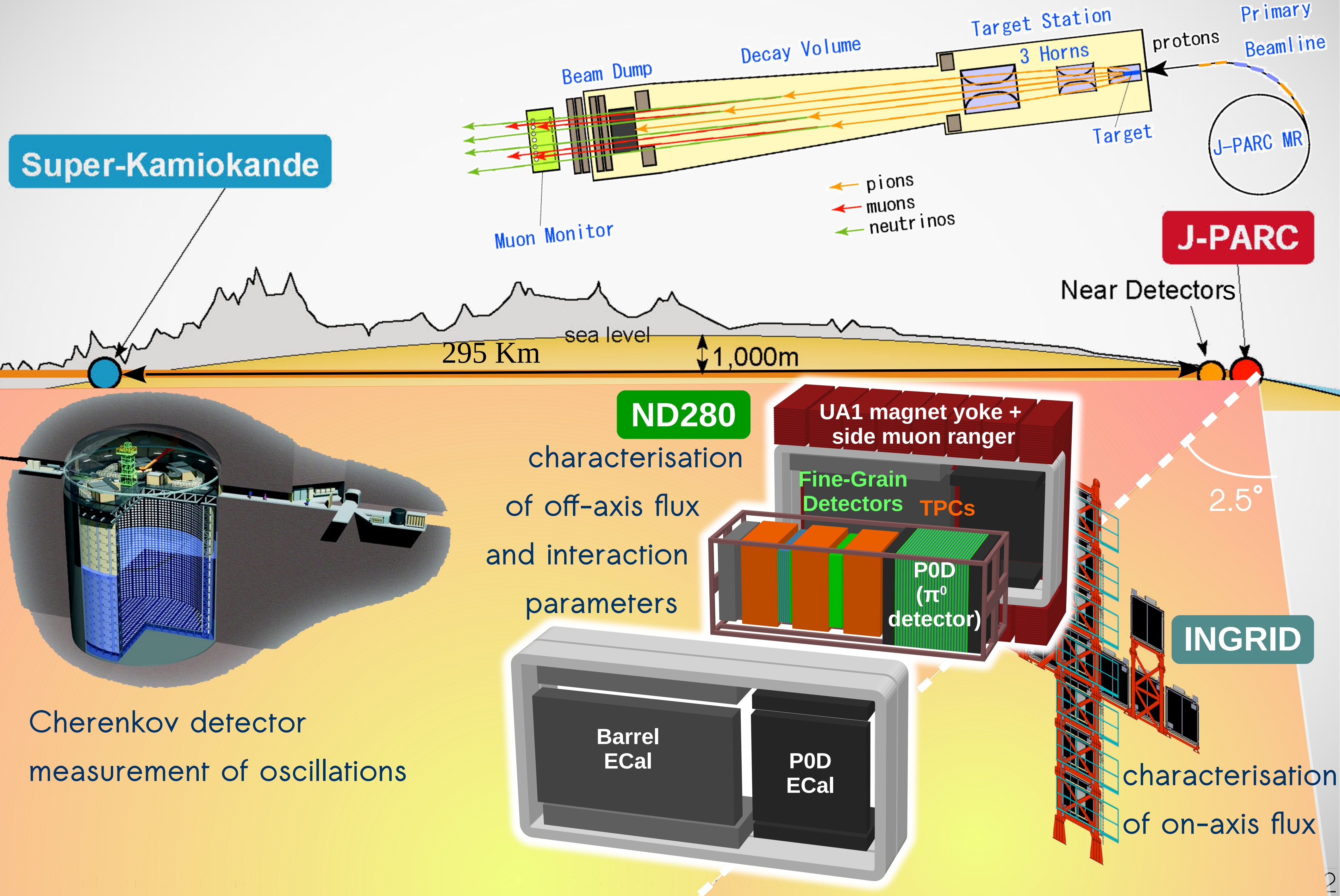

characterisation of off-axis flux and interaction parameters

Cherenkov detector measurement of oscillations

characterisation of on-axis flux

Event rate at Super-Kamiokande (ν mode)

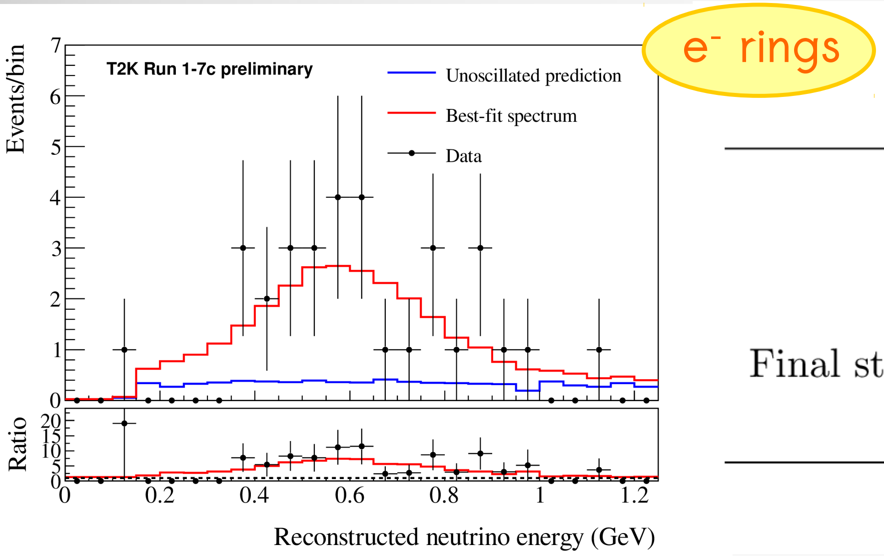

Systematic error source	$\Delta N_{SK}/N_{SK}$ before ND fit	$\Delta N_{SK}/N_{SK}$ after ND fit
Flux	8.8%	3.2%
Cross section	7.1%	4.7%
Flux and cross section	11.4%	2.7%
Final state/secondary interactions at SK	2.5%	
SK detector	2.5%	
Total	11.9%	5.2%

Fit to determine oscillation parameters minimises:

$$\ln(L) = \sum_i N_i^{pred}(x) - N_i^{data} + N_i^{data} \ln\left(N_i^{data} / N_i^{pred}(x)\right) + \frac{1}{2}\sum_i \sum_j \Delta x_i (V_x^{-1})_{i,j} \Delta x_j$$

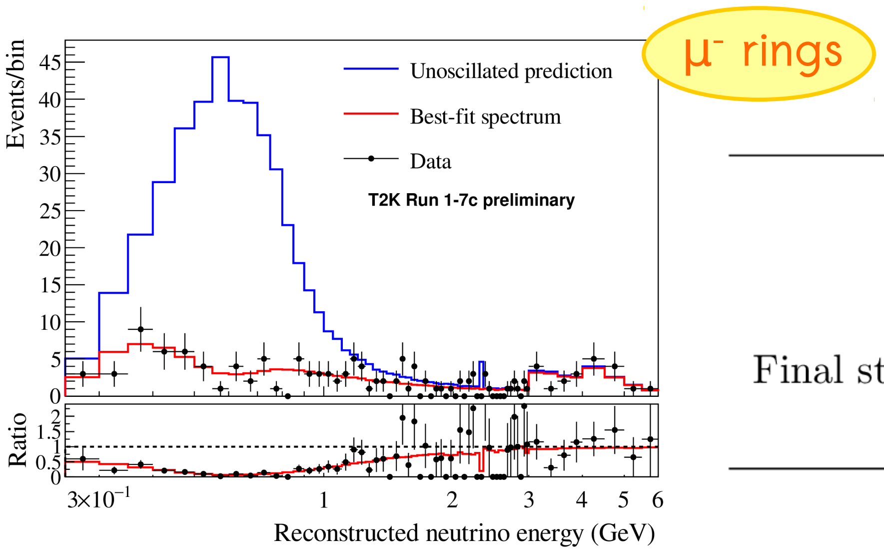

Systematic error source	$\Delta N_{SK}/N_{SK}$ before ND fit	$\Delta N_{SK}/N_{SK}$ after ND fit
Flux	7.7%	3.1%
Cross section	7.6%	3.8%
Flux and cross section	10.9%	2.5%
Final state/secondary interactions at SK	1.8%	
SK detector	4.6%	
Total	12.1%	4.9%

Analysis in stages

flux model constrained by NA61/SHINE + beam monitor measurements

Systematic error source	$\Delta N_{SK}/N_{SK}$ before ND fit	$\Delta N_{SK}/N_{SK}$ after ND fit
Flux	8.8%	3.2%
Cross section	7.1%	4.7%
Flux and cross section	11.4%	2.7%
Final state/secondary interactions at SK	2.5%	
SK detector	2.5%	
Total	11.9%	5.2%

Analysis in stages

flux model constrained by NA61/SHINE + beam monitor measurements

cross-section model constrained by measurements from other experiments

Systematic error source	$\Delta N_{SK}/N_{SK}$ before ND fit	$\Delta N_{SK}/N_{SK}$ after ND fit
Flux	8.8%	3.2%
Cross section	7.1%	4.7%
Flux and cross section	11.4%	2.7%
Final state/secondary interactions at SK	2.5%	
SK detector	2.5%	
Total	11.9%	5.2%

Analysis in stages

flux model constrained by NA61/SHINE + beam monitor measurements

cross-section model constrained by measurements from other experiments

Systematic error source	$\Delta N_{SK}/N_{SK}$ before ND fit	$\Delta N_{SK}/N_{SK}$ after ND fit
Flux	8.8%	3.2%
Cross section	7.1%	4.7%
Flux and cross section	11.4%	2.7%
Final state/secondary interactions at SK	2.5%	
SK detector	2.5%	
Total	11.9%	5.2%

lepton p-θ

ND280 fit

constrained flux and cross-section covariance matrix

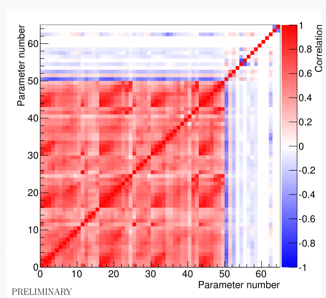

Analysis in stages

flux model constrained by NA61/SHINE + beam monitor measurements

cross-section model constrained by measurements from other experiments

Systematic error source	$\Delta N_{SK}/N_{SK}$ before ND fit	$\Delta N_{SK}/N_{SK}$ after ND fit
Flux	8.8%	3.2%
Cross section	7.1%	4.7%
Flux and cross section	11.4%	2.7%
Final state/secondary interactions at SK	2.5%	
SK detector	2.5%	
Total	11.9%	5.2%

lepton p-θ

ND280 fit

constrained flux and cross-section covariance matrix

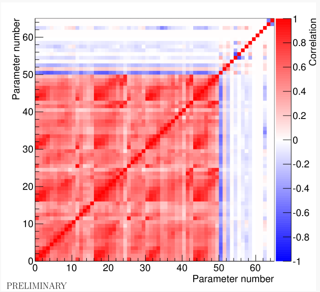

lepton E_{rec} / E_{rec}-θ / p-θ

Super-Kamiokande fit

oscillation parameters estimation

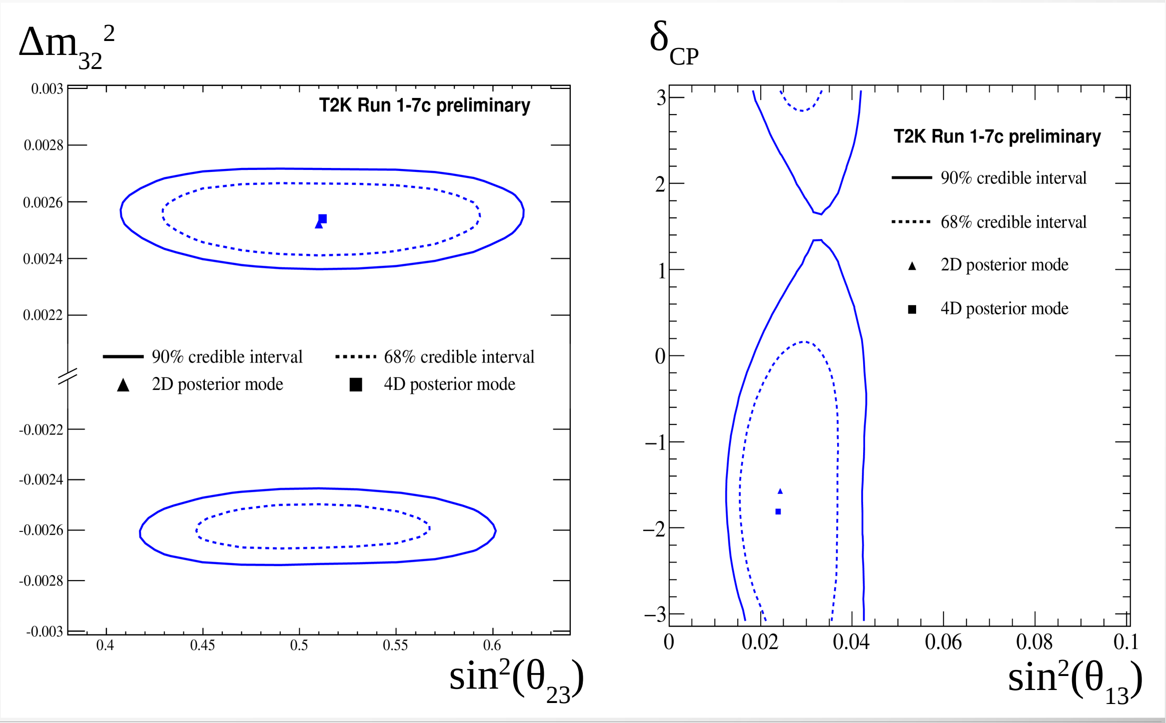

Flux model

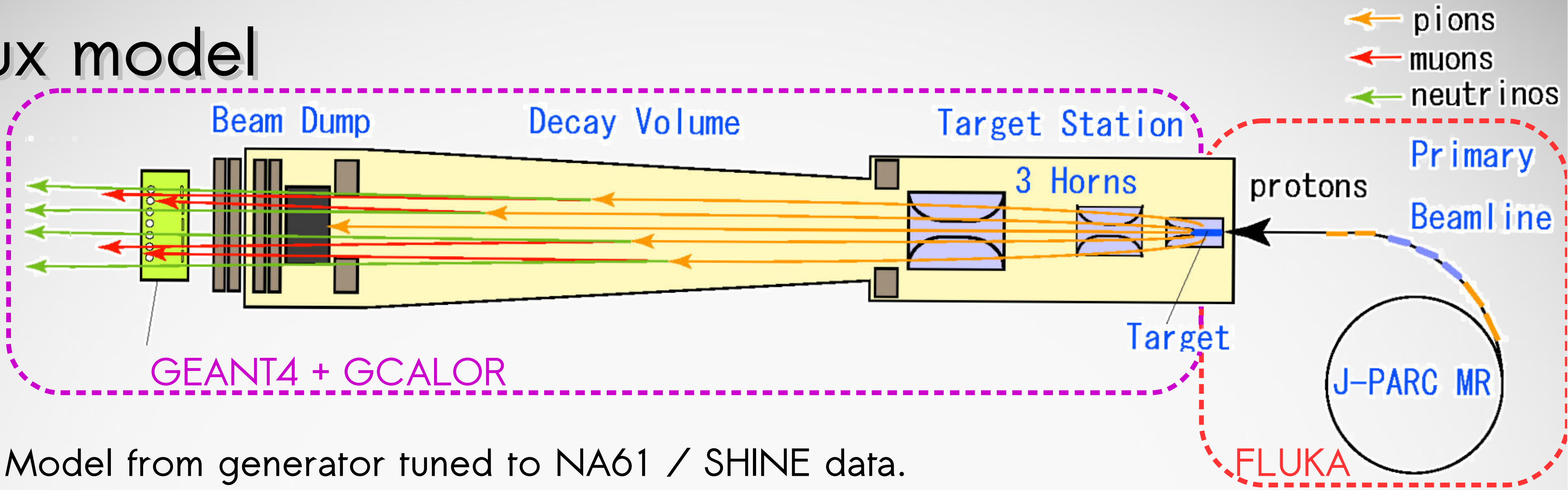

Model from generator tuned to NA61 / SHINE data.

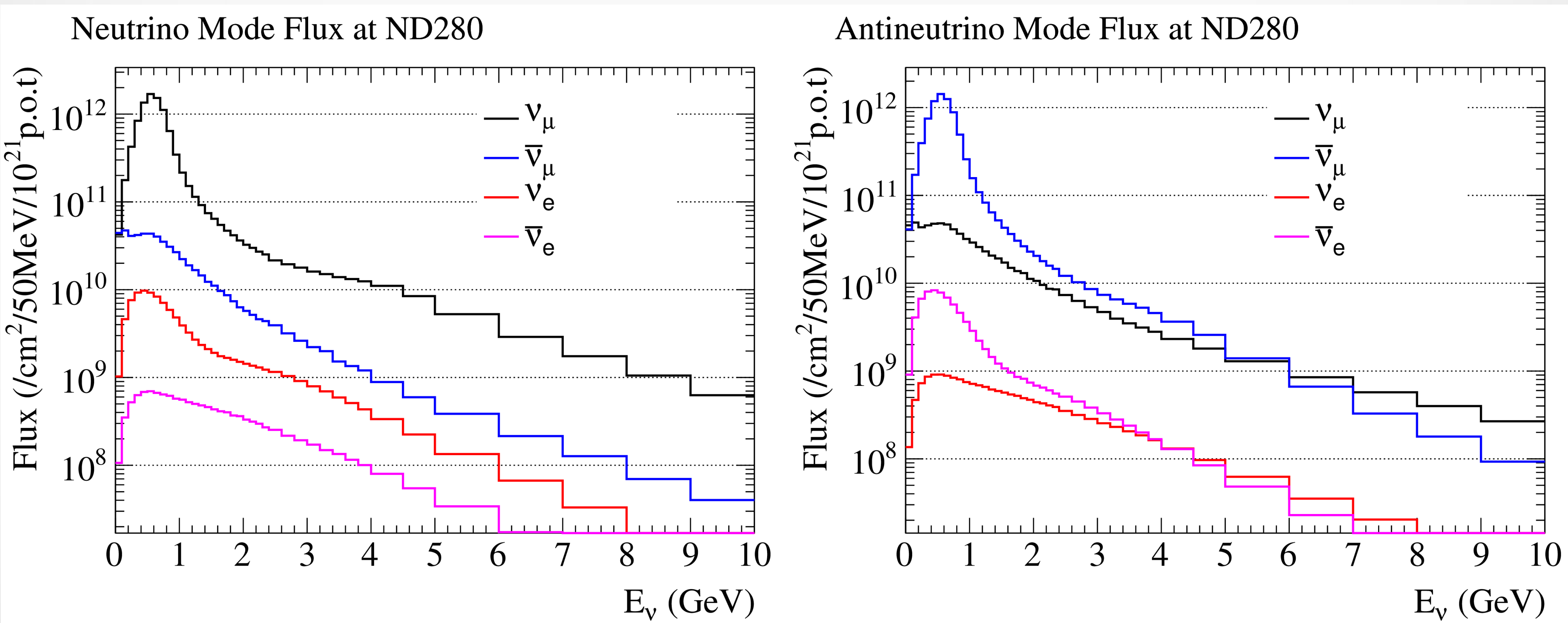

Flux constraints

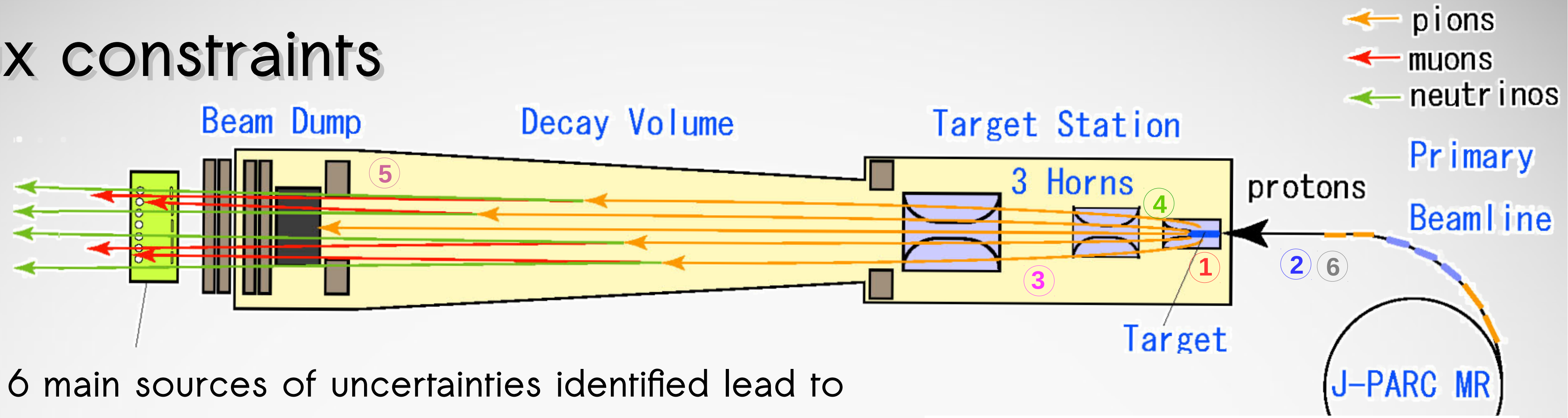

6 main sources of uncertainties identified lead to a ~10% uncertainty at flux peak.

ND280 fit significantly scales up flux parameters.

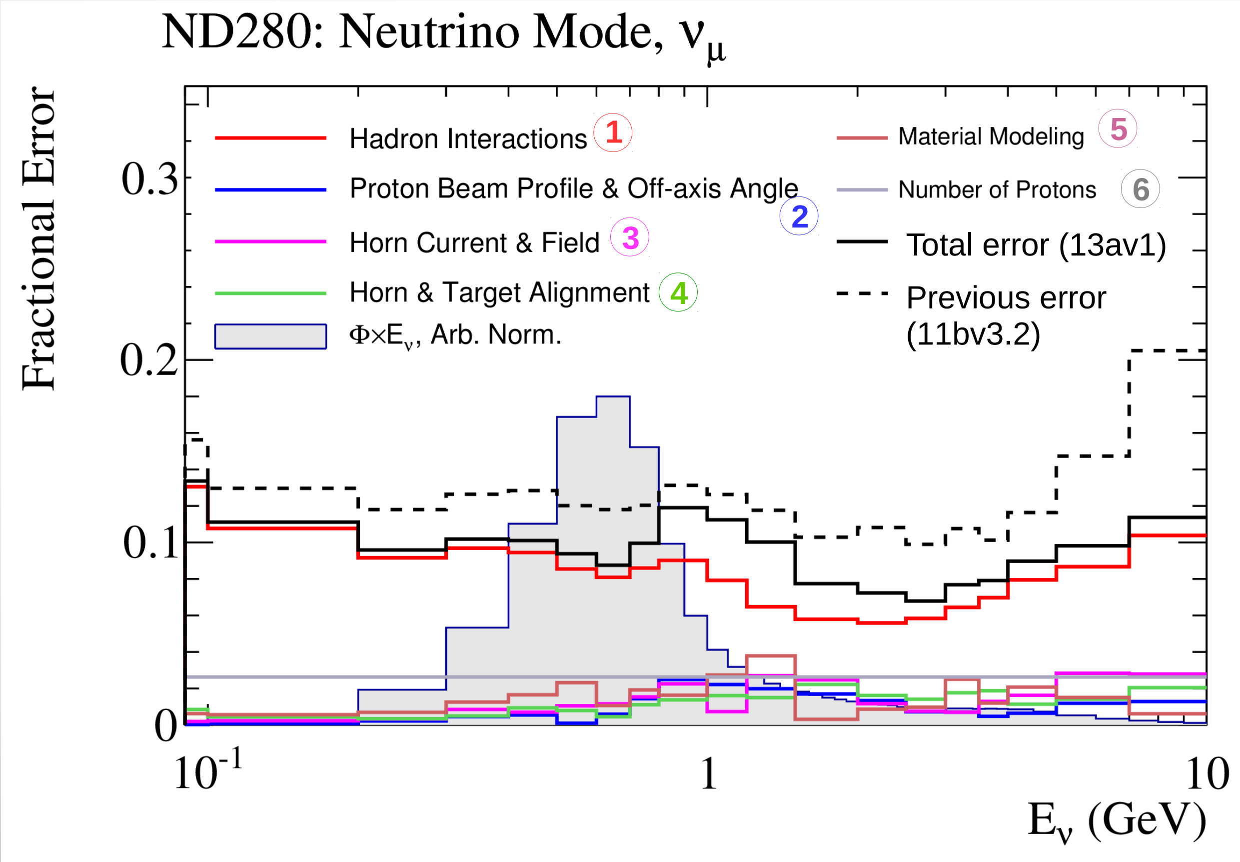

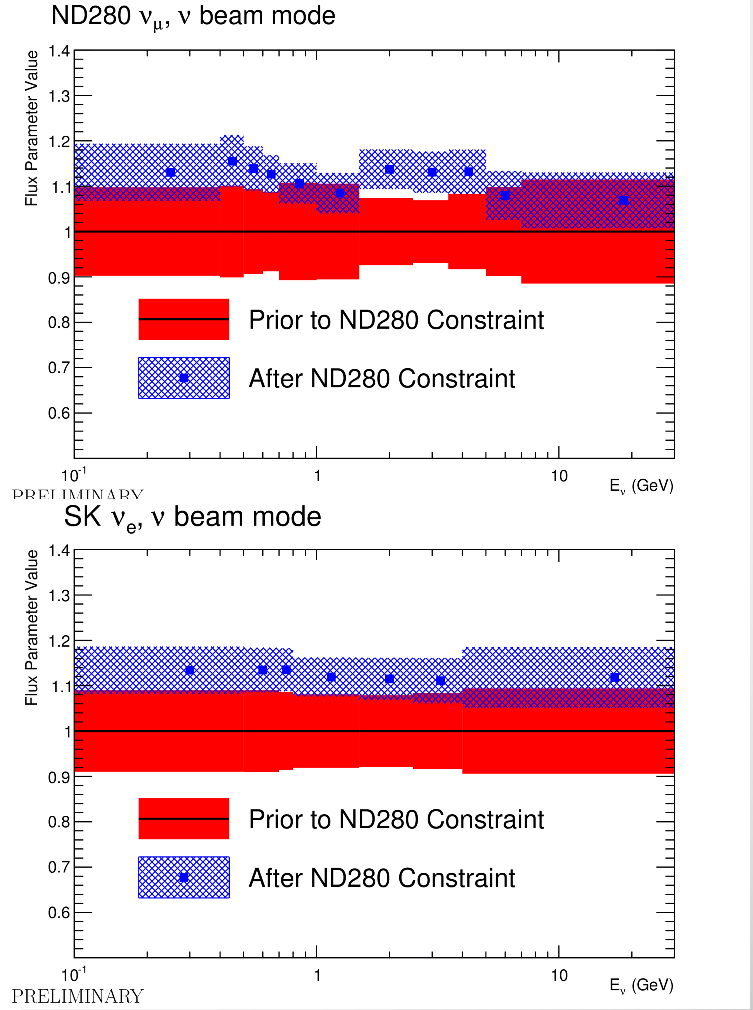

Selection in ND280

Selection of charged-current (CC) interactions of:

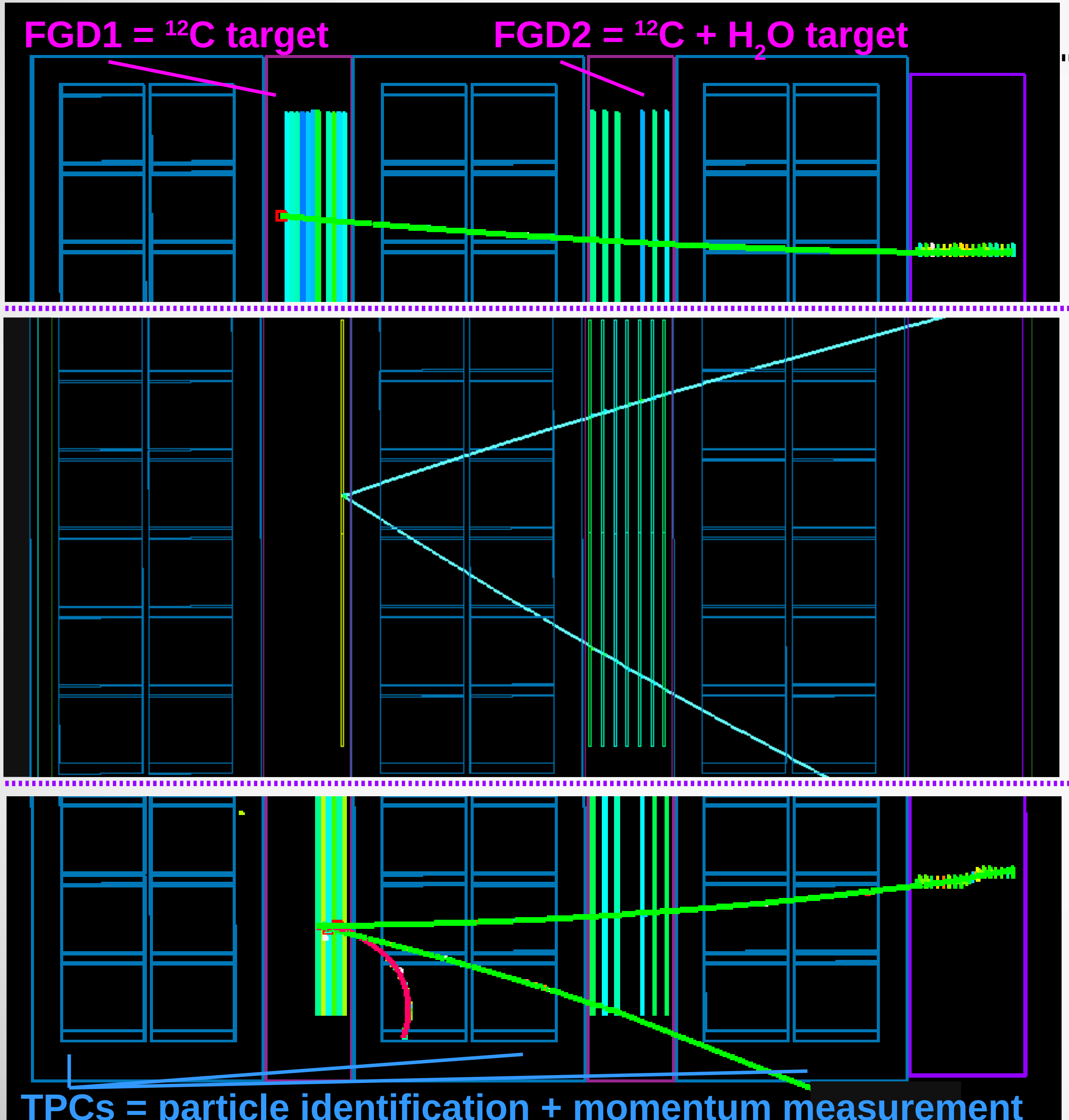

ν_μ in ν mode	$\bar{\nu}_\mu$ in $\bar{\nu}$ mode	ν_μ in $\bar{\nu}$ mode (oscillation background)
CC-0π: only 1 μ^- detected	CC-0π: only 1 μ^+ detected	CC-0π: only 1 μ^- detected
CC-1π: 1 μ^- + 1 π^+ detected	CC-other: 1 μ^+ +something other detected	CC-other: 1 μ^- +something other detected
CC-other: 1 μ^- + something other than 1π^+ detected		

Interaction model: CC-0π

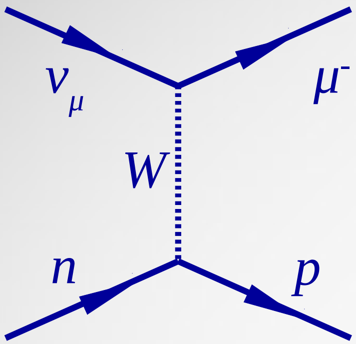

<u>CCQE: 5 parameters</u>

axial mass M_A^{QE}

Fermi momentum p_F (^{16}O; ^{12}C)

binding energy E_b (^{16}O; ^{12}C)

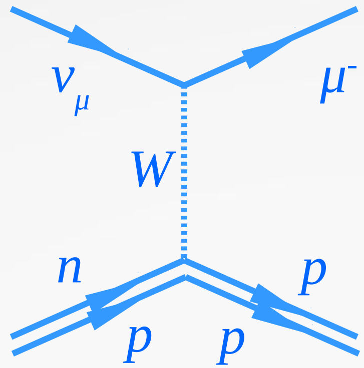

<u>2p2h: 3 parameters</u>

Nieves model

normalisation (^{16}O; ^{12}C)

(ν / $\bar{\nu}$)

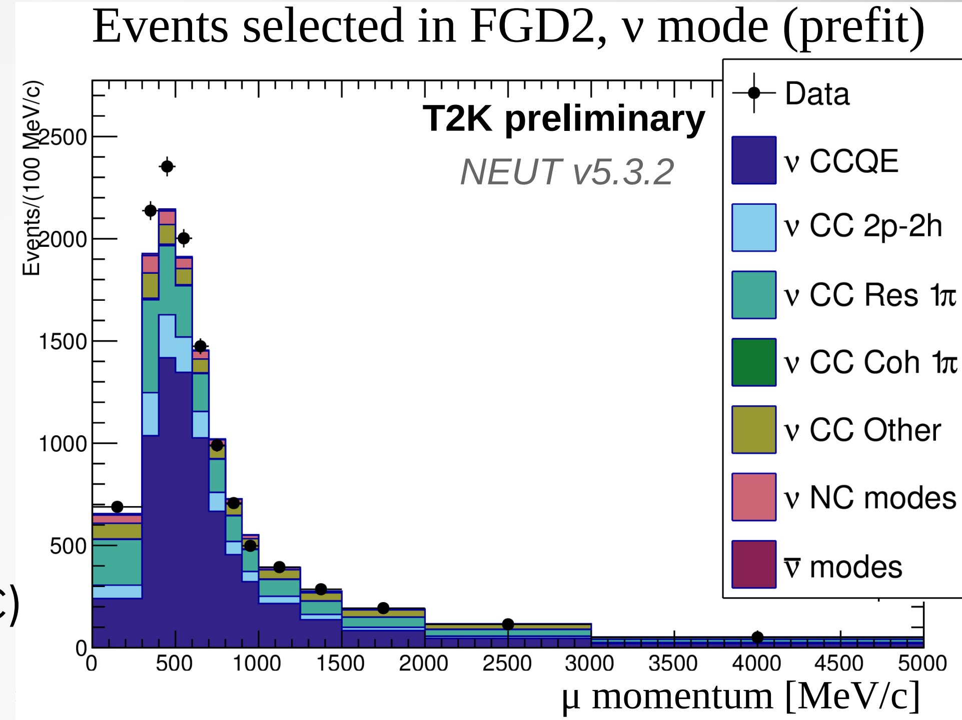

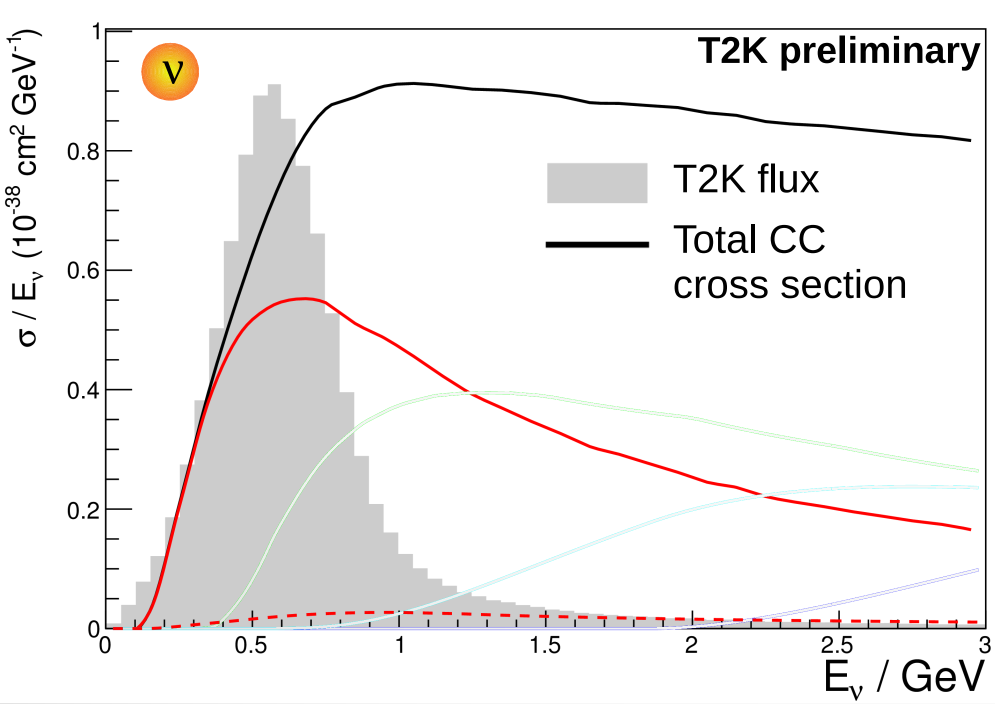

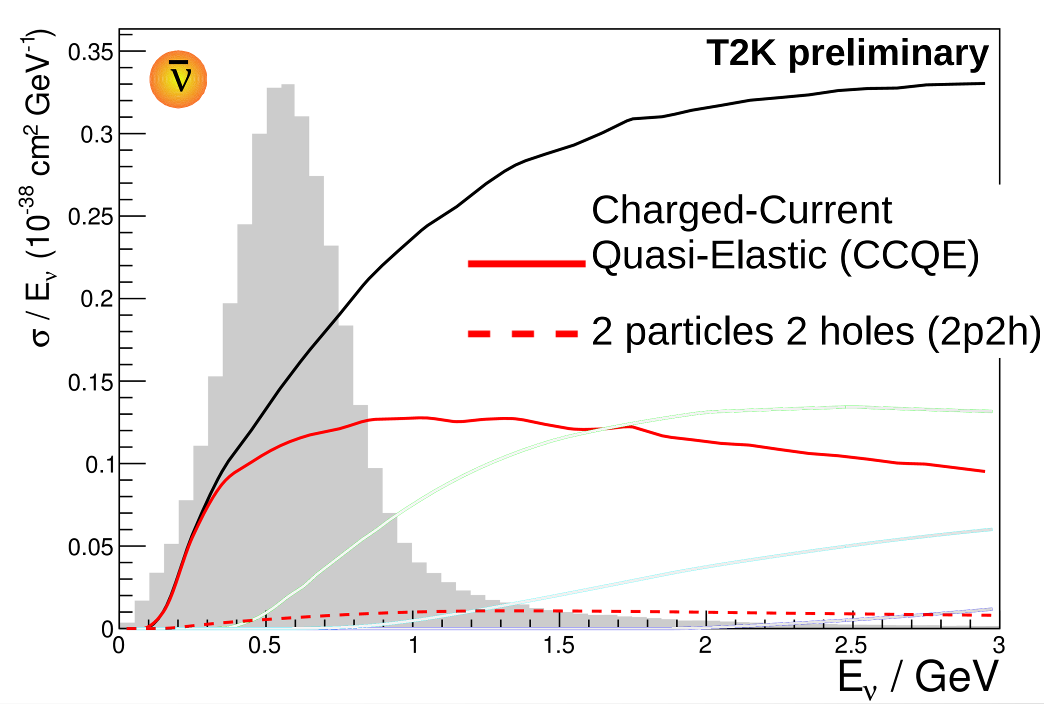

Interaction model: CC-1π

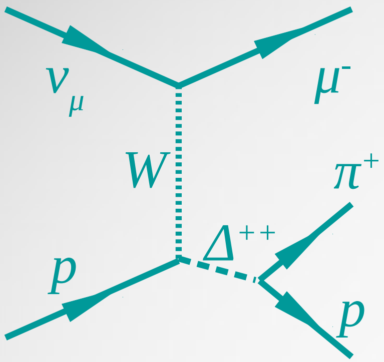

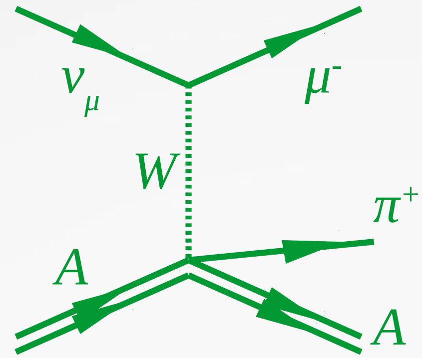

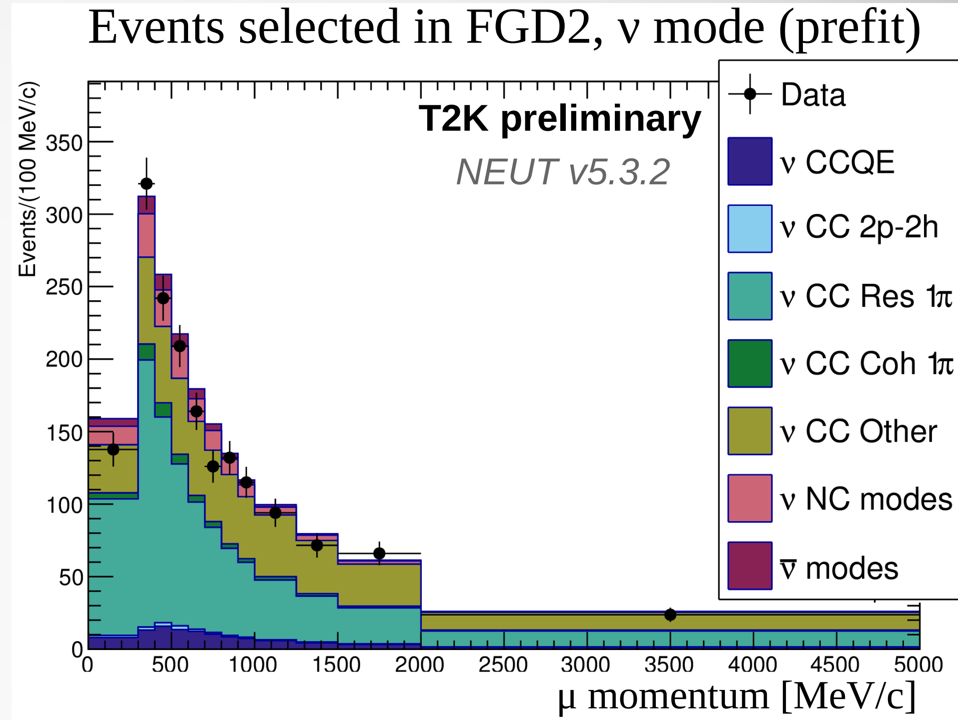

<u>CC-RES: 3 parameters</u>

axial mass M_A^{RES}

norm+shape parameter C_A^5

Isospin=1/2 background

<u>CC-COH: 1 parameter</u>

CC-coherent

cross-section

normalisation

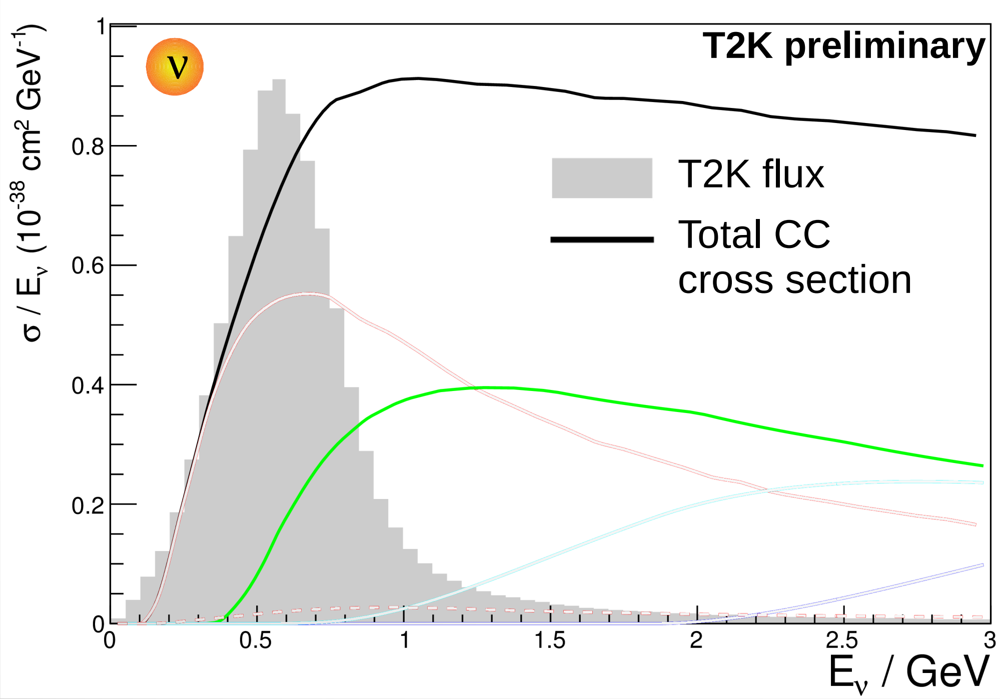

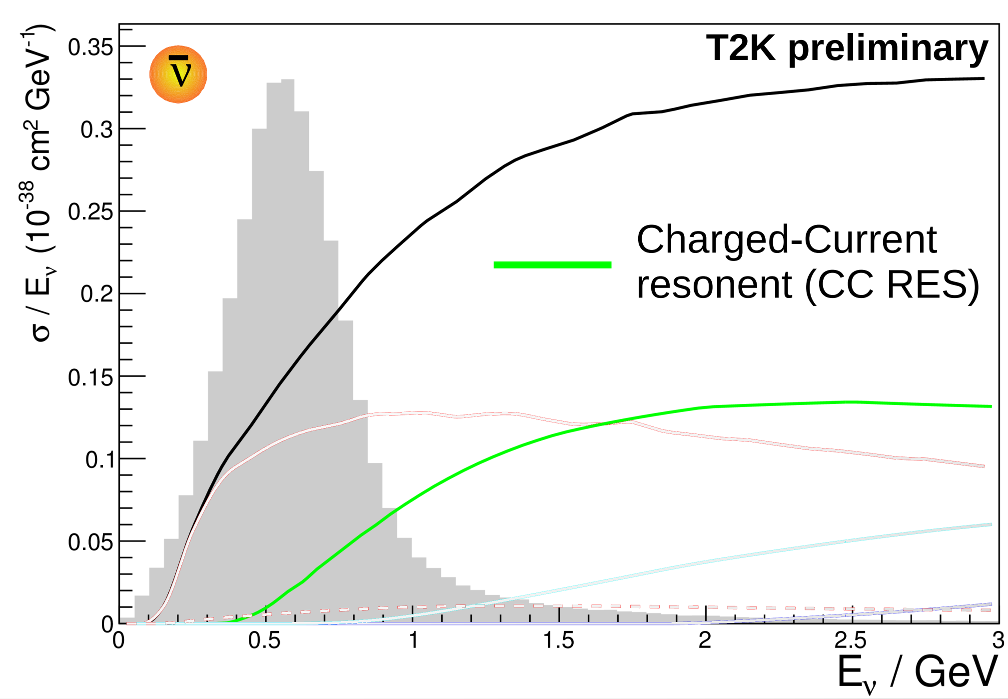

Interaction model: CC-other

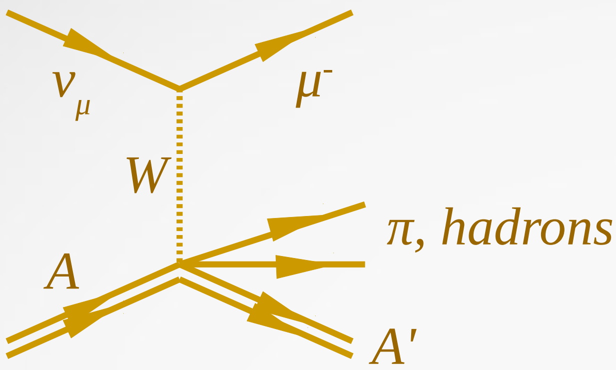

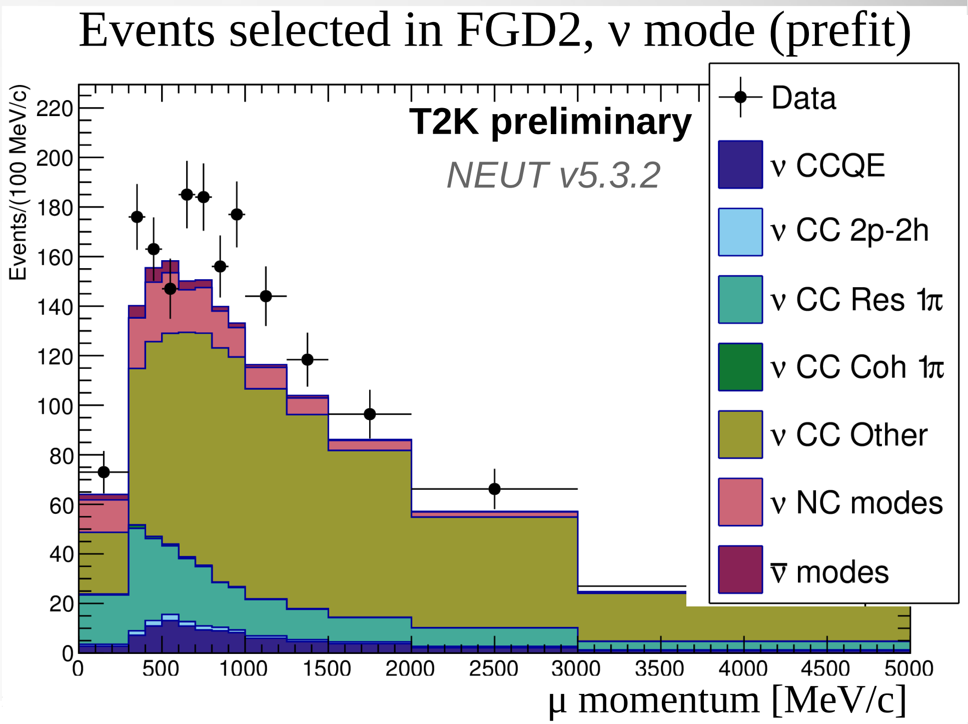

<u>CC-other: 1 parameter</u>

shape of CC-Nπ and DIS cross sections (merged)

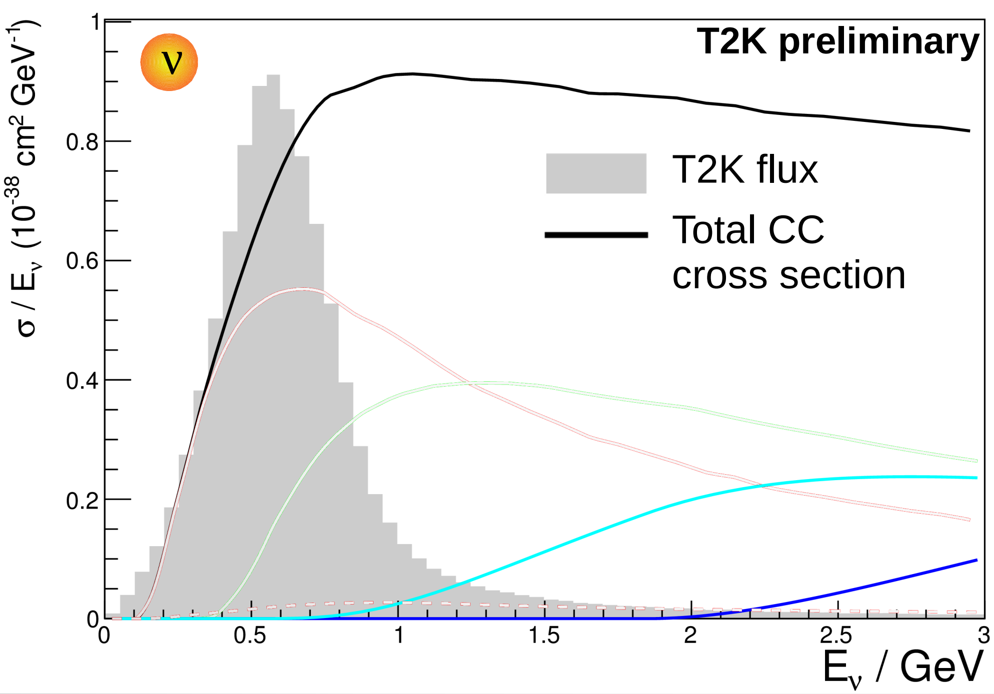

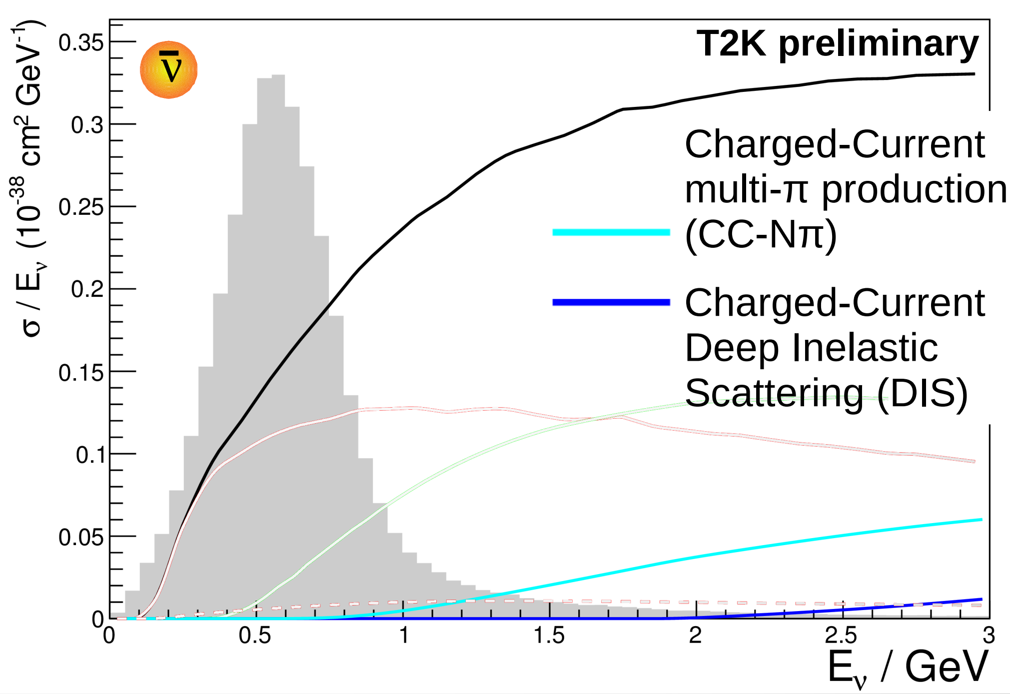

Interaction model: other parameters

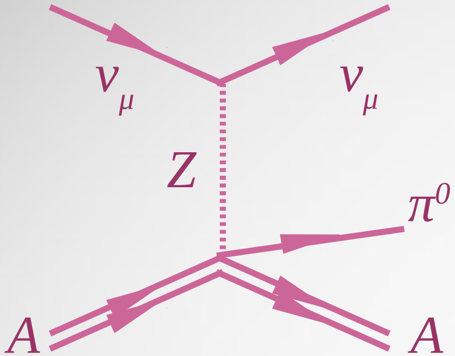

NC-COH: 1 parameter

Neutral-Current (NC) coherent cross-section normalisation

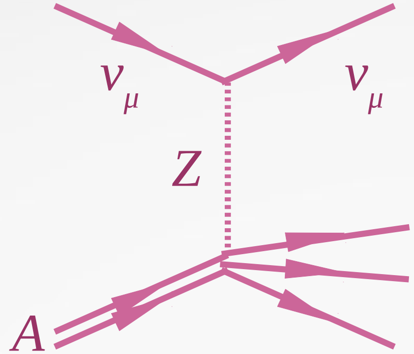

NC-other: 1 parameter

Other NC (e.g. RES, DIS) cross-section normalisation

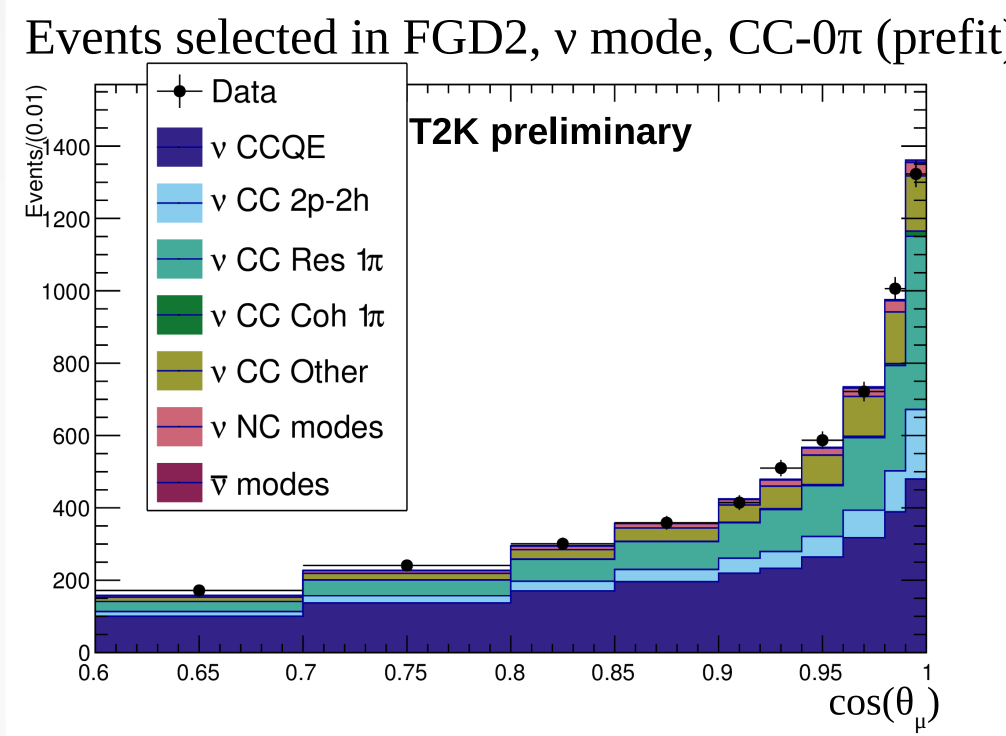

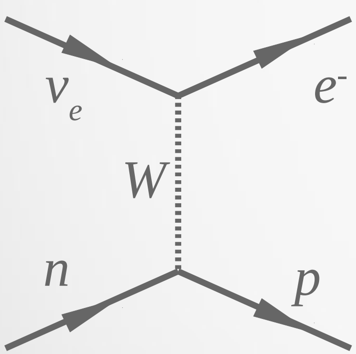

ν_e / ν_μ: 1 parameter

ν_e/ν_μ cross-section normalisation

Final State Interactions (FSI) : 6 parameters

π production / absorption in nucleus

charge exchange } (low/high energy)
inelastic scattering

Cascade model in NEUT.

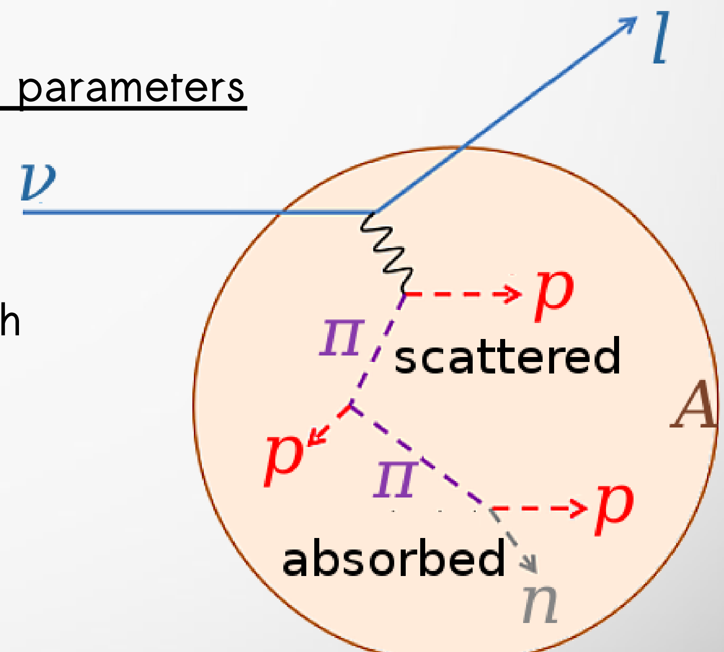

Interaction model: post-fit constraints

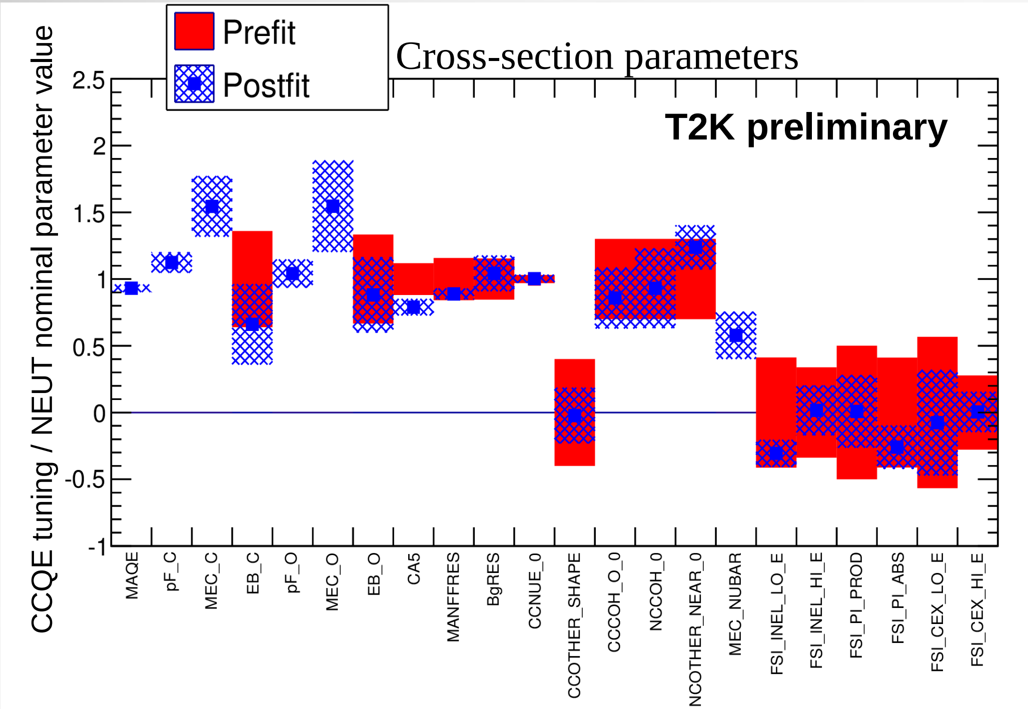

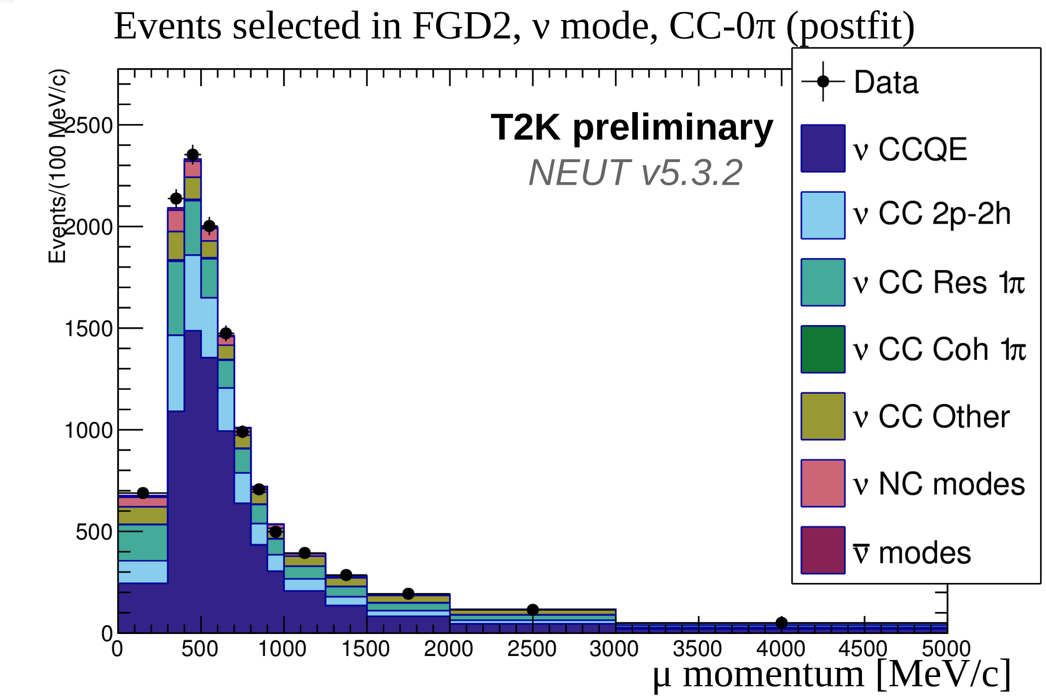

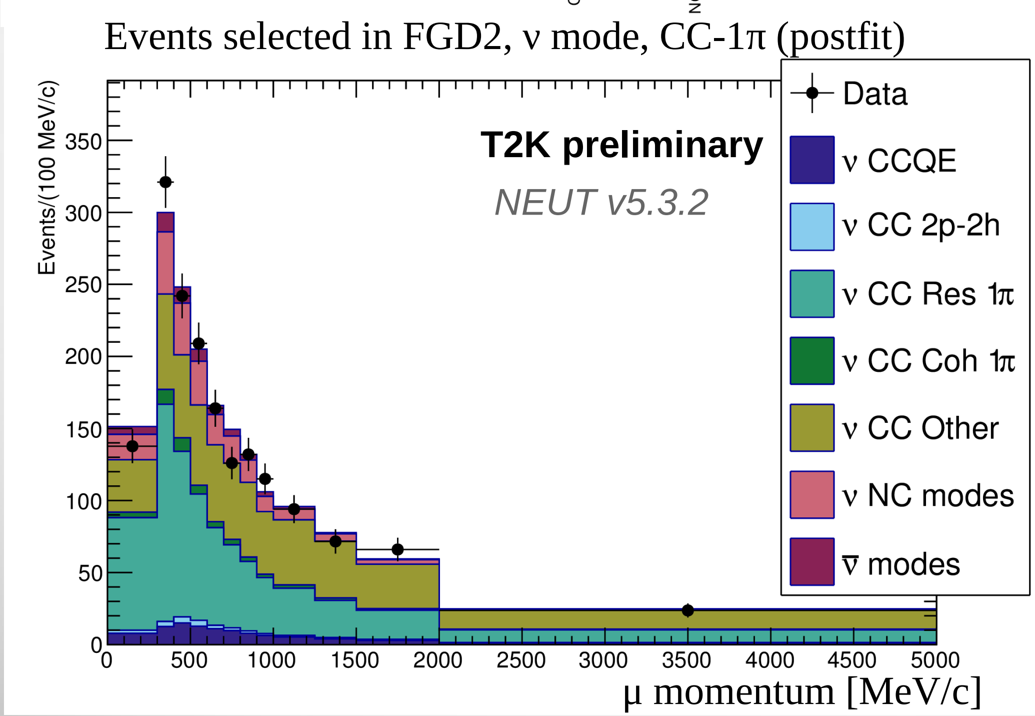

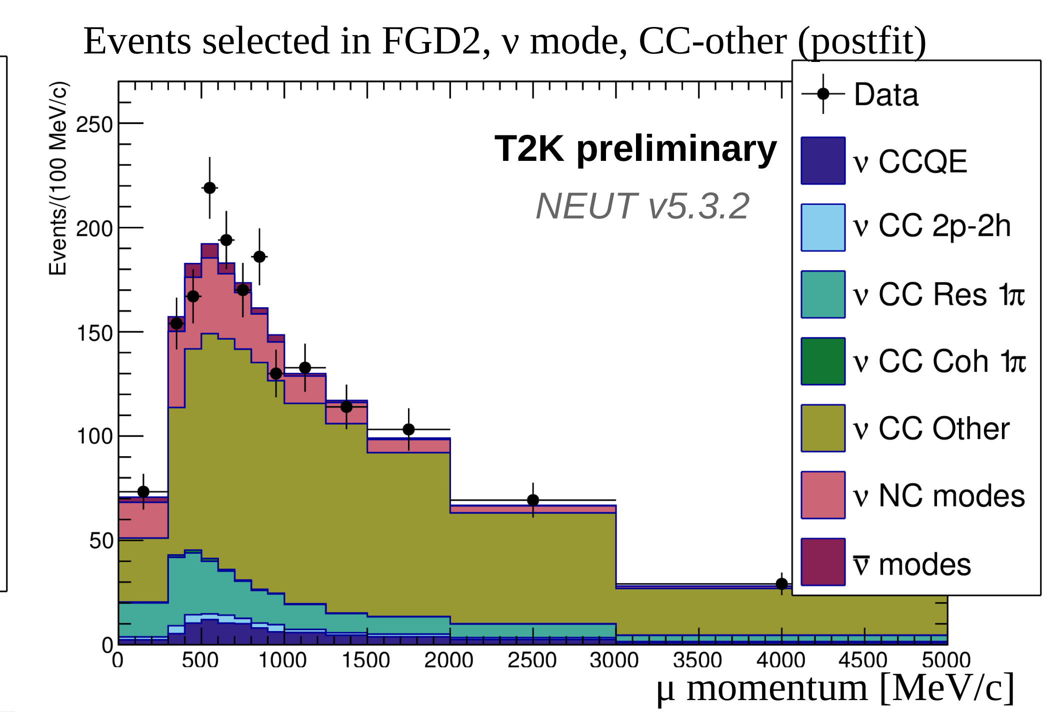

Interaction model: generator model

(1) Phys. Rev. D 93, 072010 (2016)
(2) Phys. Rev. C, 70:055503 (2004)

MC generator (NEUT v5.3.3) model chosen from Minerνa + MiniBooNE data fit [1]:

- Smith-Moniz Relativistic global Fermi Gas (RFG) model of nucleus
- 2p2h interactions from Nieves model [2]
- medium polarisation in nucleus due to relativistic Random Phase Approximation (RPA) from Nieves model [2]

cross-section enhancement, modification of kinematics

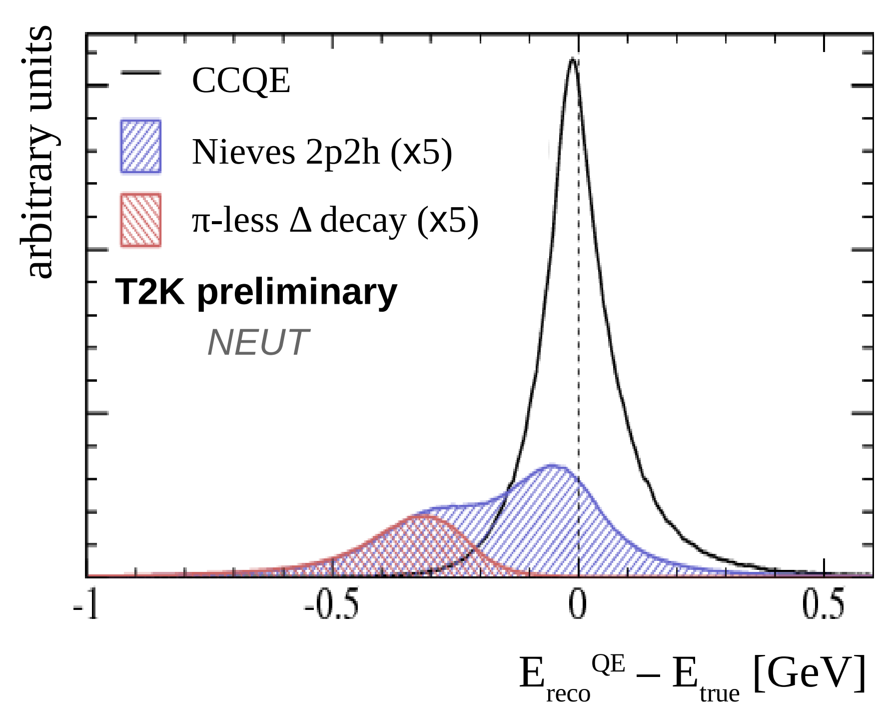

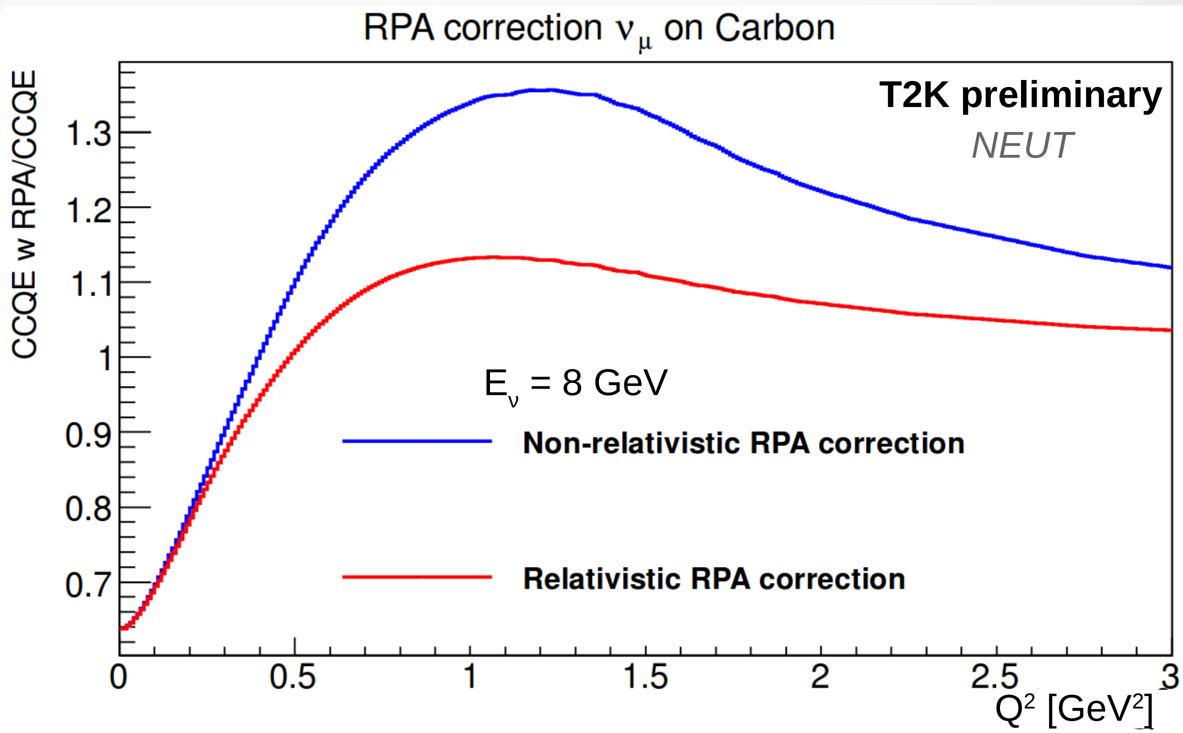

Interaction model: other parameterisations

How does the fit behave if nature follows another model, such as:

- nucleus model being Benhar's Spectral Function instead of RFG
- nucleus model being Relativistic Local Fermi Gas
- Martini's 2p2h model instead of Nieves model
- 2p2h shape parameter (adding to the normalisation parameter)
- effective RPA parameterisation with functional form

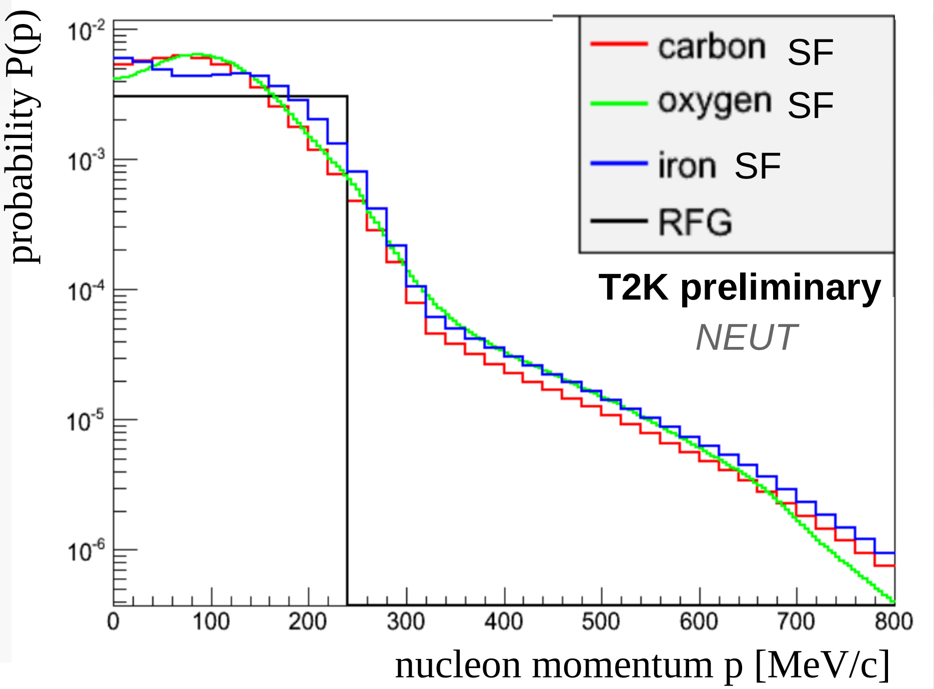

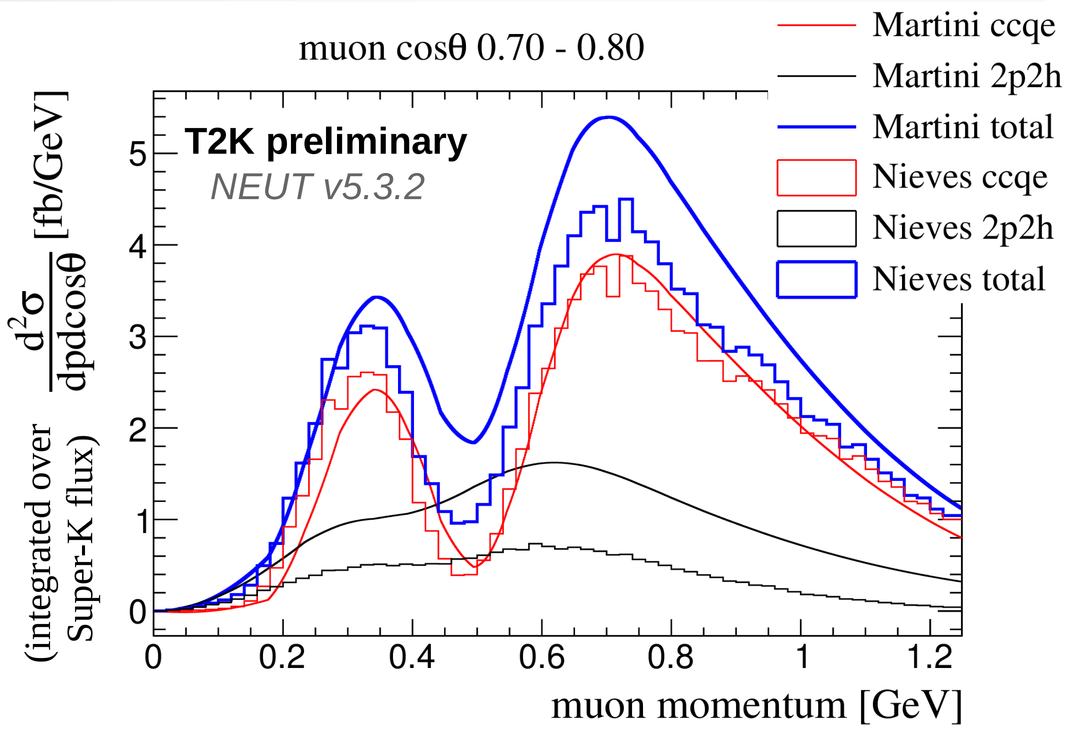

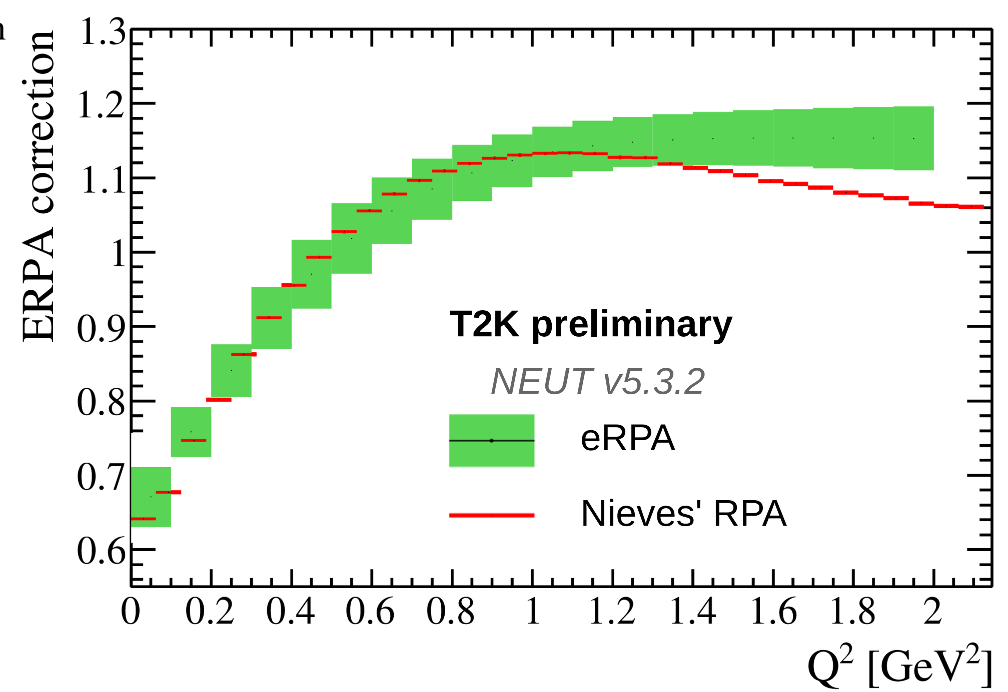

Interaction model: robustness of fit to models

How does the fit behave if nature follows another model ?

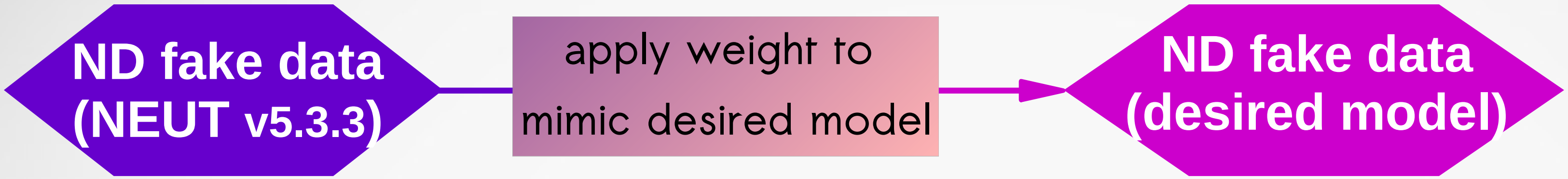

Interaction model: robustness of fit to models

How does the fit behave if nature follows another model ?

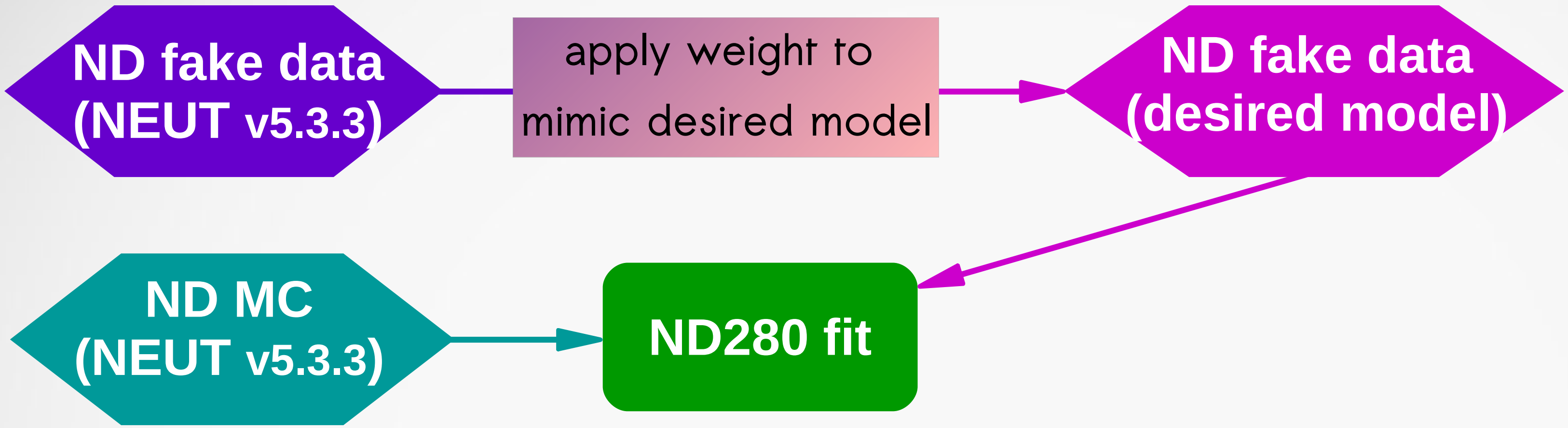

Interaction model: robustness of fit to models

How does the fit behave if nature follows another model ?

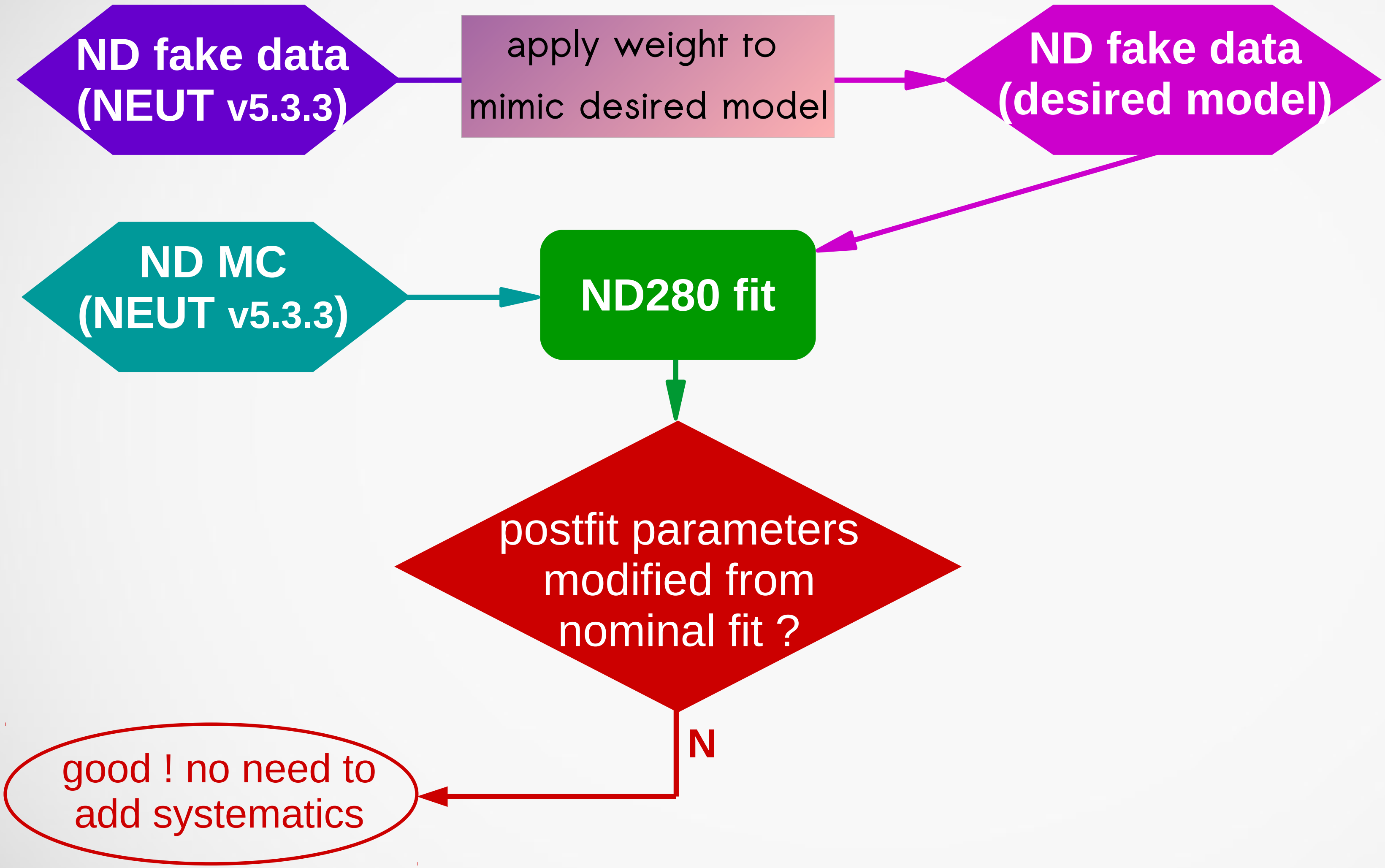

Interaction model: robustness of fit to models

How does the fit behave if nature follows another model ?

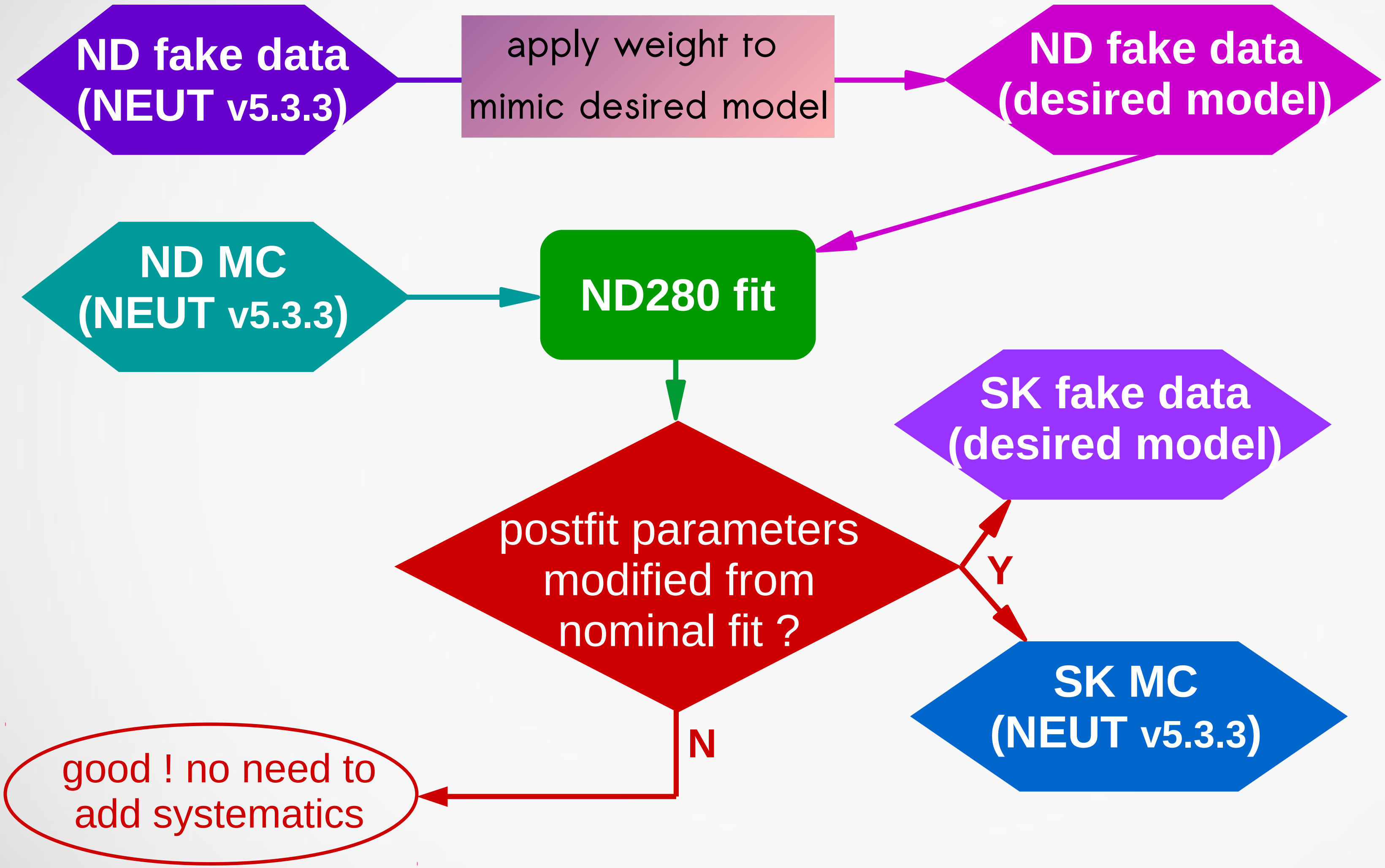

Interaction model: robustness of fit to models

How does the fit behave if nature follows another model ?

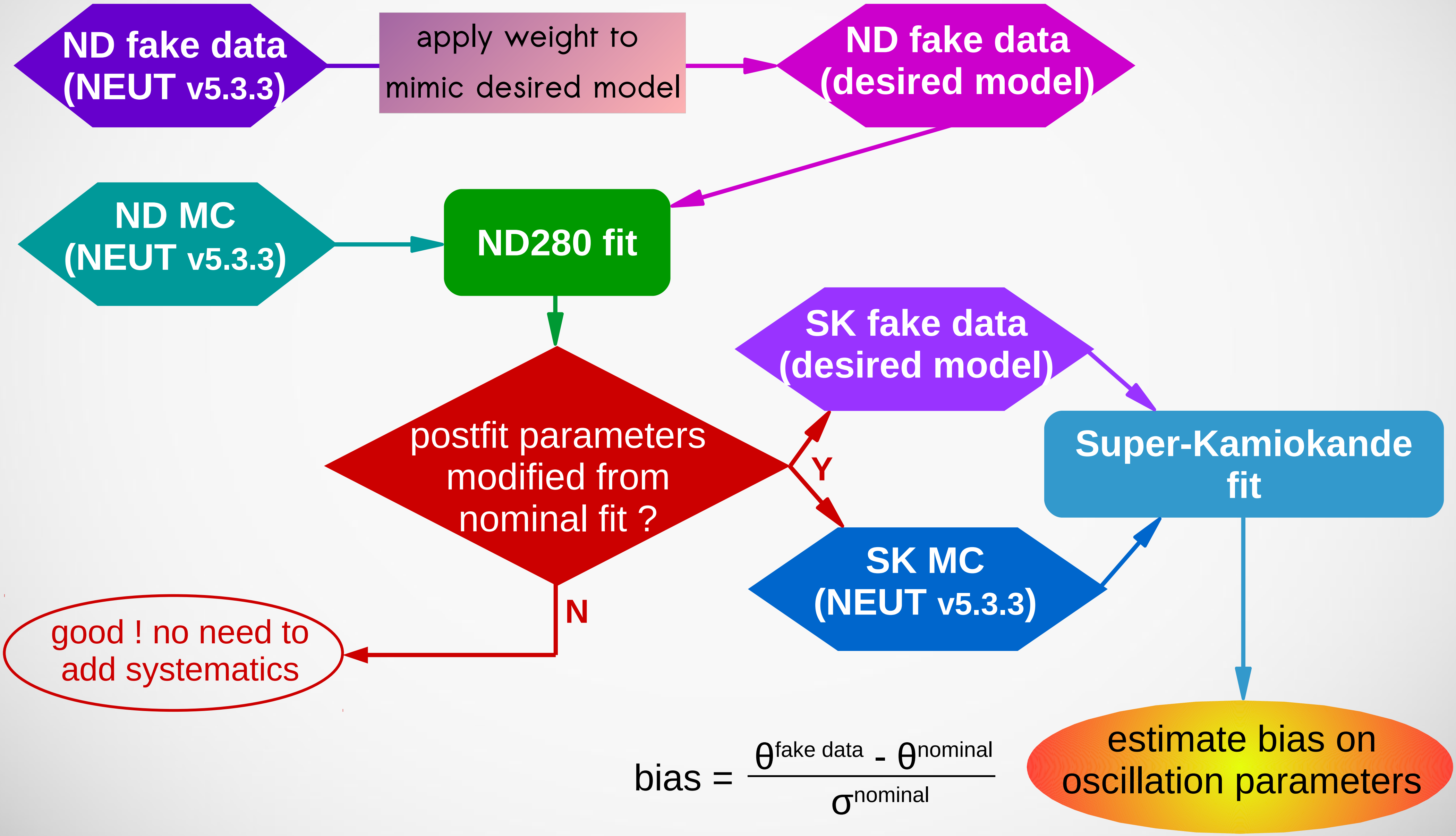

$$\text{bias} = \frac{\theta^{\text{fake data}} - \theta^{\text{nominal}}}{\sigma^{\text{nominal}}}$$

ND280 fit: final covariance matrix

How does the fit behave if nature follows another model? Results:

- ND280 post-fit parameters modified every time the model is changed ;
- bias in oscillation parameters from Local Fermi Gas taken into account by adding uncertainty in ND280 detector covariance matrix ;
- other biases are small considering statistical uncertainties.

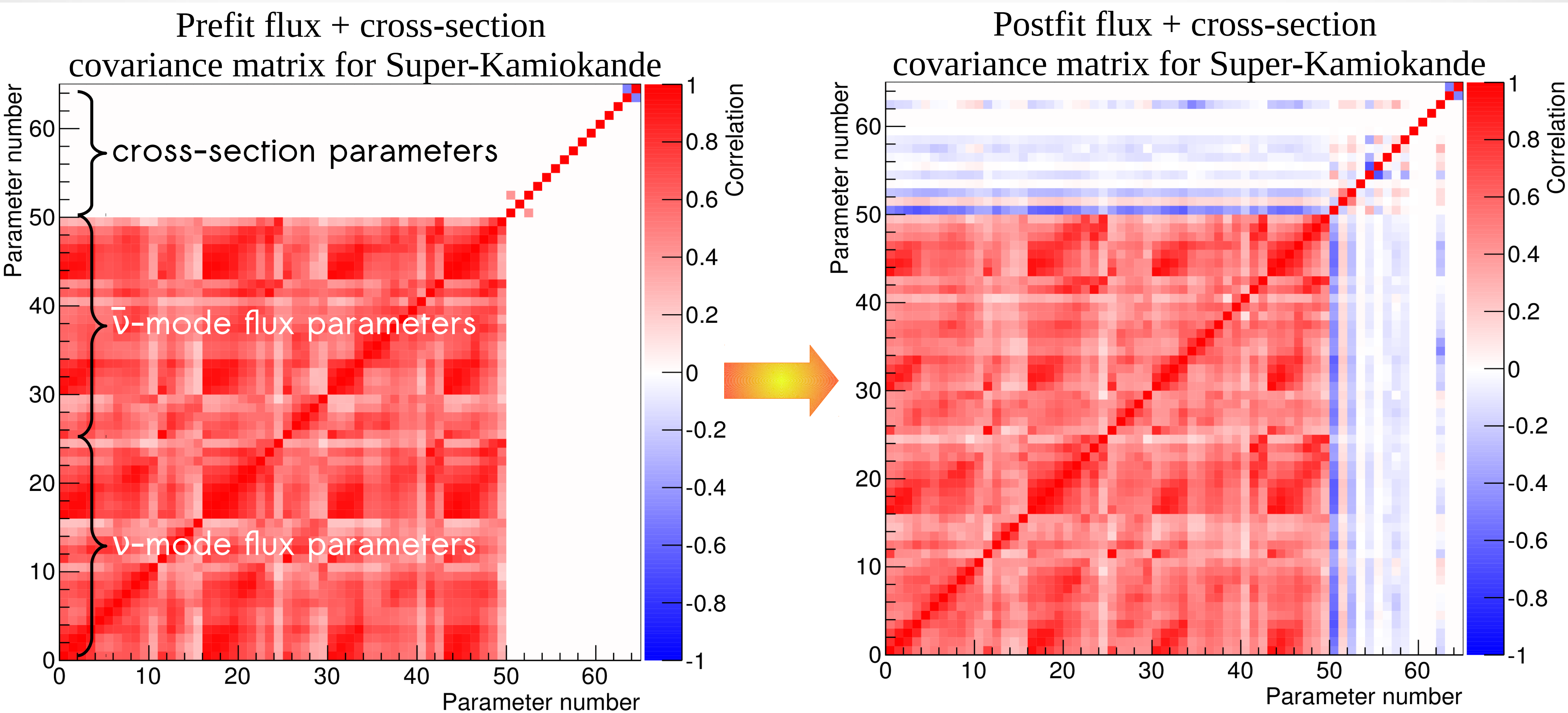

Summary and future prospects

- The ND280 fit:
  - reduces the uncertainties from ~12% to ~5% on the number of events predicted at Super-Kamiokande ;
  - predicts a higher flux than the initial model ;
  - constrains the cross-section parameters in values in the range of initial uncertainties of the model.

- Next fit improvements:
  - use inter-detector timing information to do a 360° selection in ND280 (now +/- 53°) ;
  - ν_e sample in ND280 added to the fit ;
  - add new selection in P0D subdetector ;
  - and still, flux tuning with long target NA61data, cross-section models study, MC generator improvements, more statistics.

STAY TUNED FOR MORE FROM T2K !

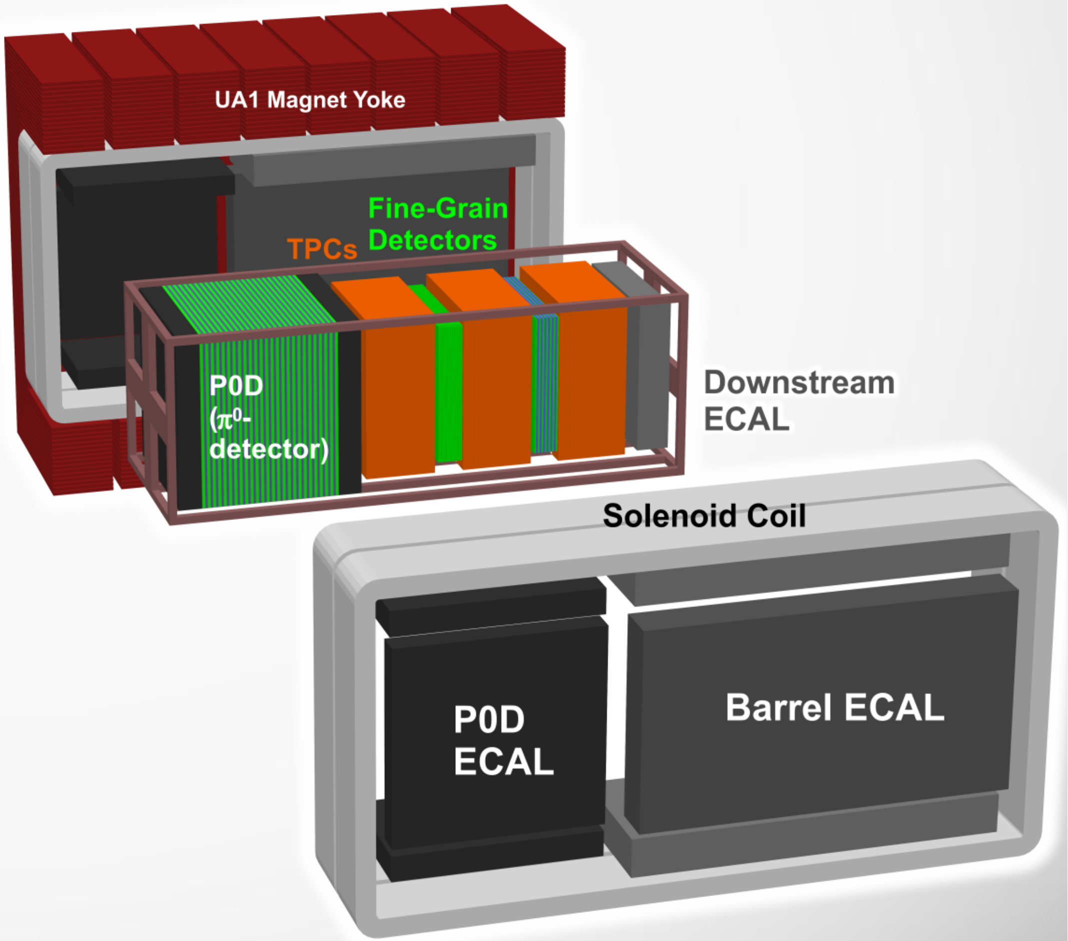

more about T2K ? S. Dolan on ν scattering

E. Reinherz-Aronis on ν cross-sections

D. Cherdack on ν interaction systematics

B. Quillain on ν_e appearance

M. Rayner on near detector upgrades

backup

T2K P.O.T.

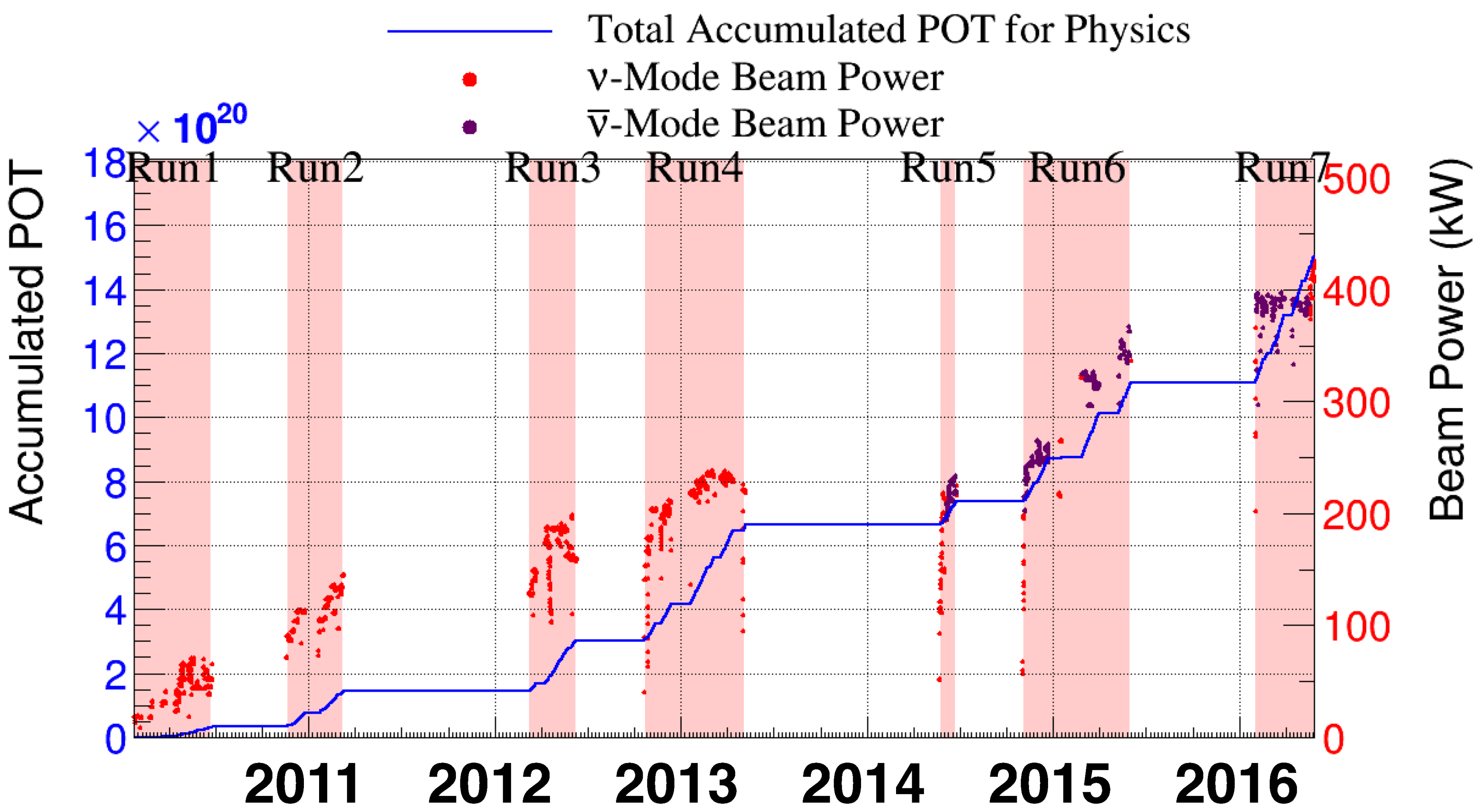

27 May 2016
POT total: 1.510×10^{21}

ν-mode POT: 7.57×10^{20} (50.14%)
ν̄-mode POT: 7.53×10^{20} (49.86%)

Near detectors

ND280

off-axis detector
characterisation of off-axis flux
and interaction parameters

INGRID

on-axis detector
beam direction monitoring

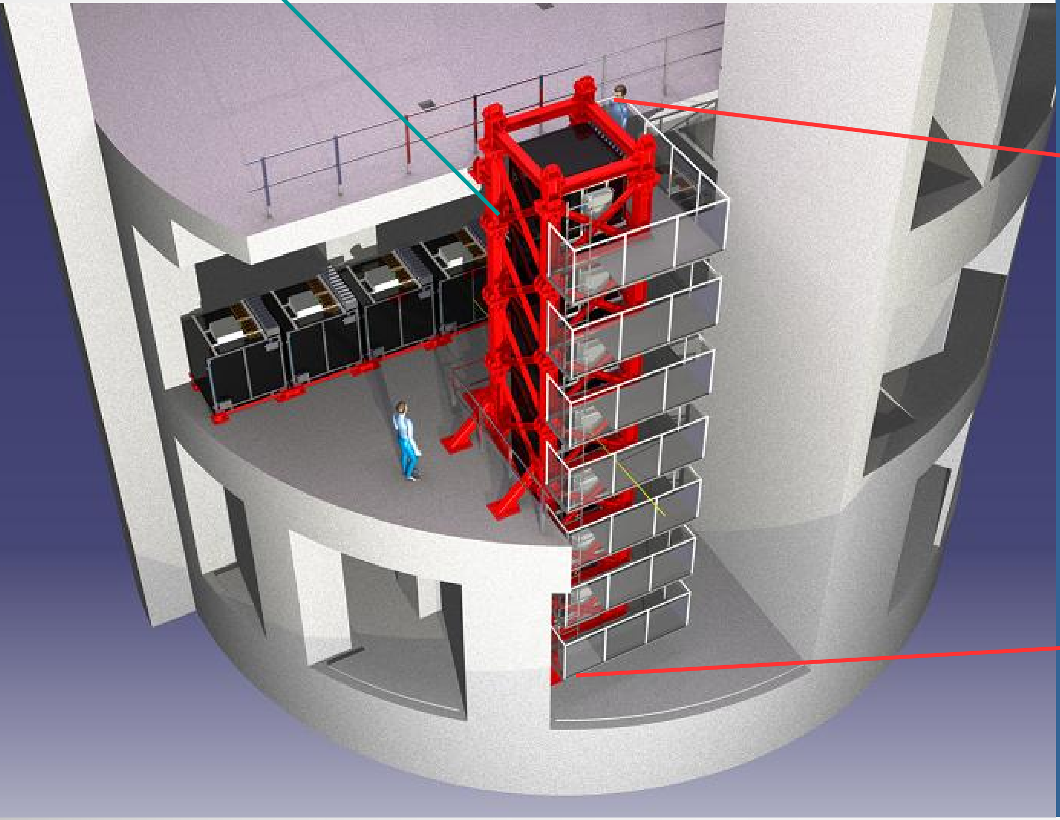

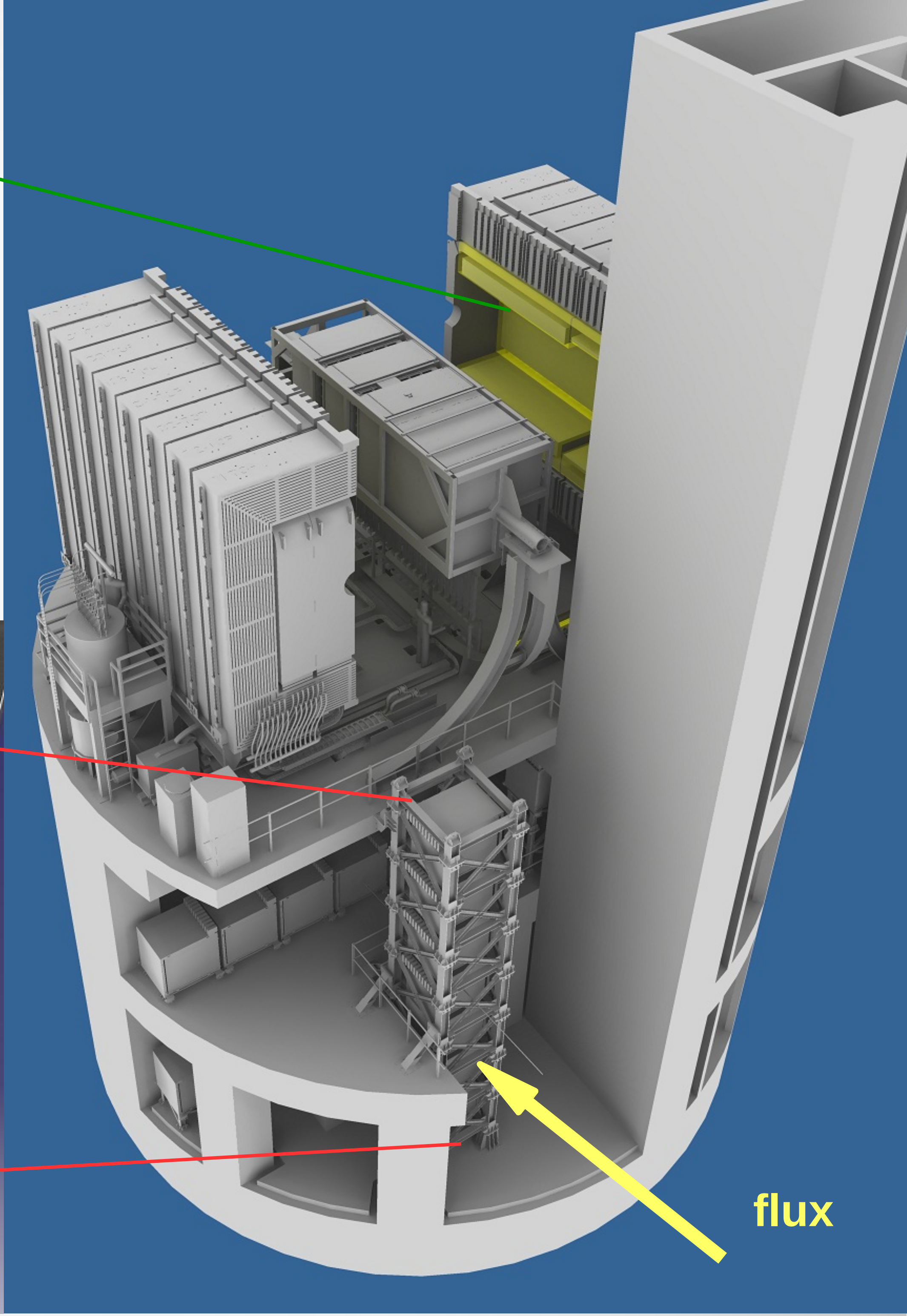

Event rate at Super-Kamiokande ($\bar{\nu}$ mode)

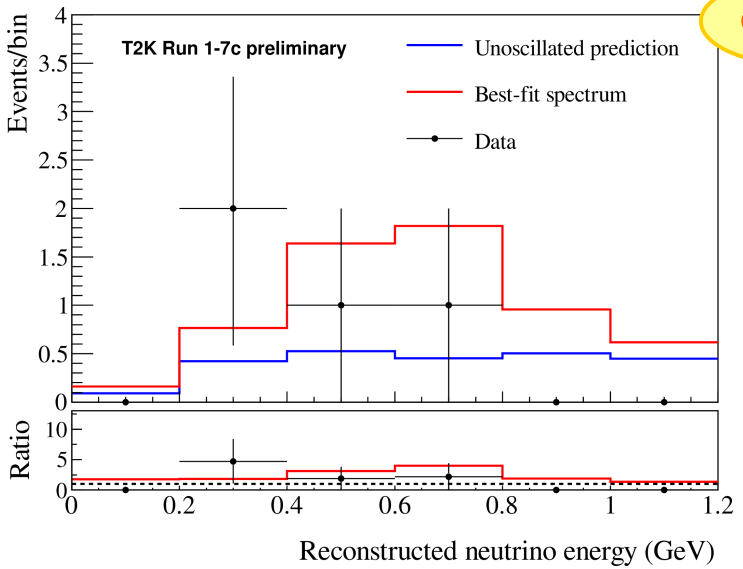

e+ rings

Systematic	$\Delta N_{SK}/N_{SK}$ before ND fit	$\Delta N_{SK}/N_{SK}$ after ND fit
Flux	7.9%	3.4%
Cross section	10.1%	5.4%
Flux and cross section	12.9%	4.5%
Final state/secondary interactions at SK	2.4%	
SK detector	3.1%	
Total	13.4%	5.7%

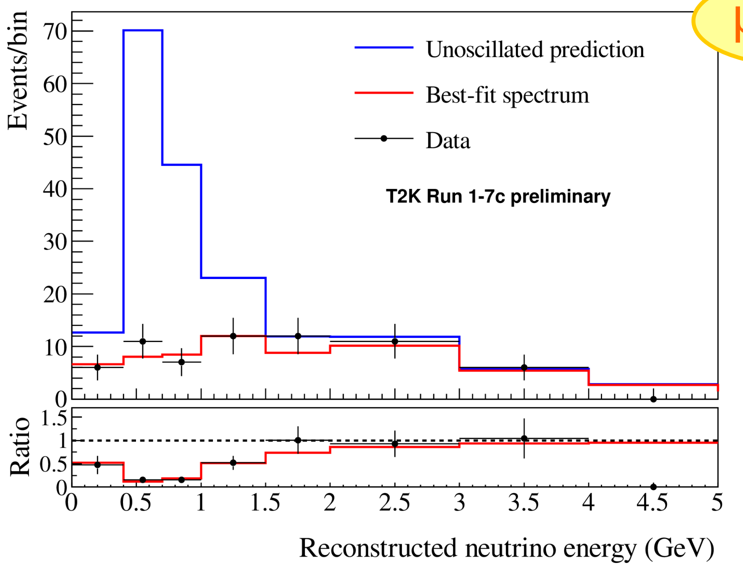

μ+ rings

Systematic	$\Delta N_{SK}/N_{SK}$ before ND fit	$\Delta N_{SK}/N_{SK}$ after ND fit
Flux	7.7%	3.1%
Cross section	7.6%	3.8%
Flux and cross section	10.9%	2.5%
Final state/secondary interactions at SK	1.8%	
SK detector	4.6%	
Total	12.1%	4.9%

T2K analysis

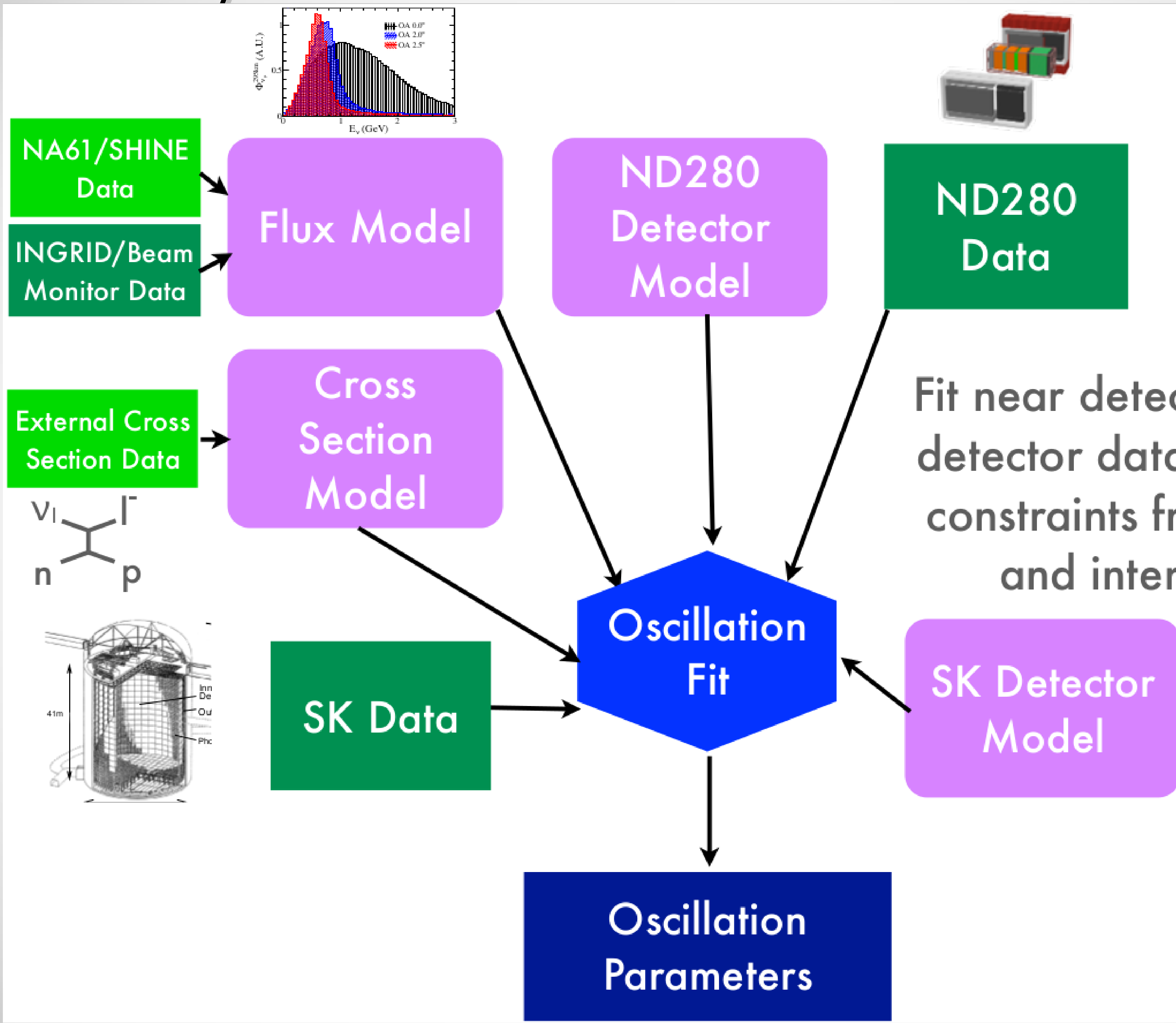

Fit near detector data, far detector data, and model constraints from external and internal data

ND280 fit likelihood

$$
\begin{aligned}
\Delta\chi^2_{ND280} =& 2\sum_i^{Nbins} N_i^p(\vec{b},\vec{x},\vec{d}) - N_i^d + N_i^d \ln[N_i^d/N_i^p(\vec{b},\vec{x},\vec{d})] + \\
& \sum_i^{E_\nu\ bins}\sum_j^{E_\nu\ bins} \Delta b_i (V_b^{-1})_{i,j}\Delta b_j + \sum_i^{xsec\ pars}\sum_j^{xsec\ pars} \Delta x_i (V_x^{-1})_{i,j}\Delta x_j + \\
& \sum_i^{N_{bins}}\sum_j^{N_{bins}} \Delta d_i (V^{-1})_d \Delta d_j
\end{aligned} \tag{1}
$$

Here, N_i^d is the numbers of events observed in each of the i bins of the analysis where i ranges over the lepton $p-\cos\theta$ bins and samples. N_i^p is the predicted number of events for each of the i bins and depends on the flux, $\vec{b}$, cross section, $\vec{x}$, and detector, $\vec{d}$, systematic parameters. The systematic parameters have prior probability distributions that are modeled as multivariate Gaussians with covariances of V_b, V_x and V_d for the flux, cross section and detector parameters respectively. Δb, Δx and Δd are the deviations of the systematic parameters away from their prior mean values.

Flux prediction at Super-Kamiokande

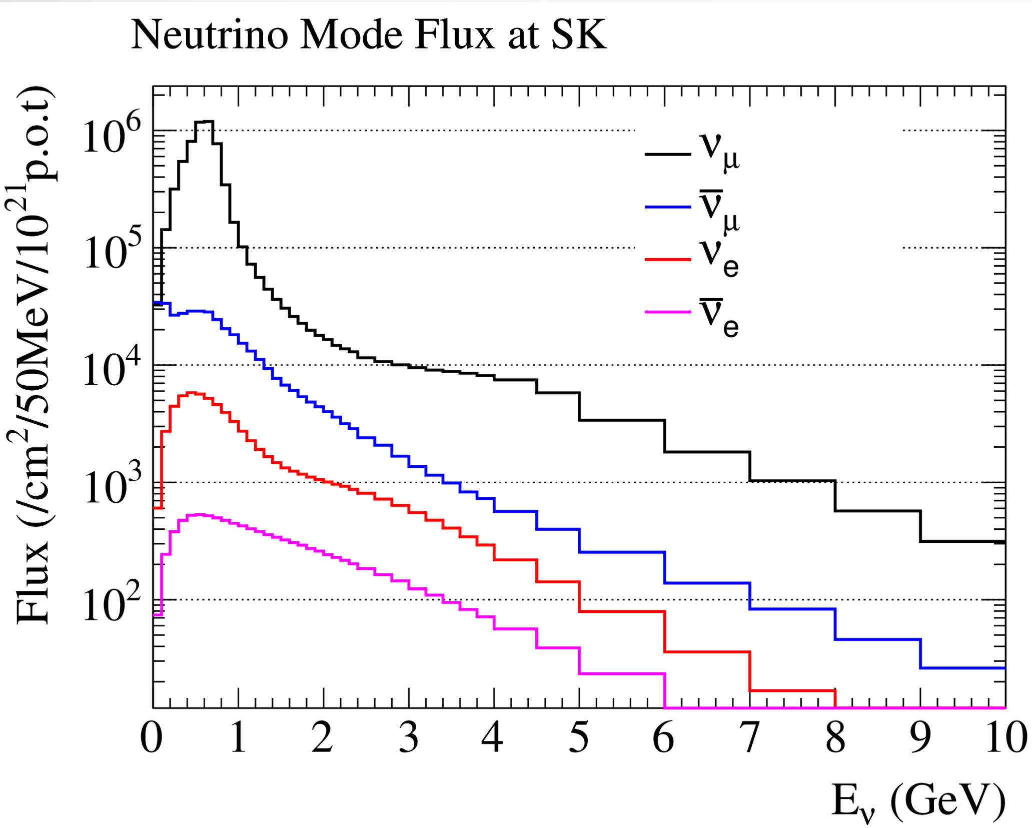

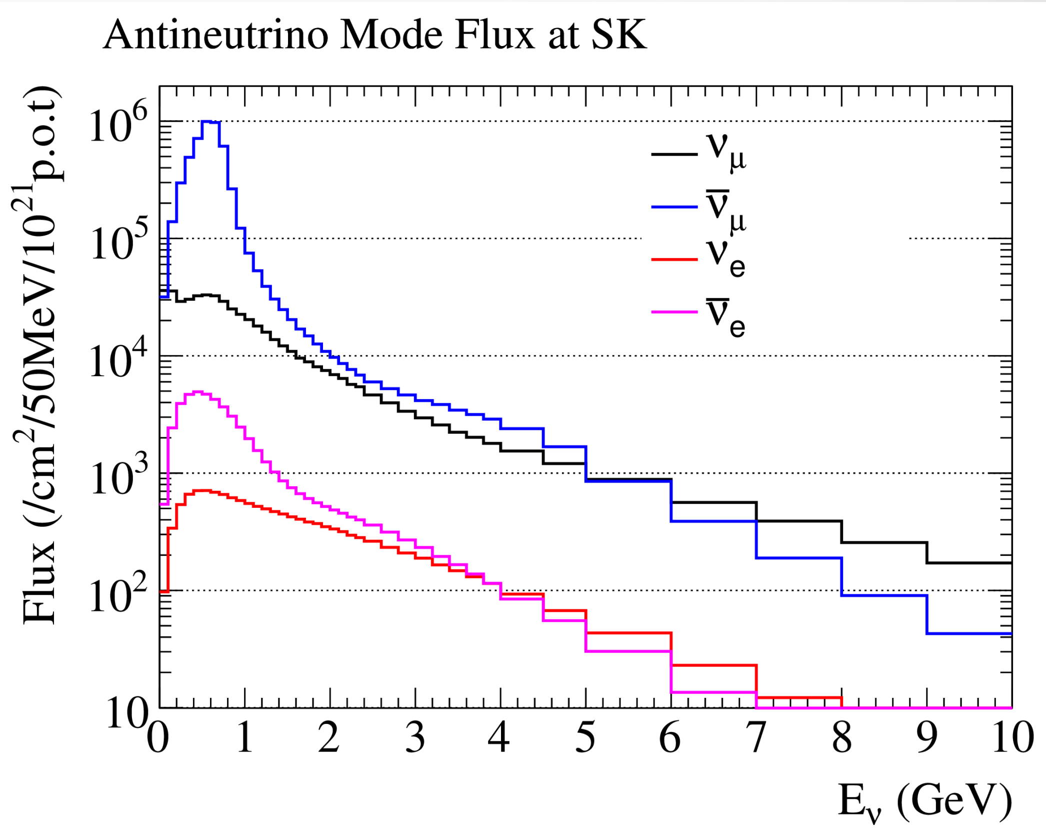

Flux correlations before ND280 fit

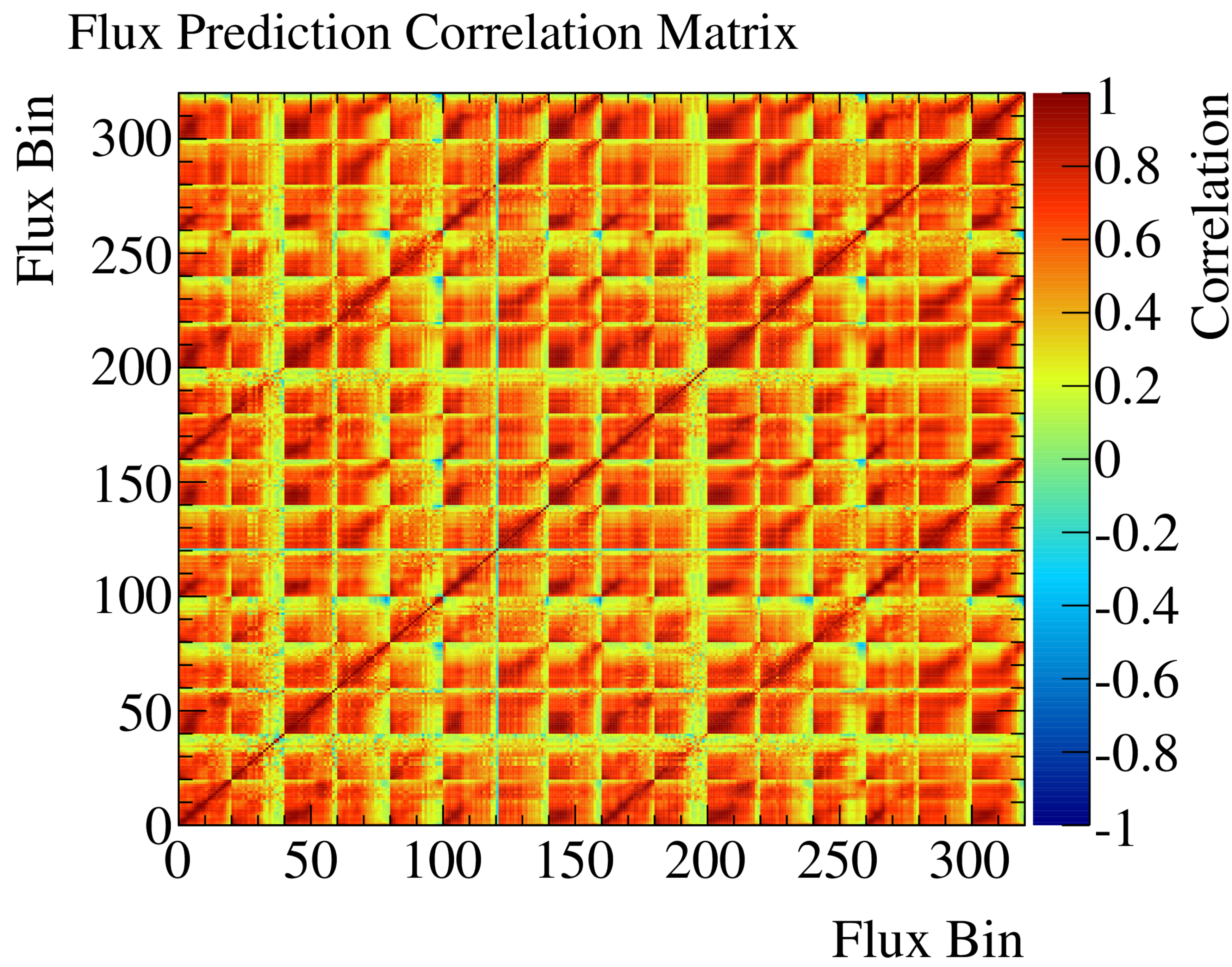

00-19 : ND280, ν mode, ν_μ

20-39 : ND280, ν mode, $\bar{\nu}_\mu$

40-59 : ND280, ν mode, ν_e

60-79 : ND280, ν mode, ν_e

80-99 : ND280, $\bar{\nu}$ mode, ν_μ

100-119 : ND280, $\bar{\nu}$ mode, $\bar{\nu}_\mu$

120-139 : ND280, $\bar{\nu}$ mode, ν_e

140-159 : ND280, $\bar{\nu}$ mode, ν_e

160-179 : SK, ν mode, ν_μ

180-199 : SK, ν mode, $\bar{\nu}_\mu$

200-219 : SK, ν mode, ν_e

220-239 : SK, ν mode, ν_e

240-259 : SK, $\bar{\nu}$ mode, ν_μ

260-279 : SK, $\bar{\nu}$ mode, $\bar{\nu}_\mu$

280-299 : SK, $\bar{\nu}$ mode, ν_e

300-319 : SK, $\bar{\nu}$ mode, ν_e

Flux correlations before ND280 fit : zoom

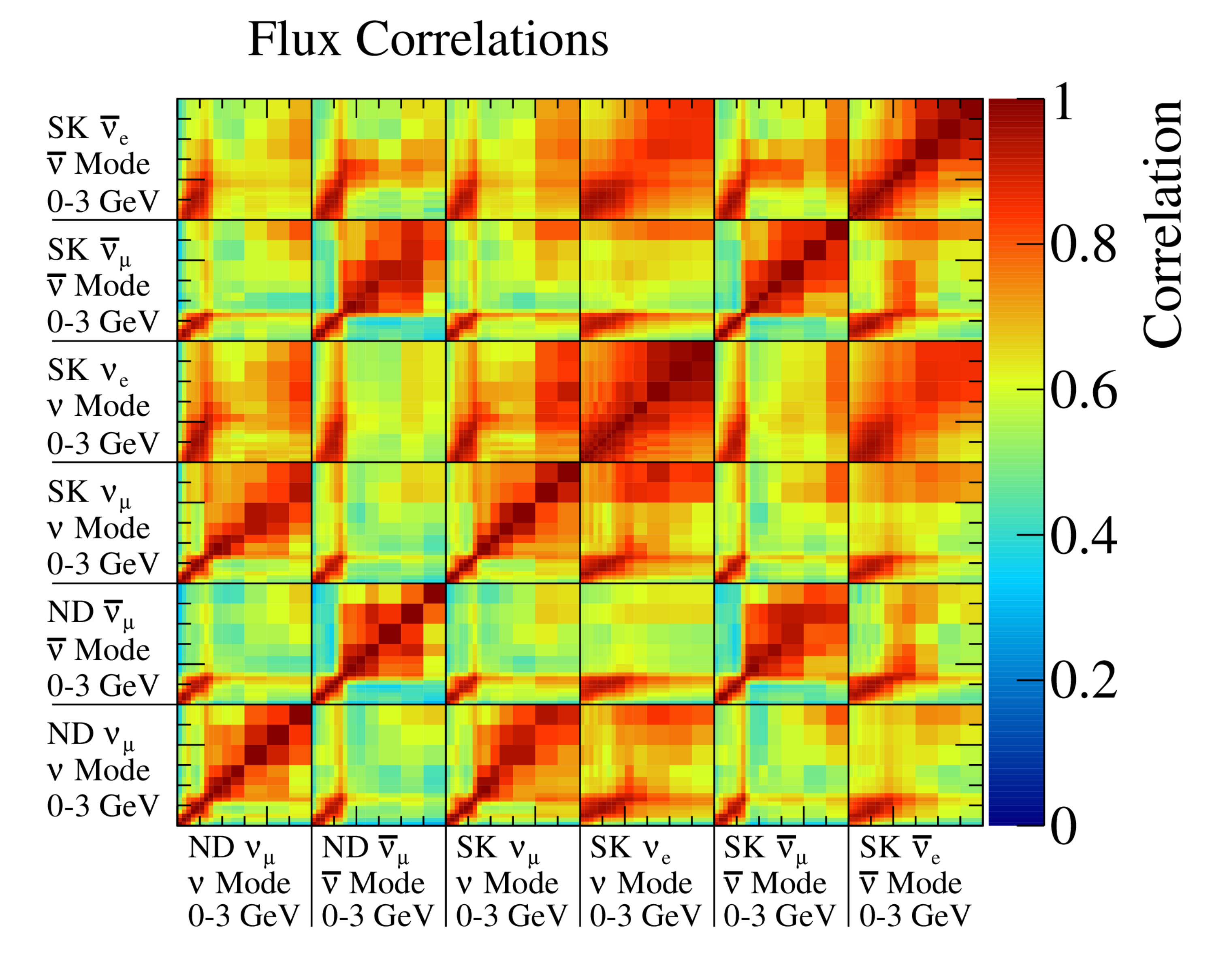

Flux uncertainties : ND280 ν mode

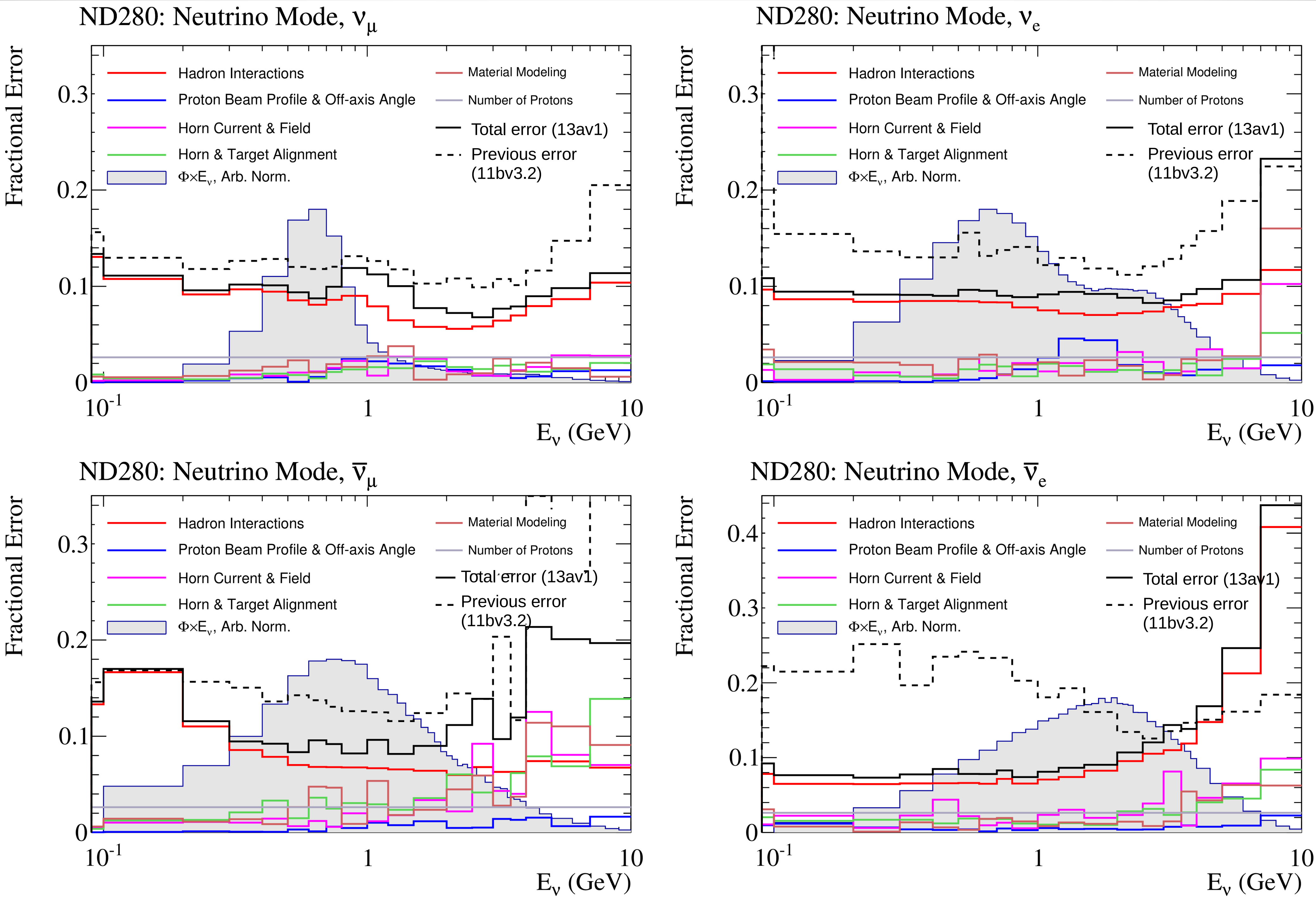

Flux uncertainties : ND280 $\bar{\nu}$ mode

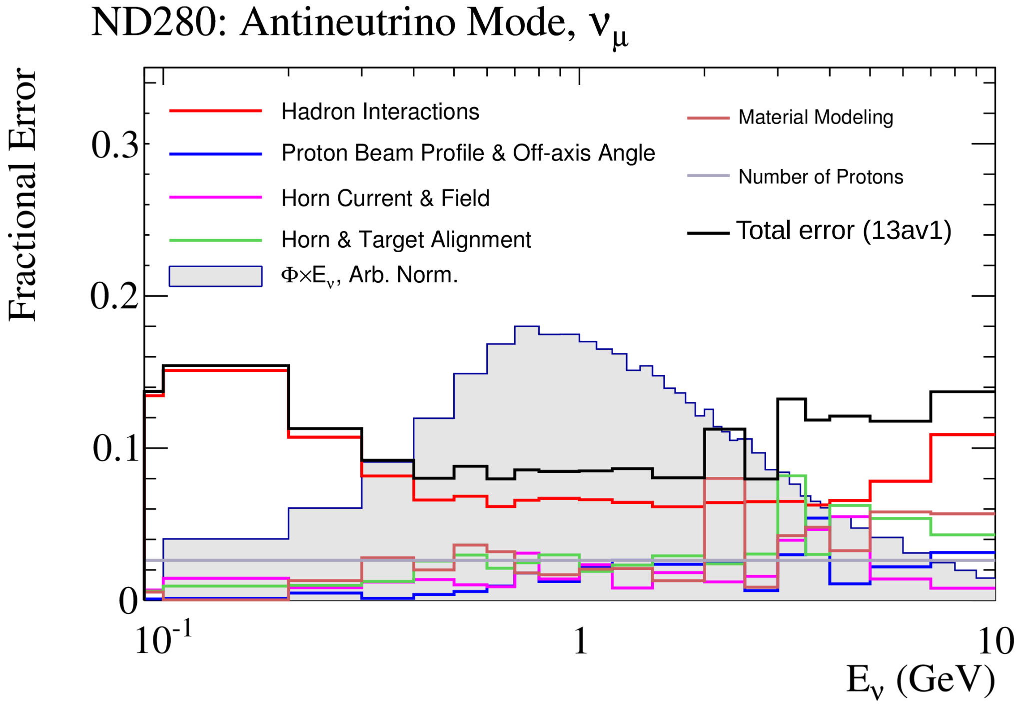

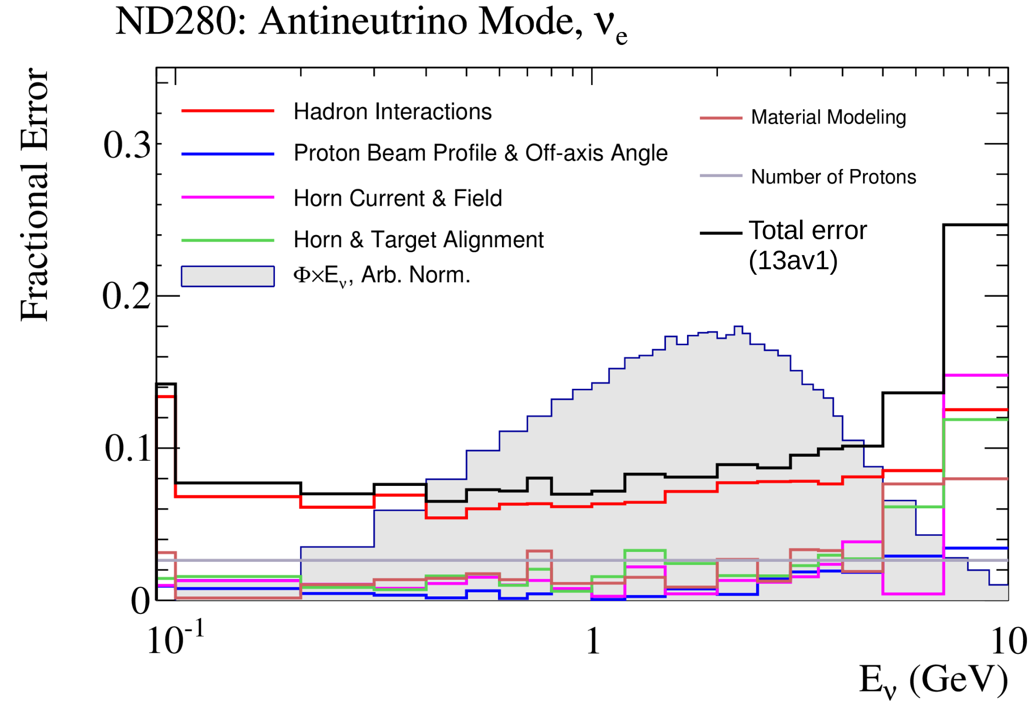

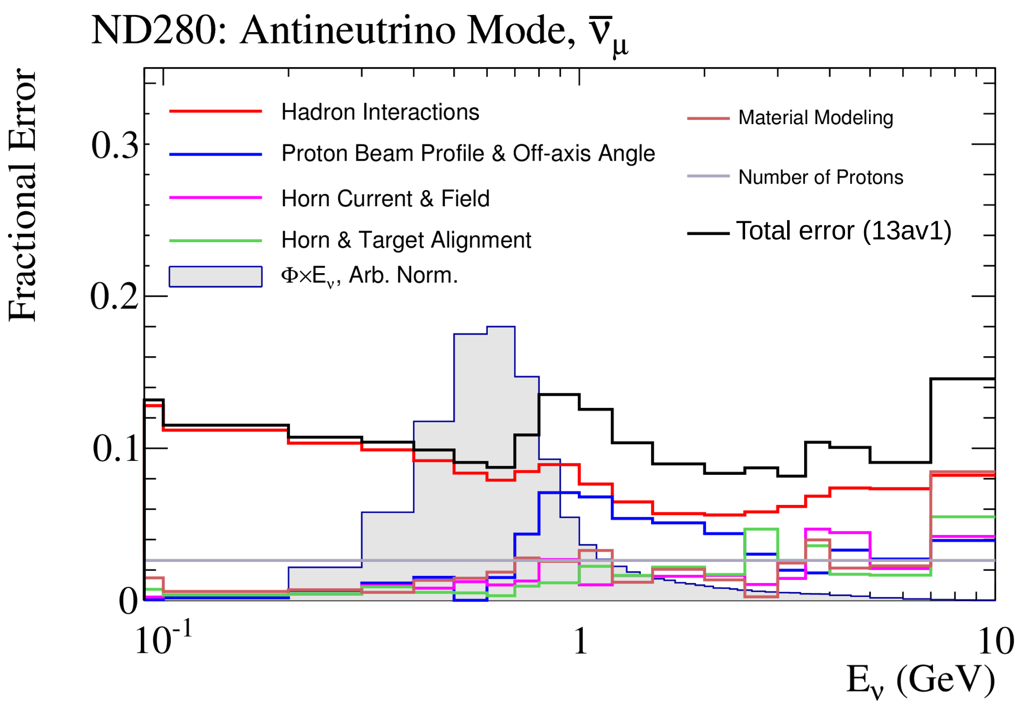

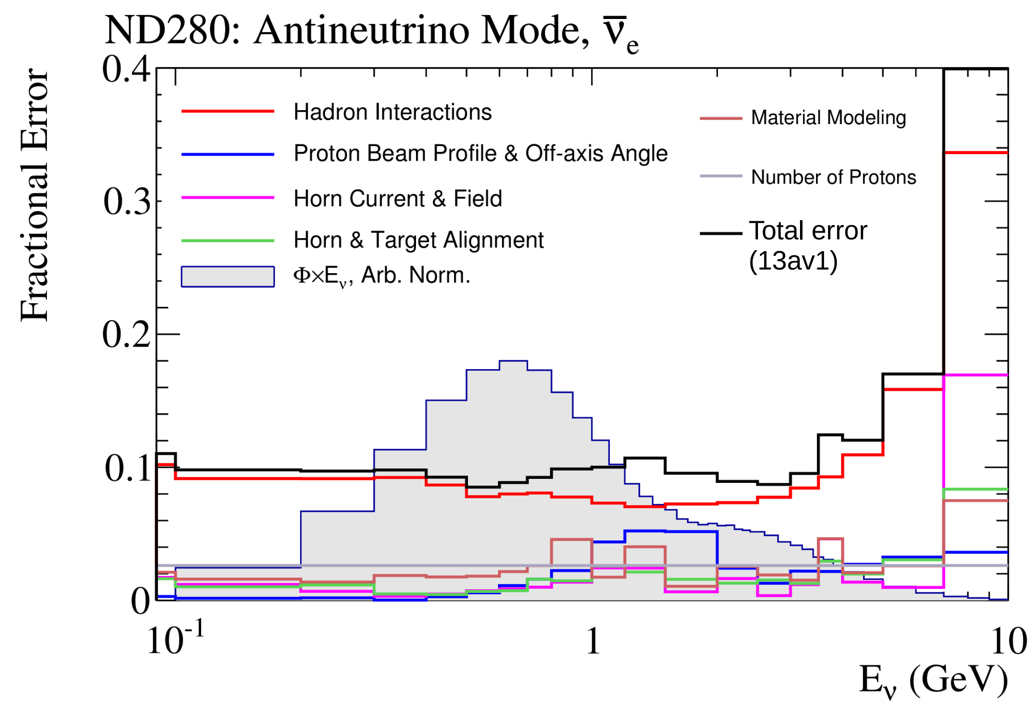

Flux uncertainties : Super-Kamiokande ν mode

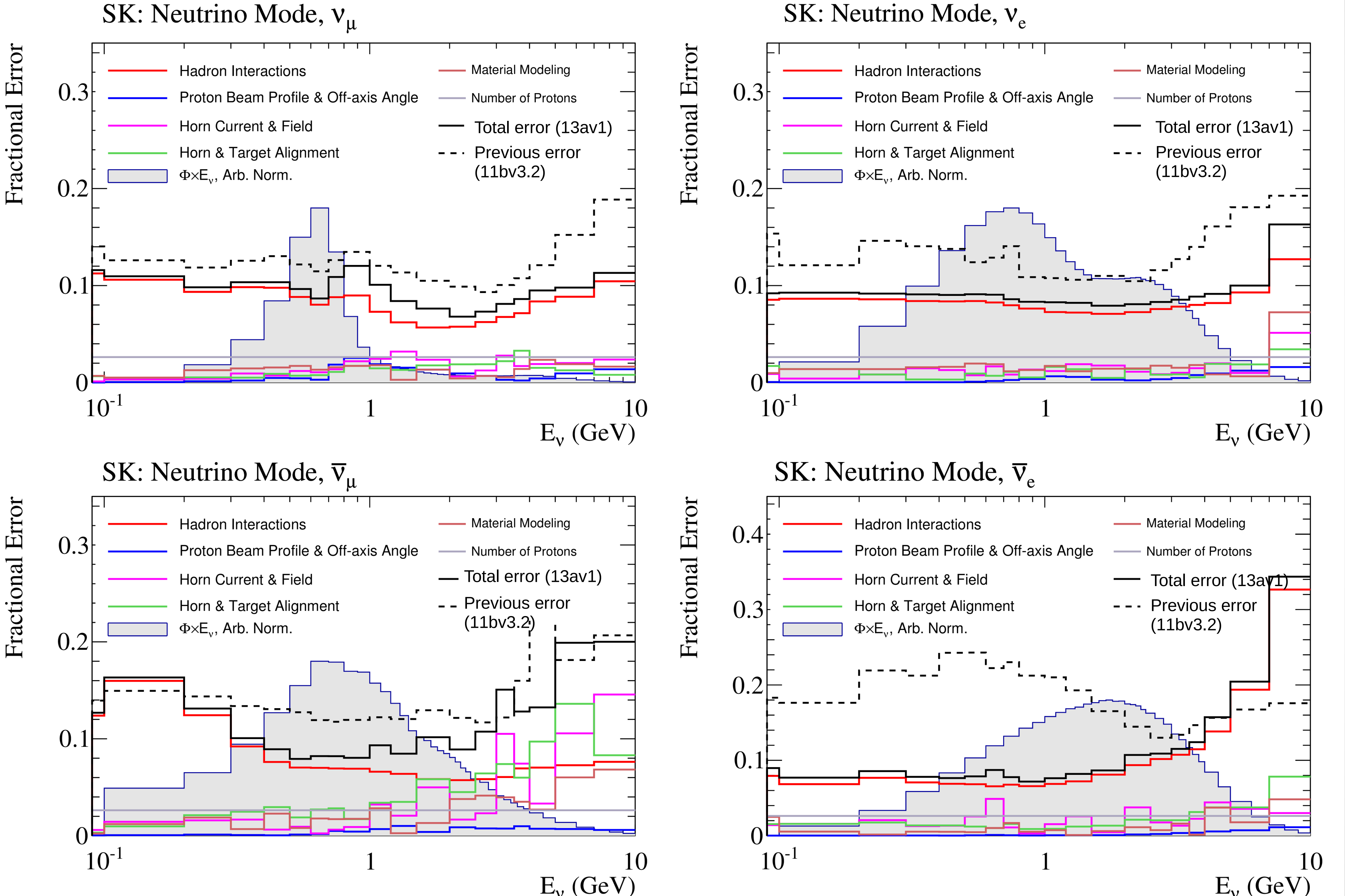

Flux uncertainties : Super-Kamiokande $\bar{\nu}$ mode

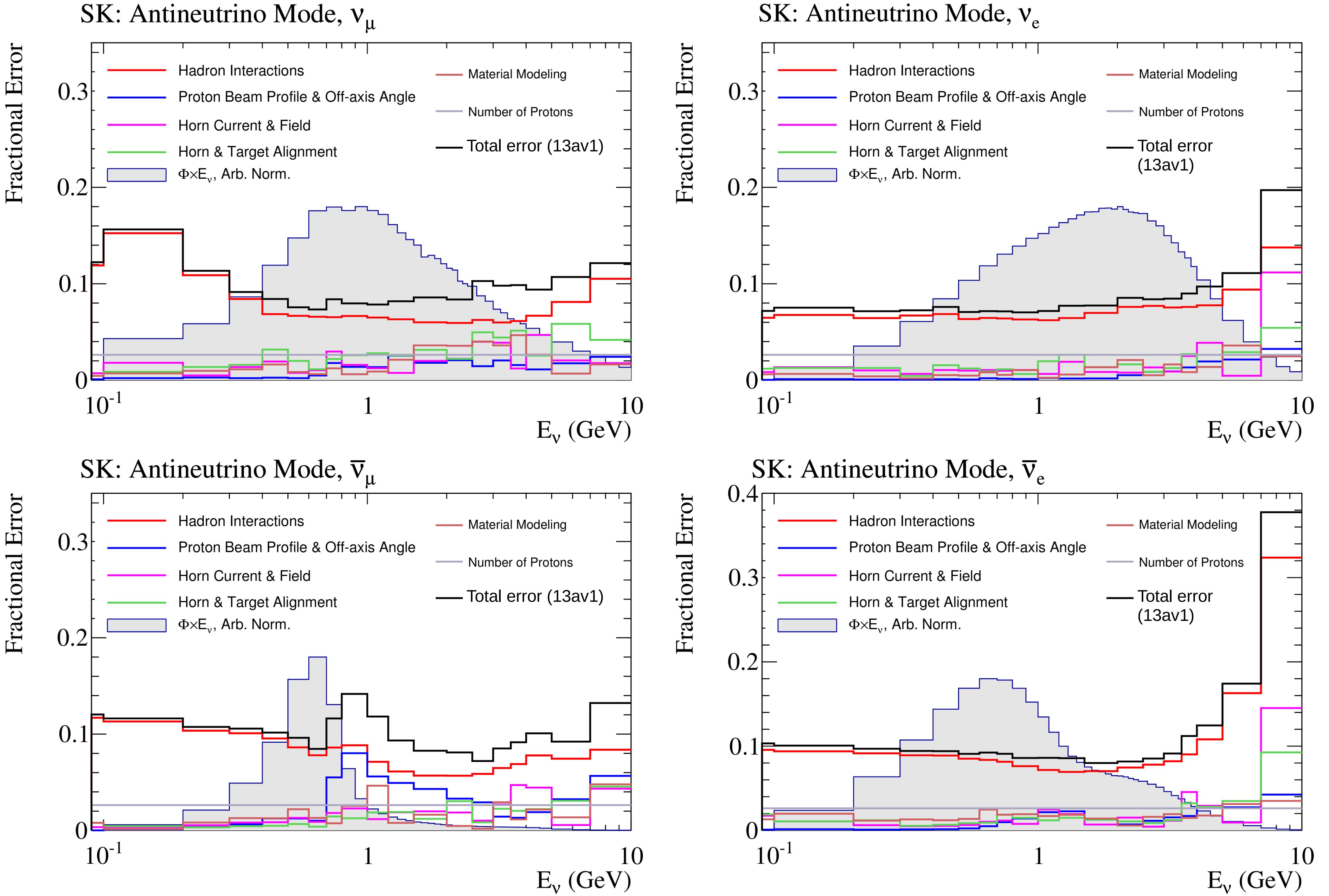

Flux constraints : expectation

sensitivity of ND280 fit to MC fake data

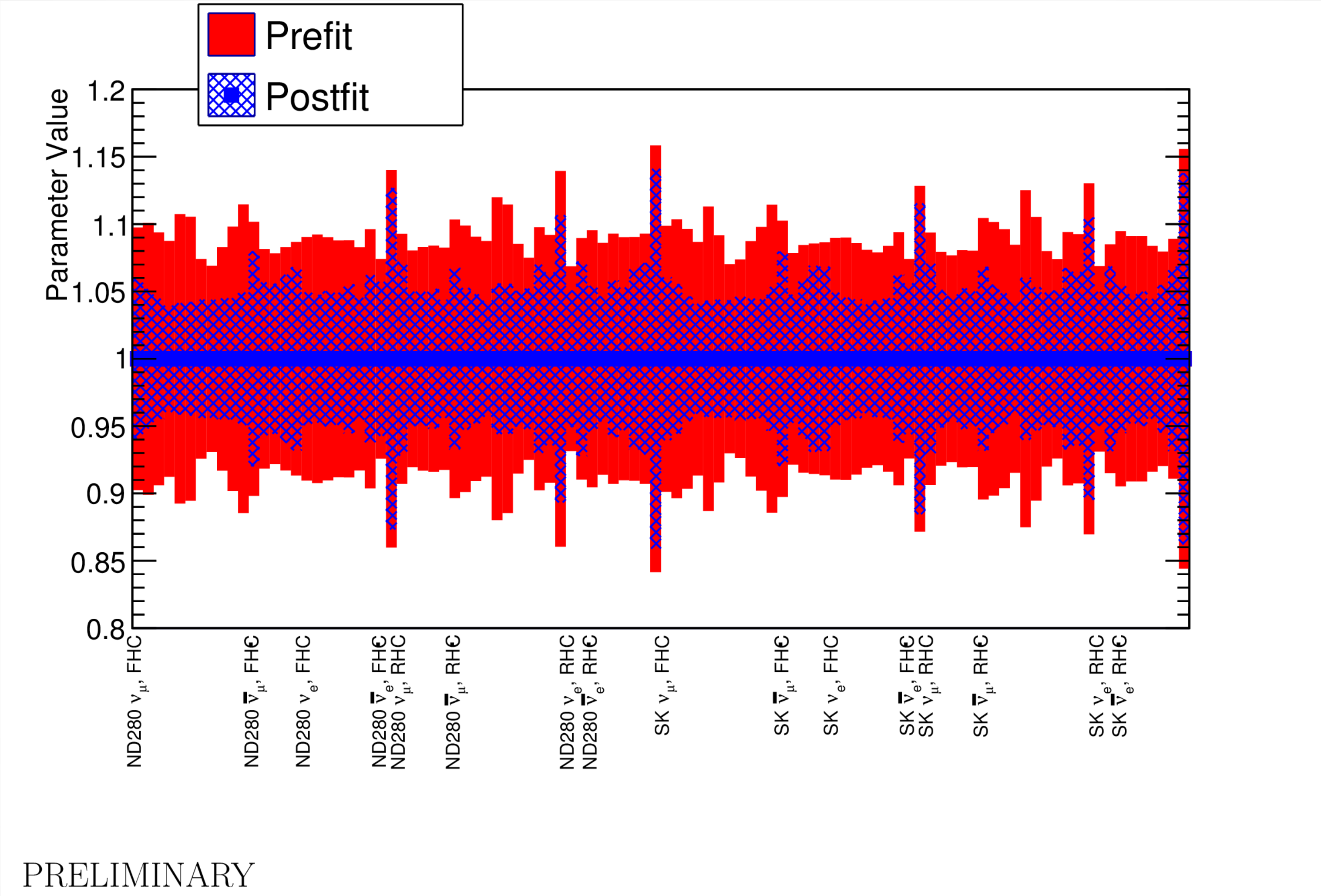

Flux constraints : ND280 ν mode

ND280 ν_μ, ν beam mode

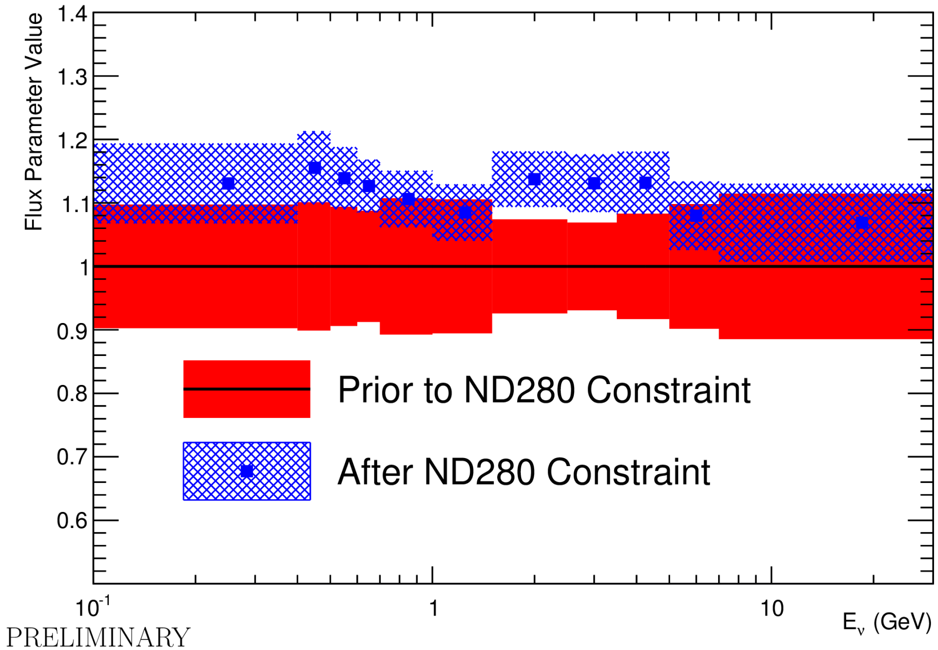

ND280 ν_e, ν beam mode

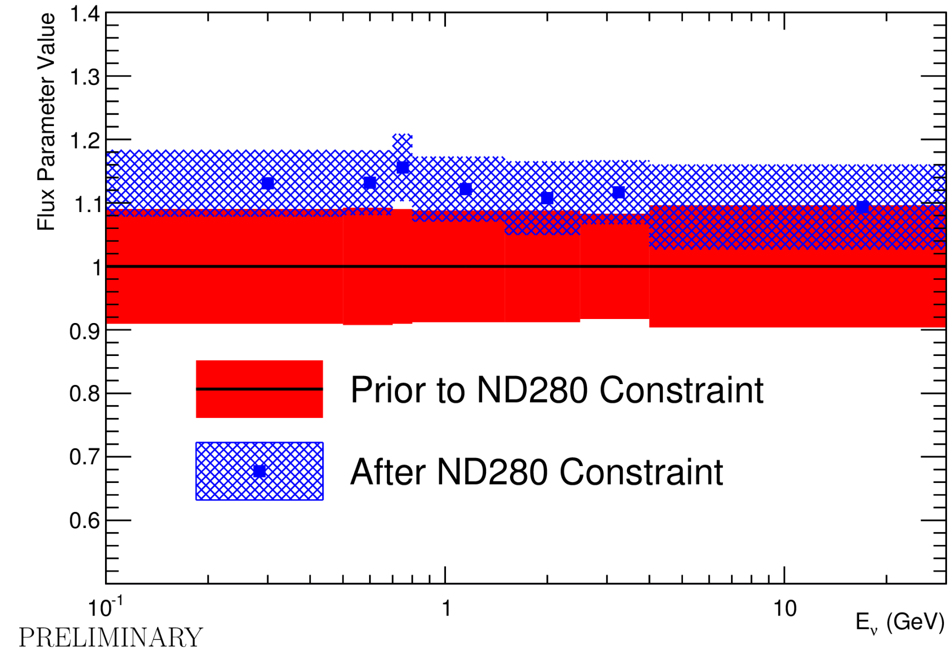

ND280 $\bar{\nu}_\mu$, ν beam mode

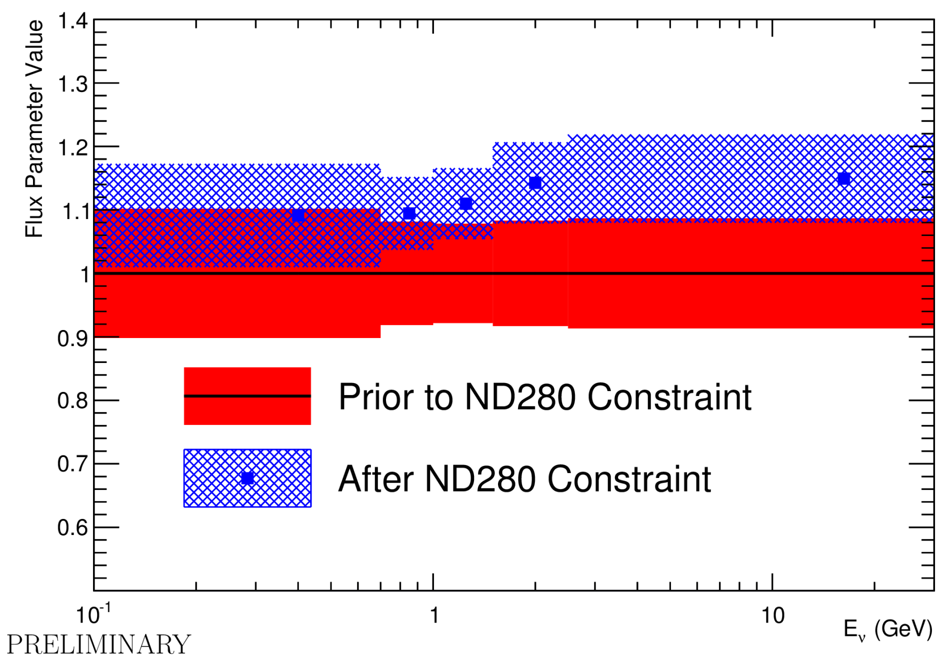

ND280 $\bar{\nu}_e$, ν beam mode

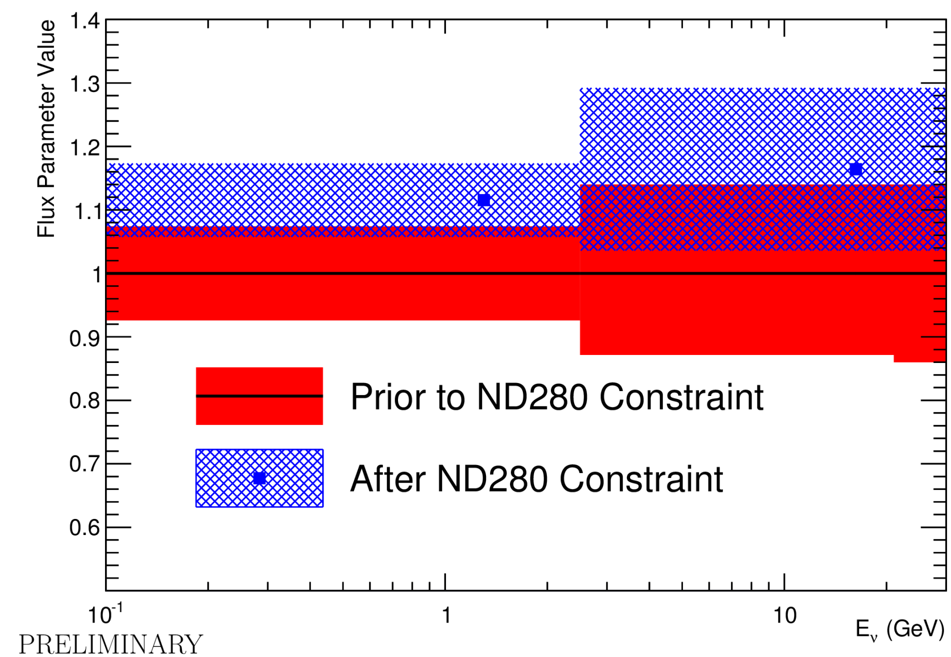

Flux constraints : ND280 $\overline{\nu}$ mode

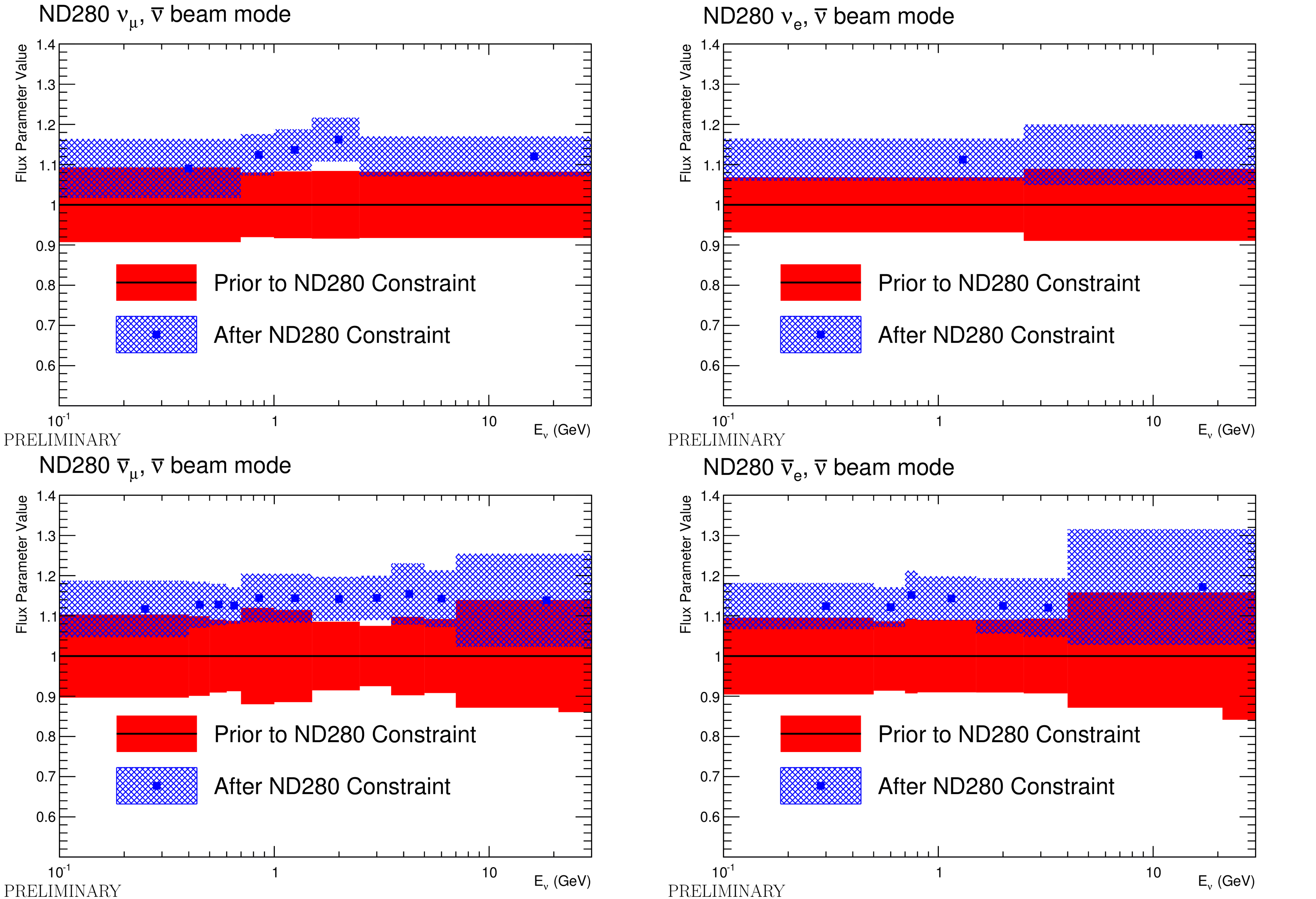

Flux constraints : Super-Kamiokande ν mode

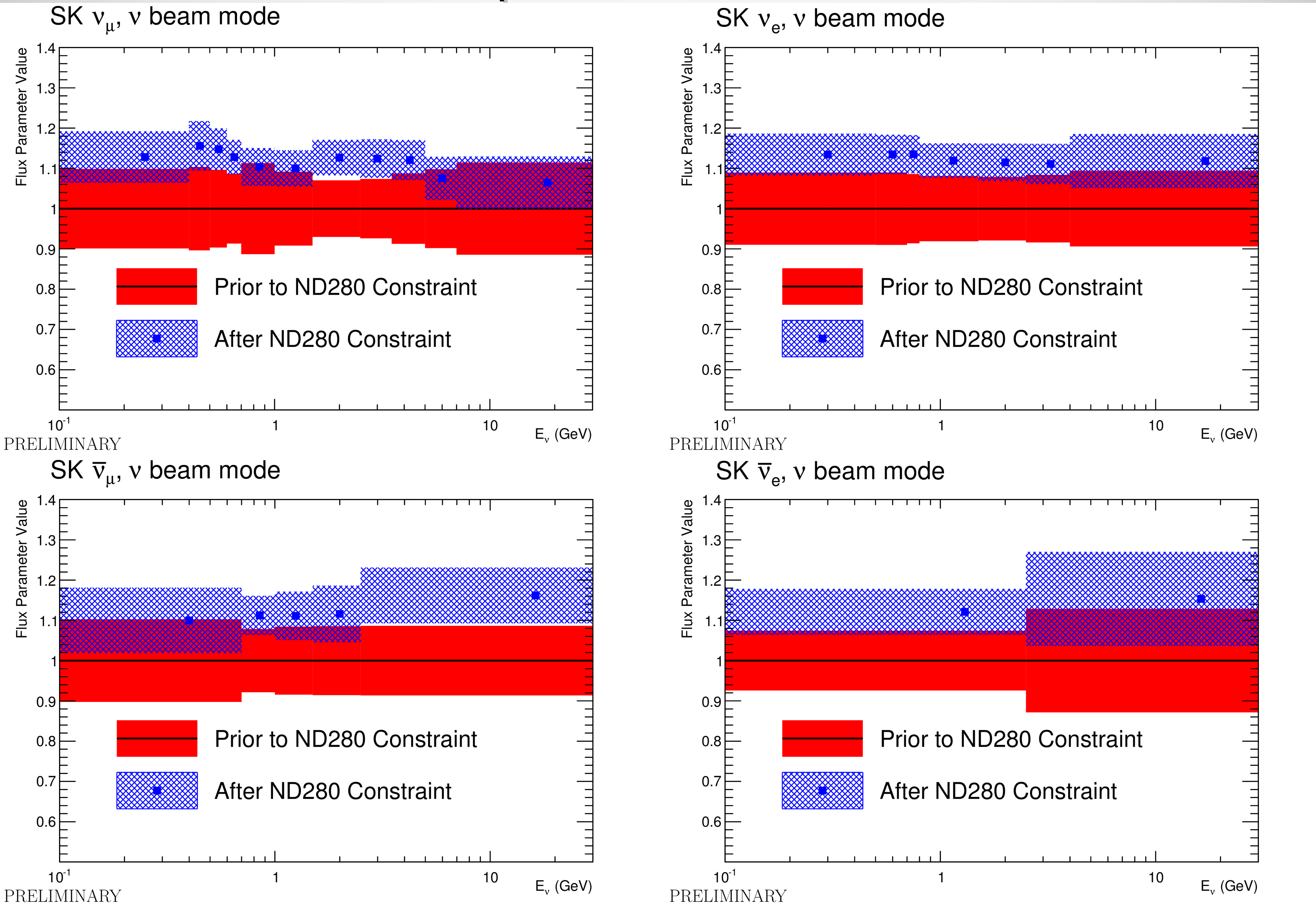

Flux constraints : Super-Kamiokande $\bar{\nu}$ mode

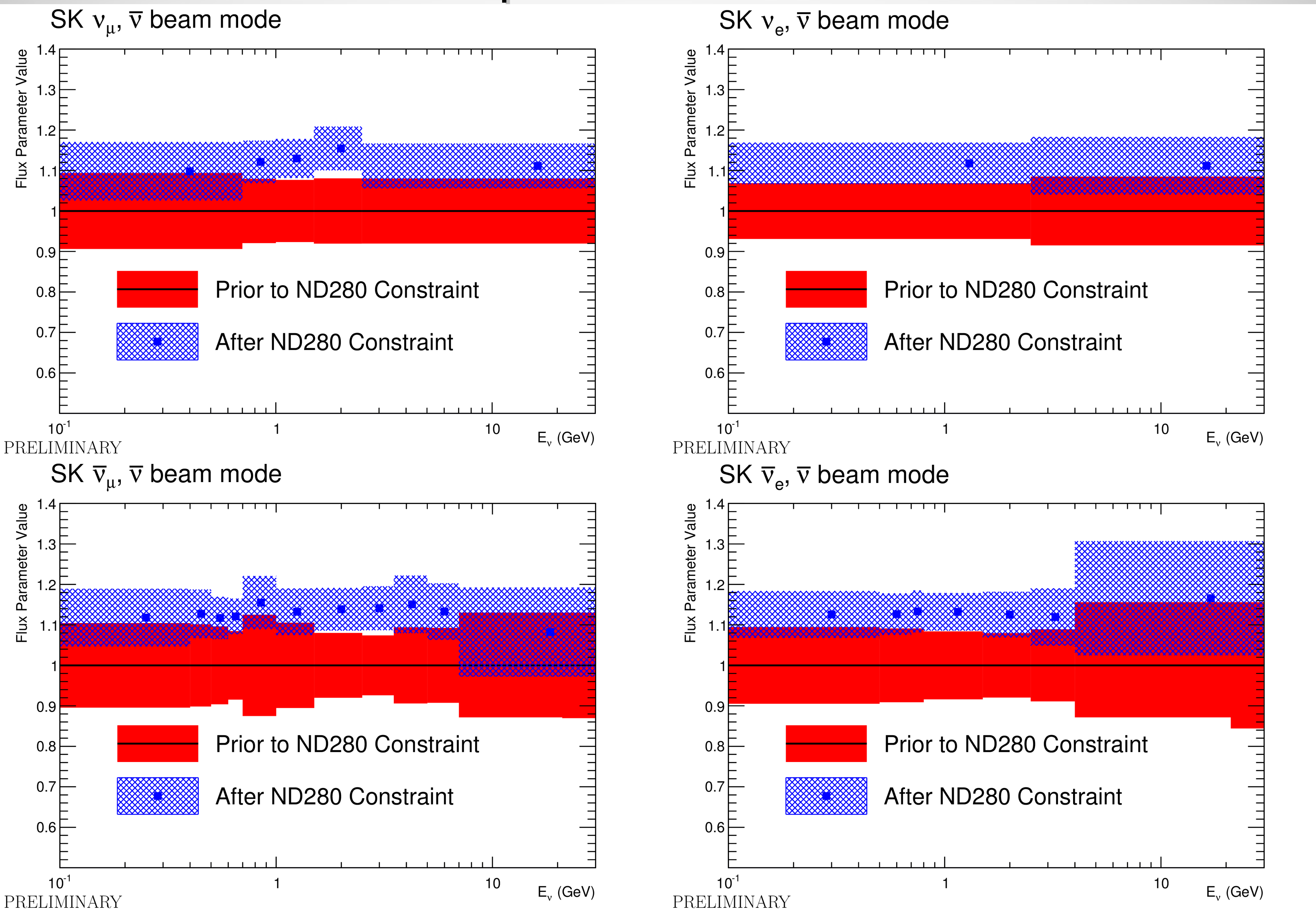

Interaction model: post-fit constraints

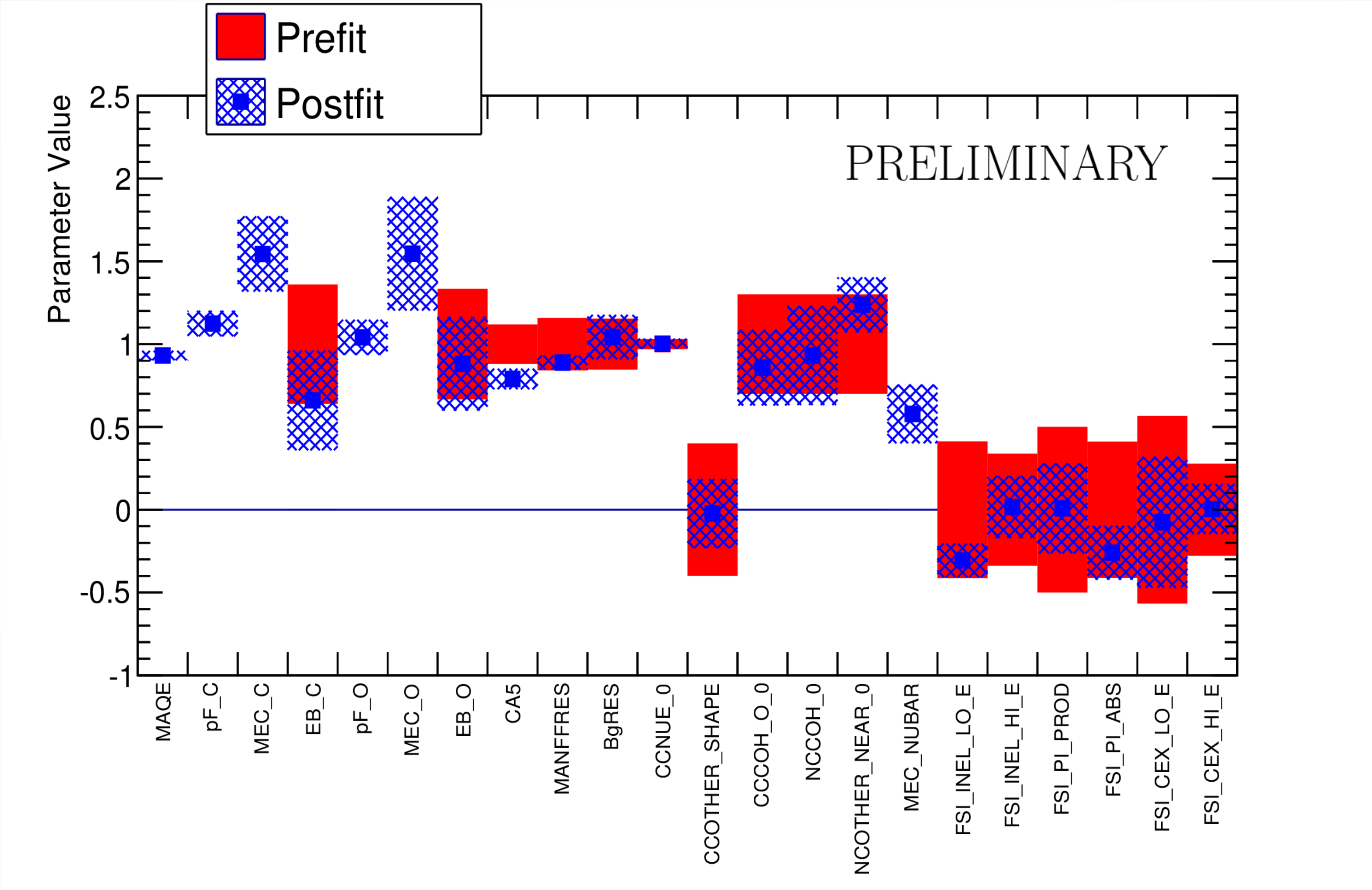

<u>Parameters used at Super-Kamiokande without being constrained in ND280:</u>

- NC-other$_{SK}$ (different interactions than NC-other$_{ND280}$)
- FSI$_{SK}$ (different interaction than FSI$_{ND280}$)
- NC-1γ (100% uncertainty)

Interaction model: post-fit constraints

PRELIMINARY

Cross Section Parameter	Prefit	ND280 postfit
M_A^{QE} (GeV/c^2)	1.2 ± 0.069607	1.1173 ± 0.033882
p_F ^{12}C (MeV/c)	217.0 ± 12.301	243.9 ± 16.608
MEC ^{12}C	100.0 ± 29.053	154.45 ± 22.691
E_B ^{12}C (MeV)	25.0 ± 9.0	16.512 ± 7.5267
p_F ^{16}O (MeV/c)	225.0 ± 12.301	234.24 ± 23.732
MEC ^{16}O	100.0 ± 35.228	154.59 ± 34.254
E_B ^{16}O (MeV)	27.0 ± 9.0	23.802 ± 7.6101
$CA5^{RES}$	1.01 ± 0.12	0.79724 ± 0.06235
M_A^{RES} (GeV/c^2)	0.95 ± 0.15	0.84426 ± 0.038816
Isospin=$\frac{1}{2}$ Background	1.3 ± 0.2	1.3551 ± 0.17389
CC Other Shape	0.0 ± 0.4	-0.022288 ± 0.20831
CC Coh	1.0 ± 0.3	0.85798 ± 0.22842
NC Coh	1.0 ± 0.3	0.93101 ± 0.29816
NC Other	1.0 ± 0.3	1.2376 ± 0.16482
MEC $\bar{\nu}$	1.0 ± 1.0	0.57804 ± 0.17661
FSI Inel. Low E	0.0 ± 0.41231	-0.30599 ± 0.10133
FSI Inel. High E	0.0 ± 0.33793	0.016198 ± 0.18624
FSI Pion Prod.	0.0 ± 0.5	0.0083399 ± 0.27151
FSI Pion Abs.	0.0 ± 0.41161	-0.25953 ± 0.16182
FSI Ch. Exch. Low E	0.0 ± 0.56679	-0.075981 ± 0.39526
FSI Ch. Exch. High E	0.0 ± 0.27778	0.0044852 ± 0.15084

oscillation fit: pre-ND280 fit covariance matrix

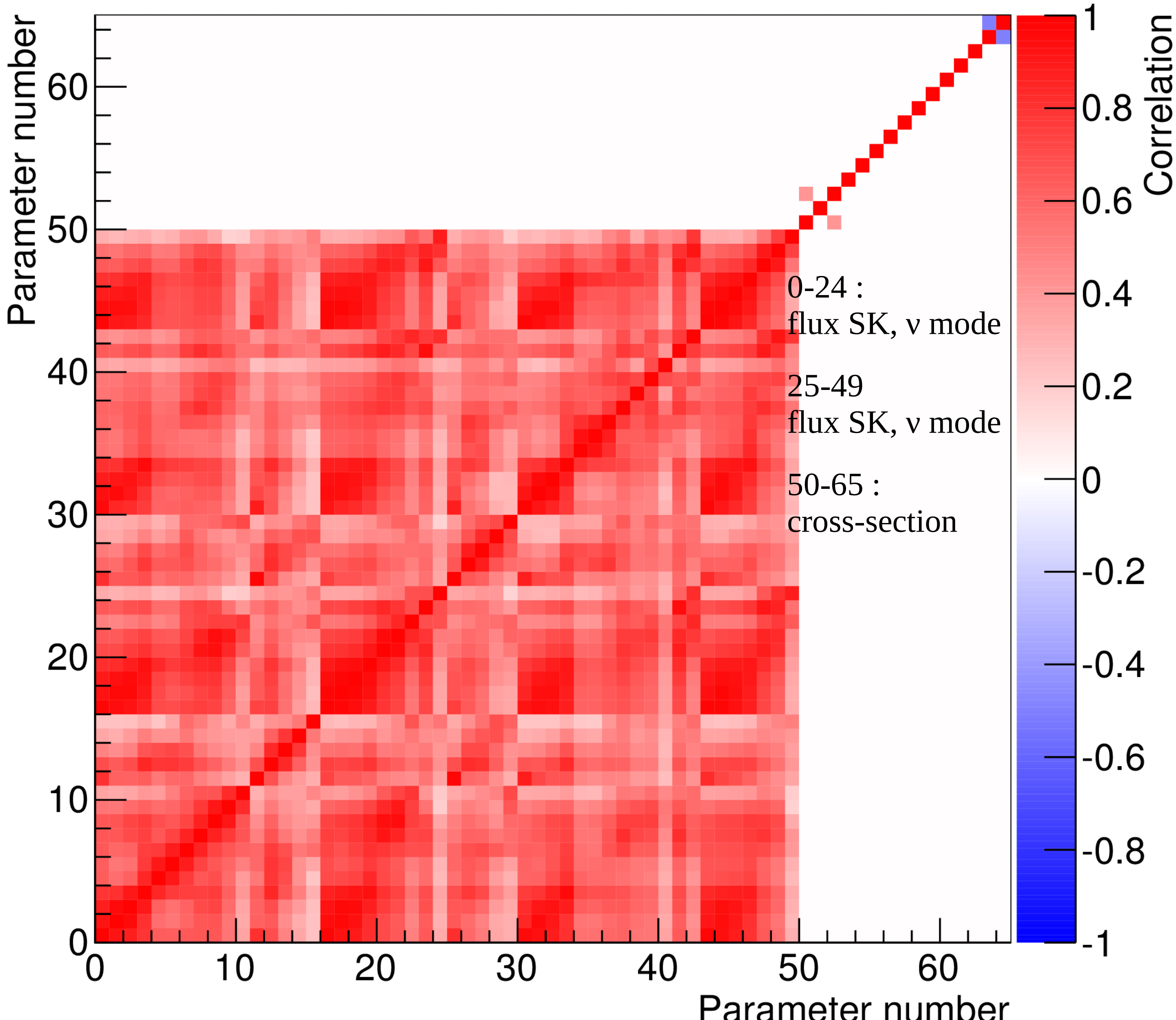

PRELIMINARY

SK flux NuMode Numu
11 energy range
SK flux NuMode Numub
5 energy range
SK flux NuMode Nue
6 energy range
SK flux NuMode Nueb
2 energy range
SK flux ANuMode Numu
5 energy range
SK flux ANuMode Numub
11 energy range
SK flux ANuMode Nue
2 energy range
SK flux ANuMode Nueb
7 energy range
MA_QE
pF_O
MEC_2p2h_O
EB_O
CA5
MA_RES
BgRES I=1/2
CC-other
CC-COH_O
NC-COH
NC-1GAMMA
NC-OTHER_FAR
MEC_NUBAR
Nue/Numu cross-section
Nuebar/Numubar cross-section

oscillation fit: post-ND280 fit covariance matrix

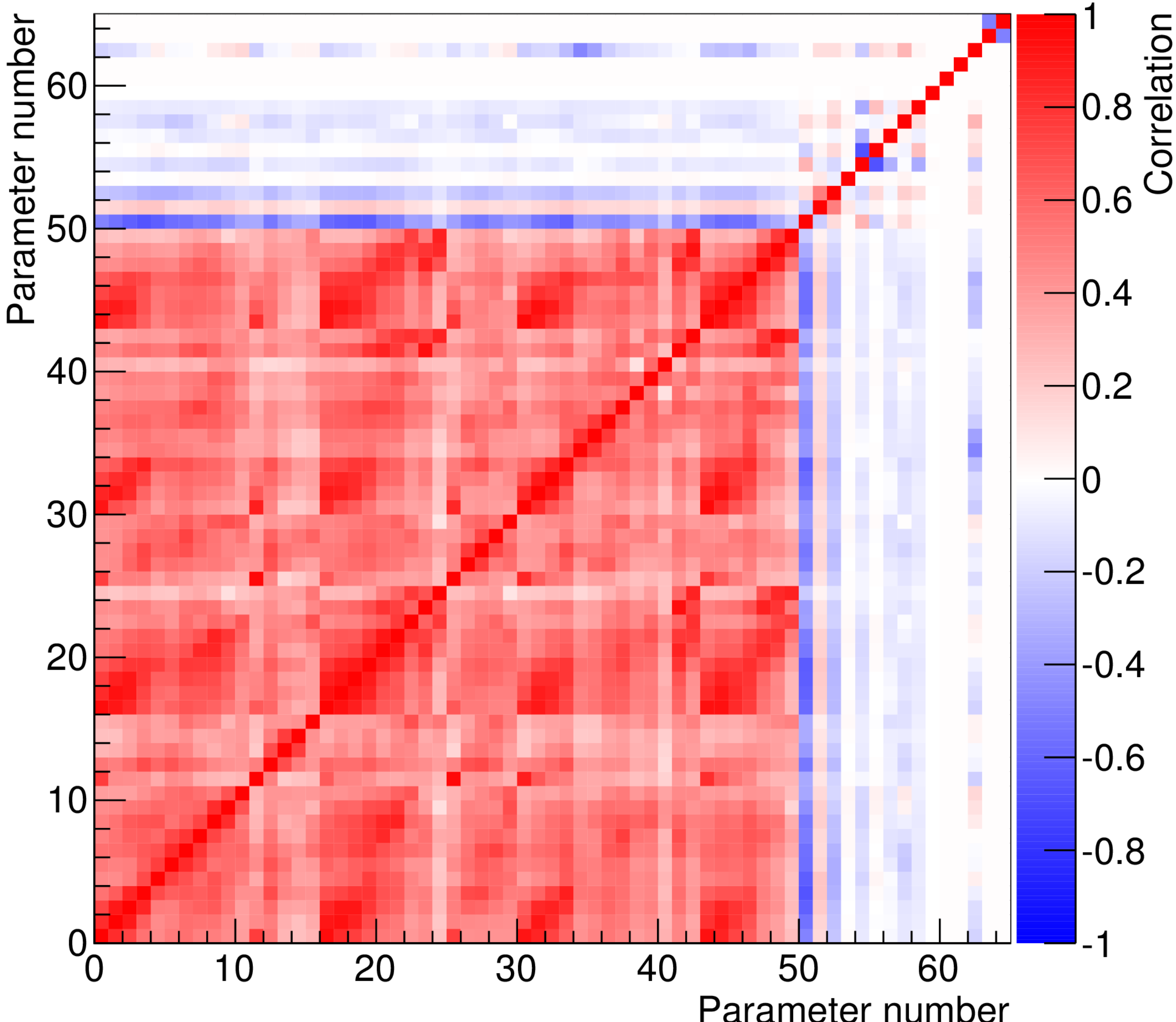

SK flux NuMode Numu 11 energy range
SK flux NuMode Numub 5 energy range
SK flux NuMode Nue 6 energy range
SK flux NuMode Nueb 2 energy range
SK flux ANuMode Numu 5 energy range
SK flux ANuMode Numub 11 energy range
SK flux ANuMode Nue 2 energy range
SK flux ANuMode Nueb 7 energy range
MA_QE
pF_O
MEC_2p2h_O
EB_O
CA5
MA_RES
BgRES I=1/2
CC-other
CC-COH_O
NC-COH
NC-1GAMMA
NC-OTHER_FAR
MEC_NUBAR
Nue/Numu cross-section
Nuebar/Numubar cross-section

PRELIMINARY

FGD2 selection distributions: ν mode CC-0π

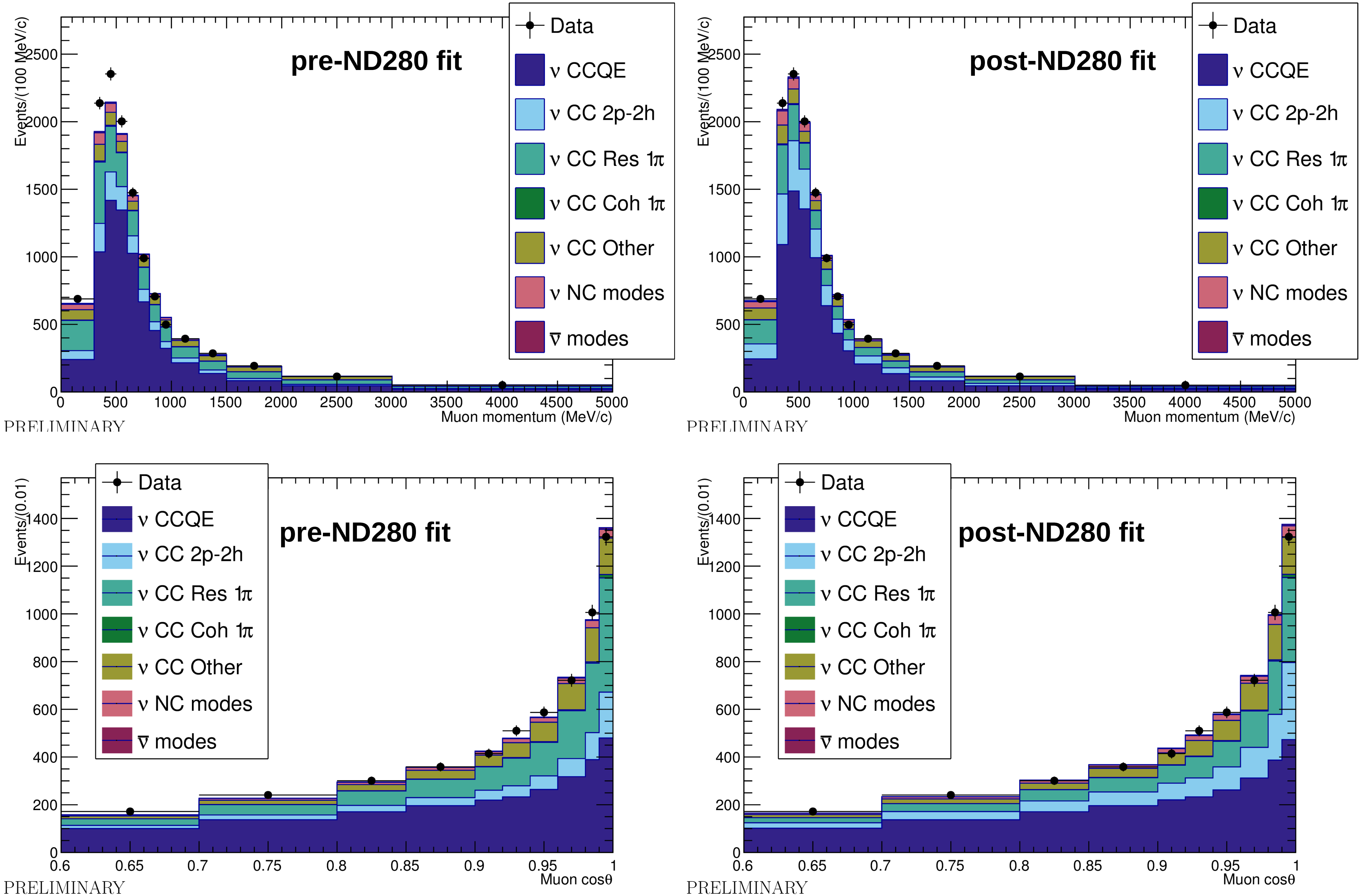

FGD2 selection distributions: ν mode CC-1π

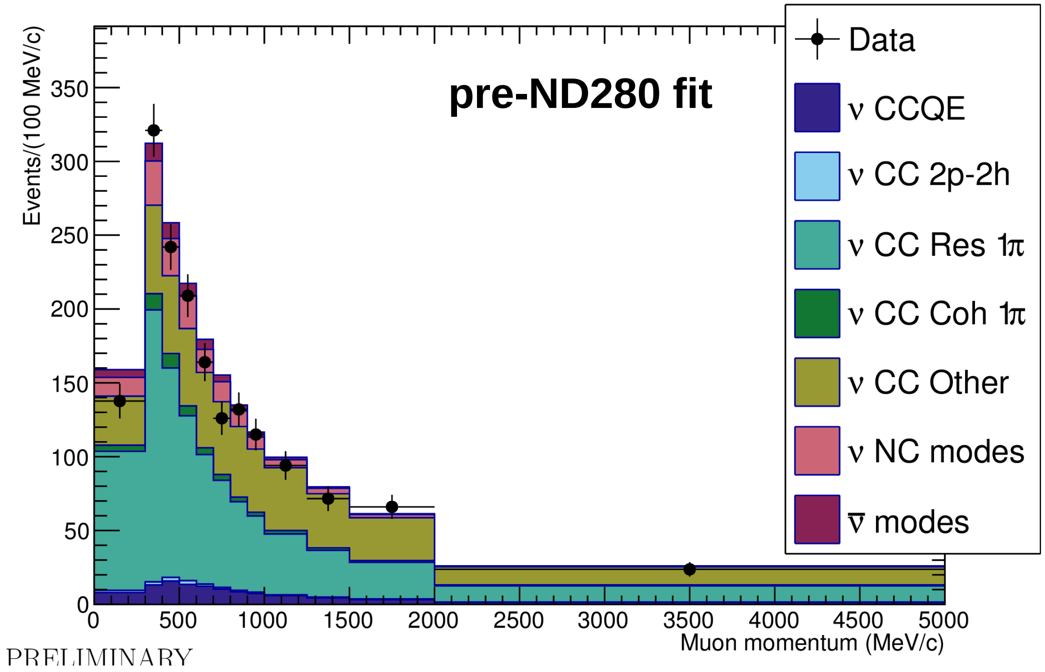

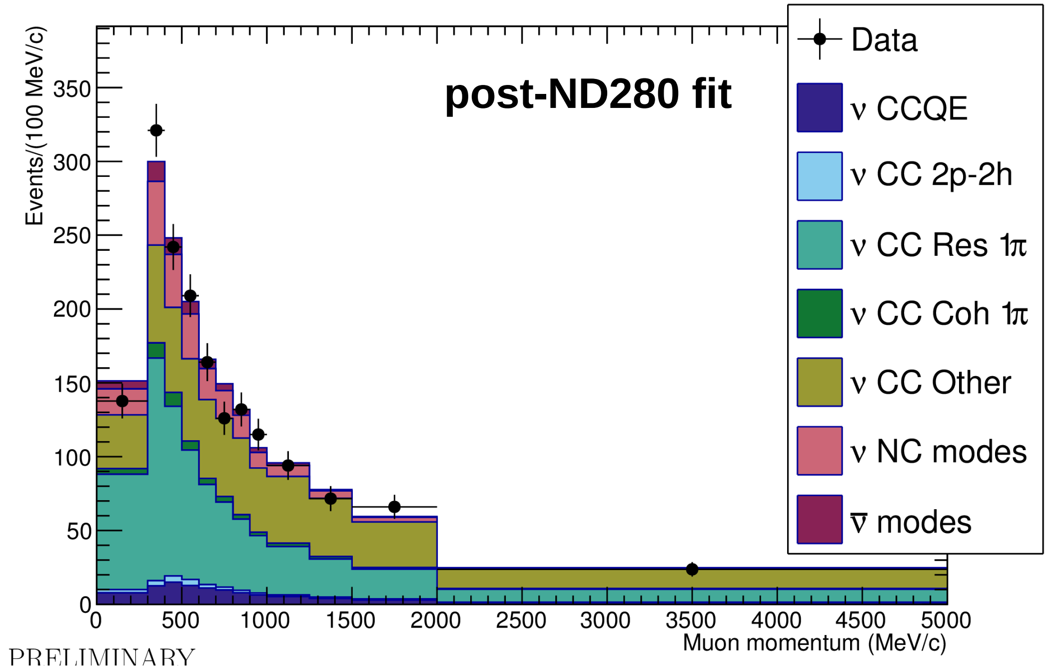

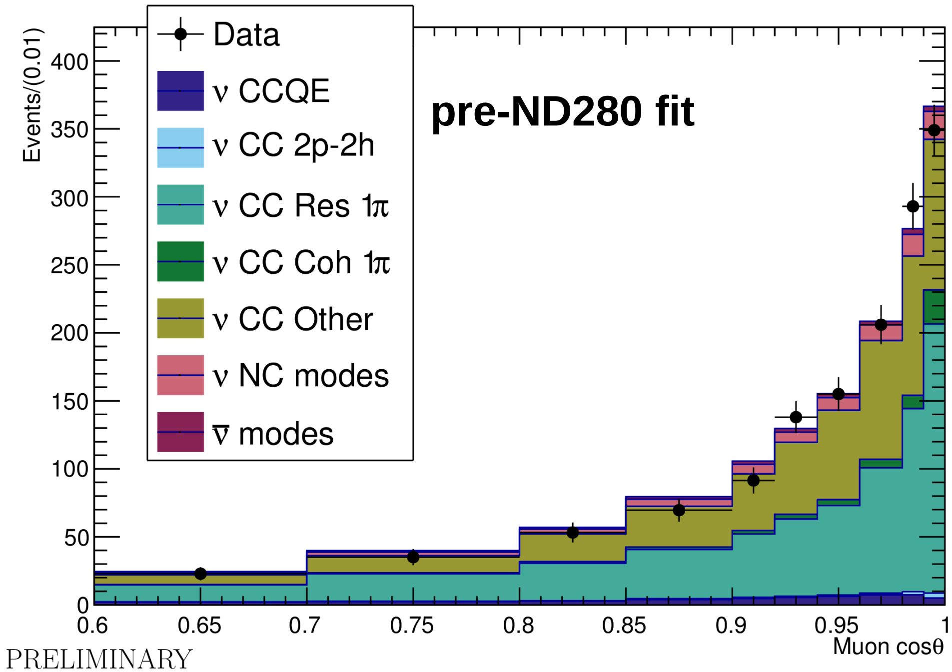

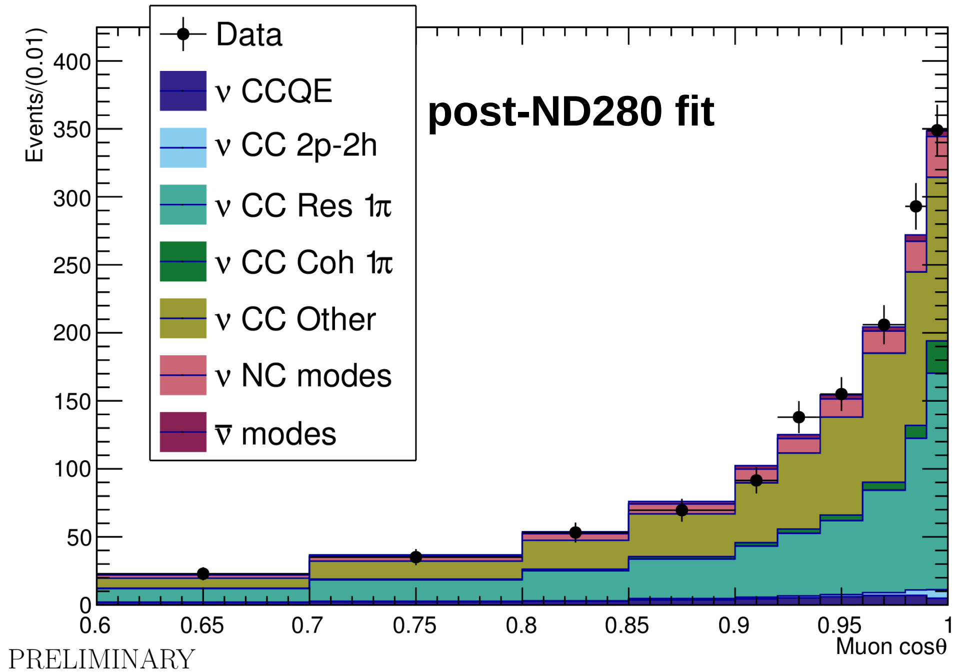

FGD2 selection distributions: ν mode CC-other

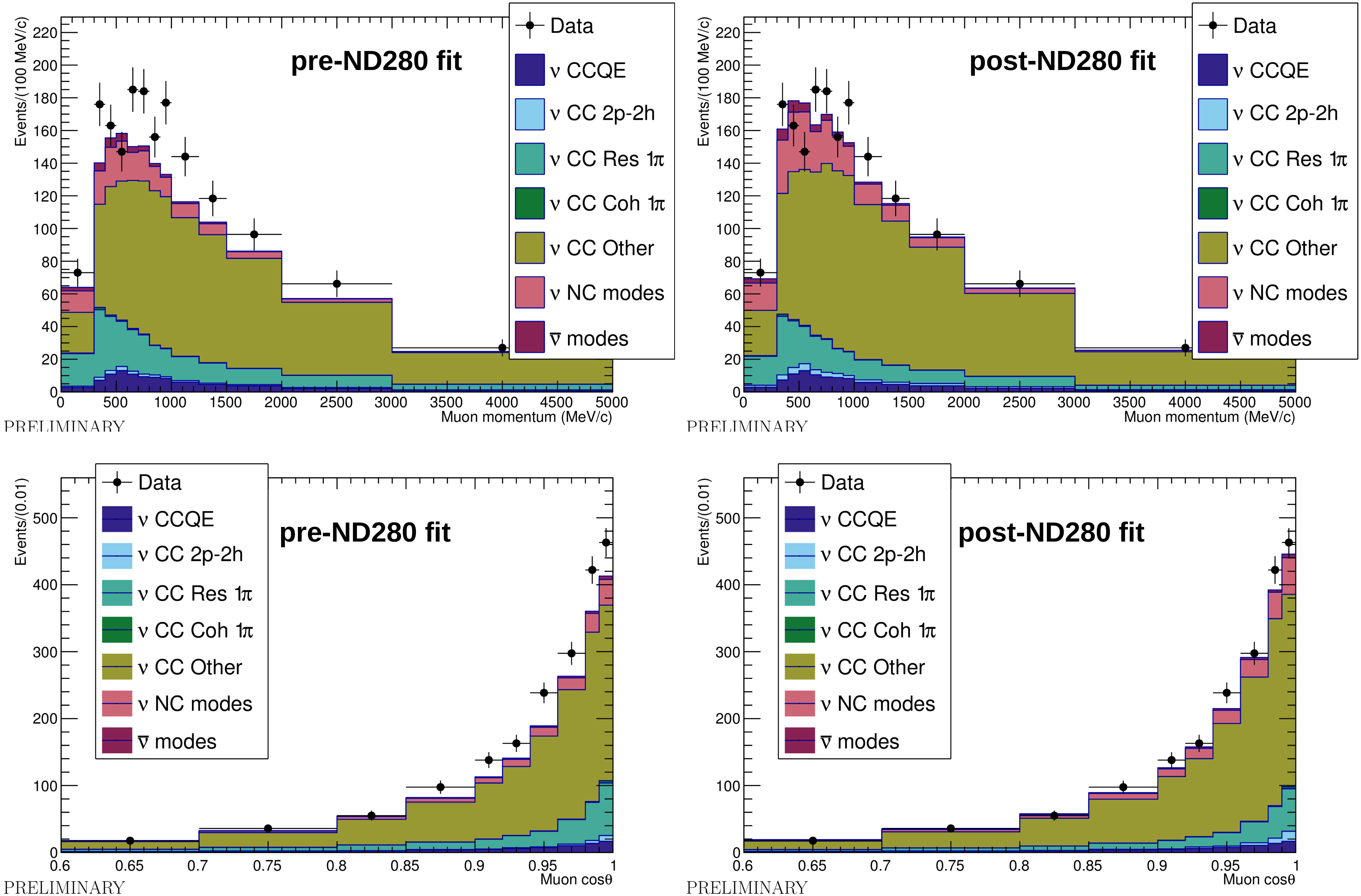

FGD2 selection distributions: ν in $\bar{\nu}$ mode CC-0π

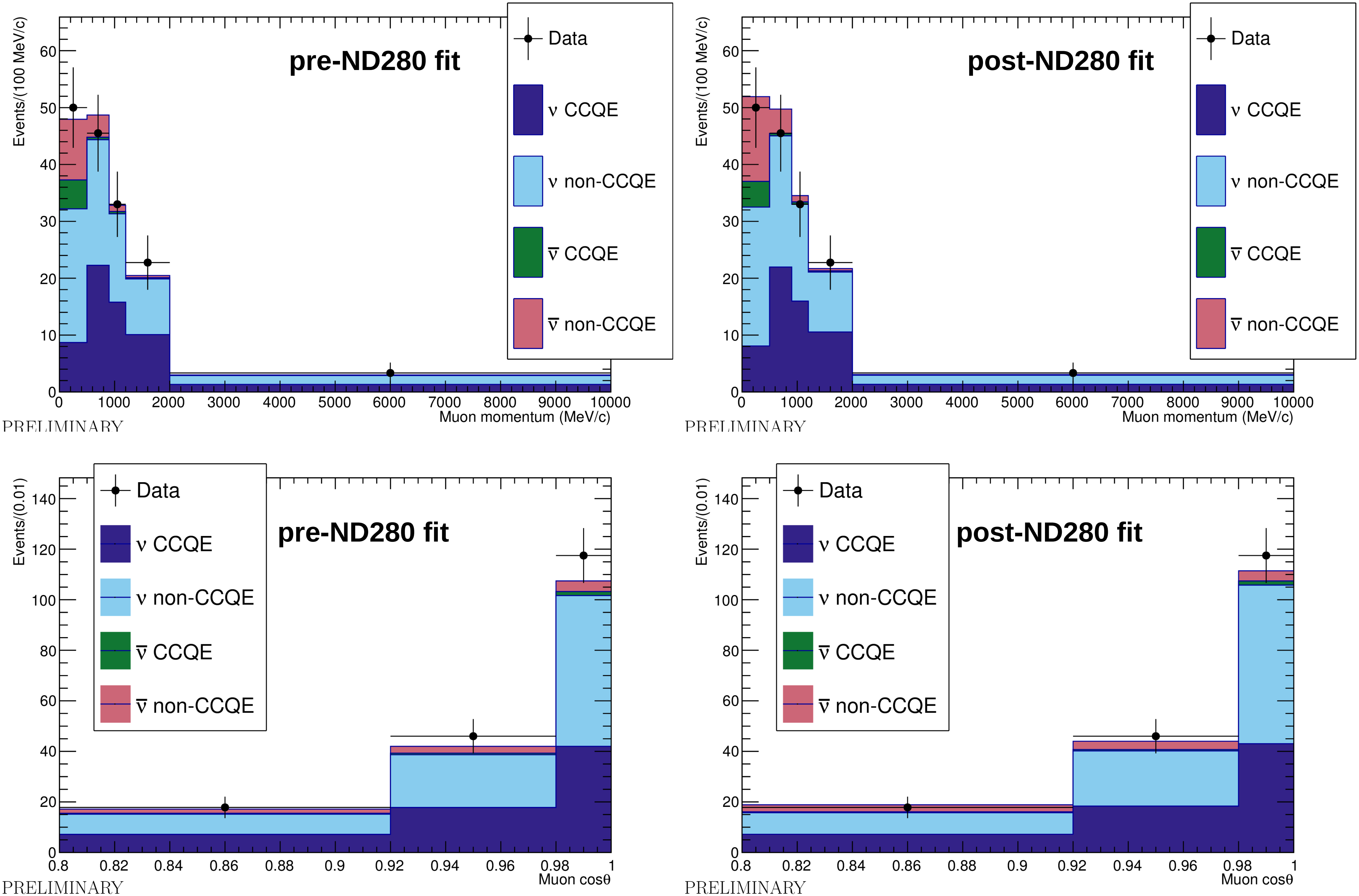

FGD2 selection distributions: ν in $\bar{\nu}$ mode CC-1π+oth

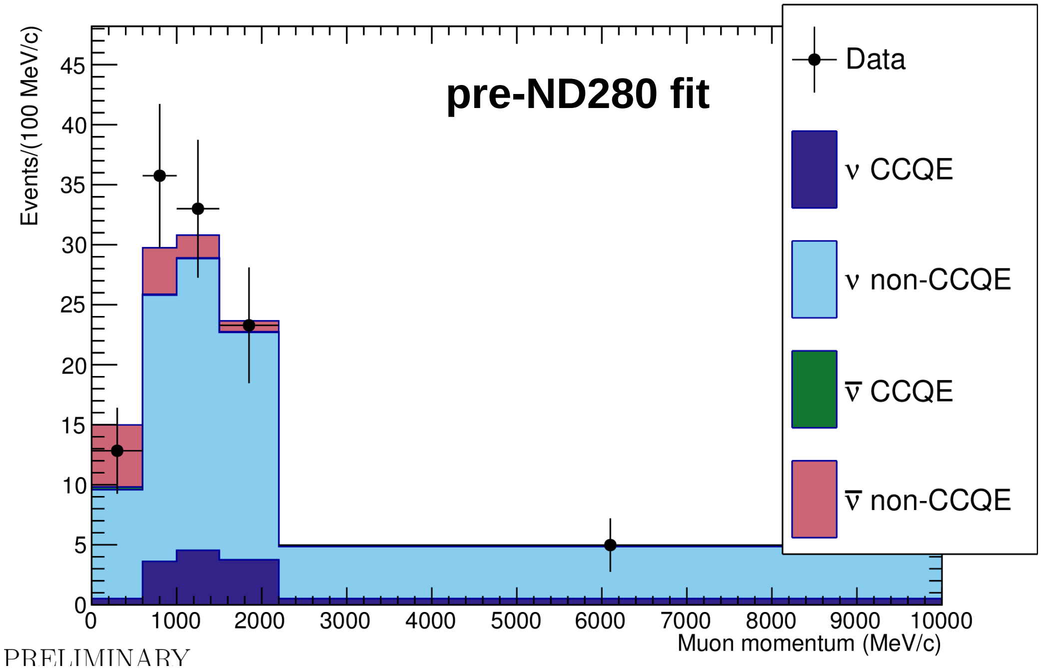

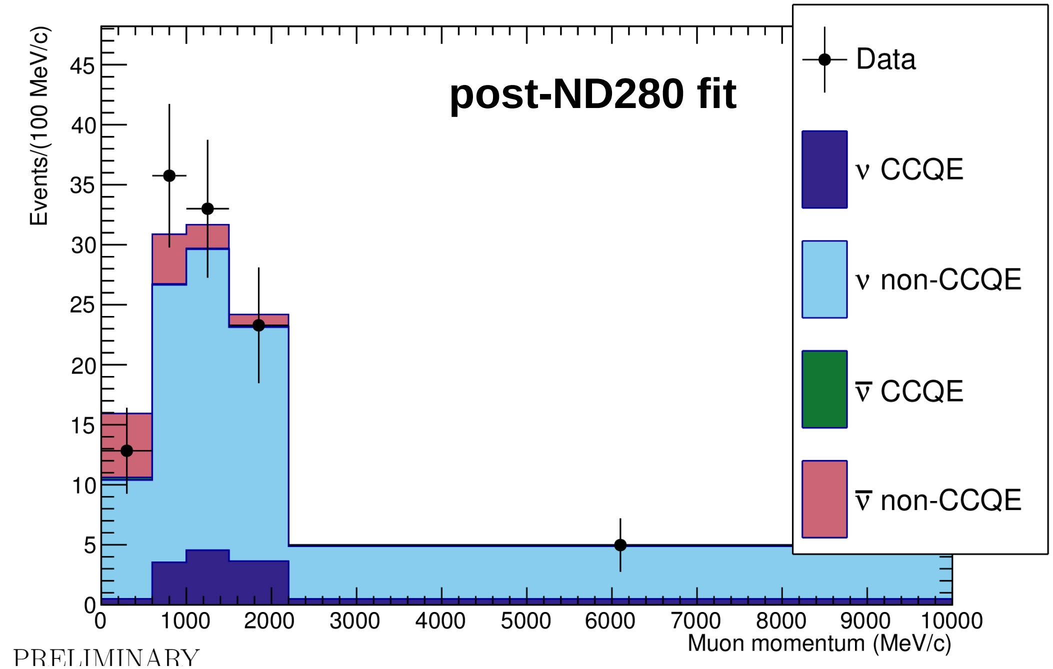

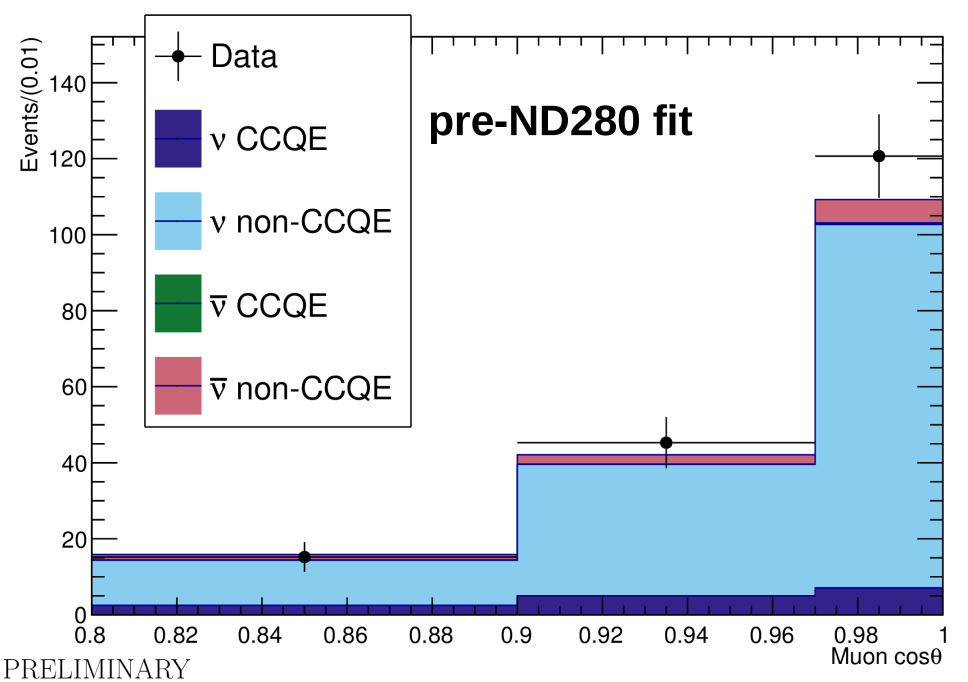

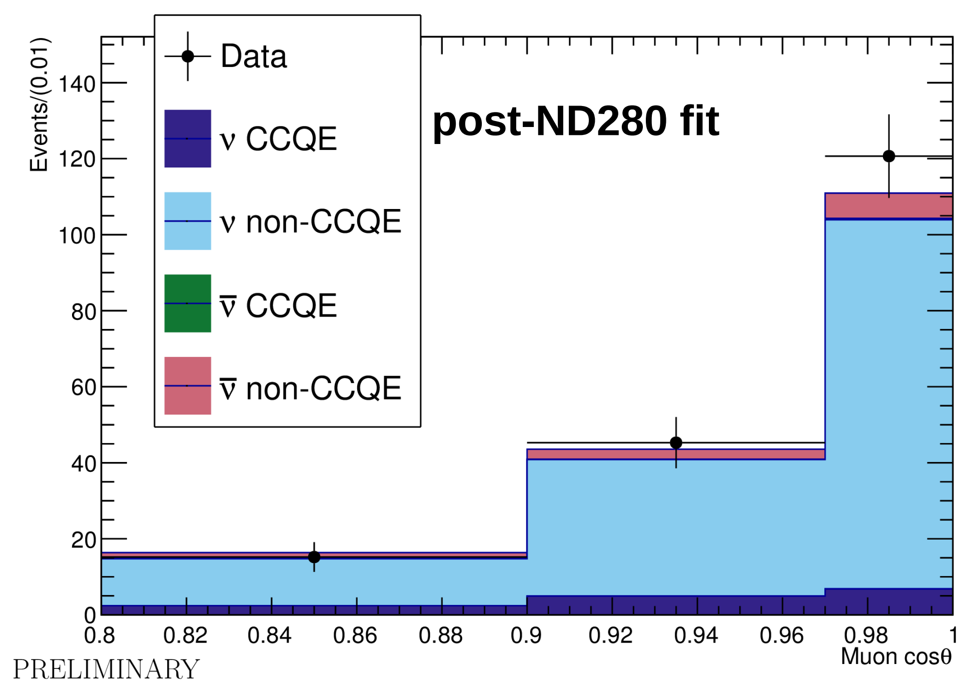

FGD2 selection distributions: $\bar{\nu}$ in $\bar{\nu}$ mode CC-0π

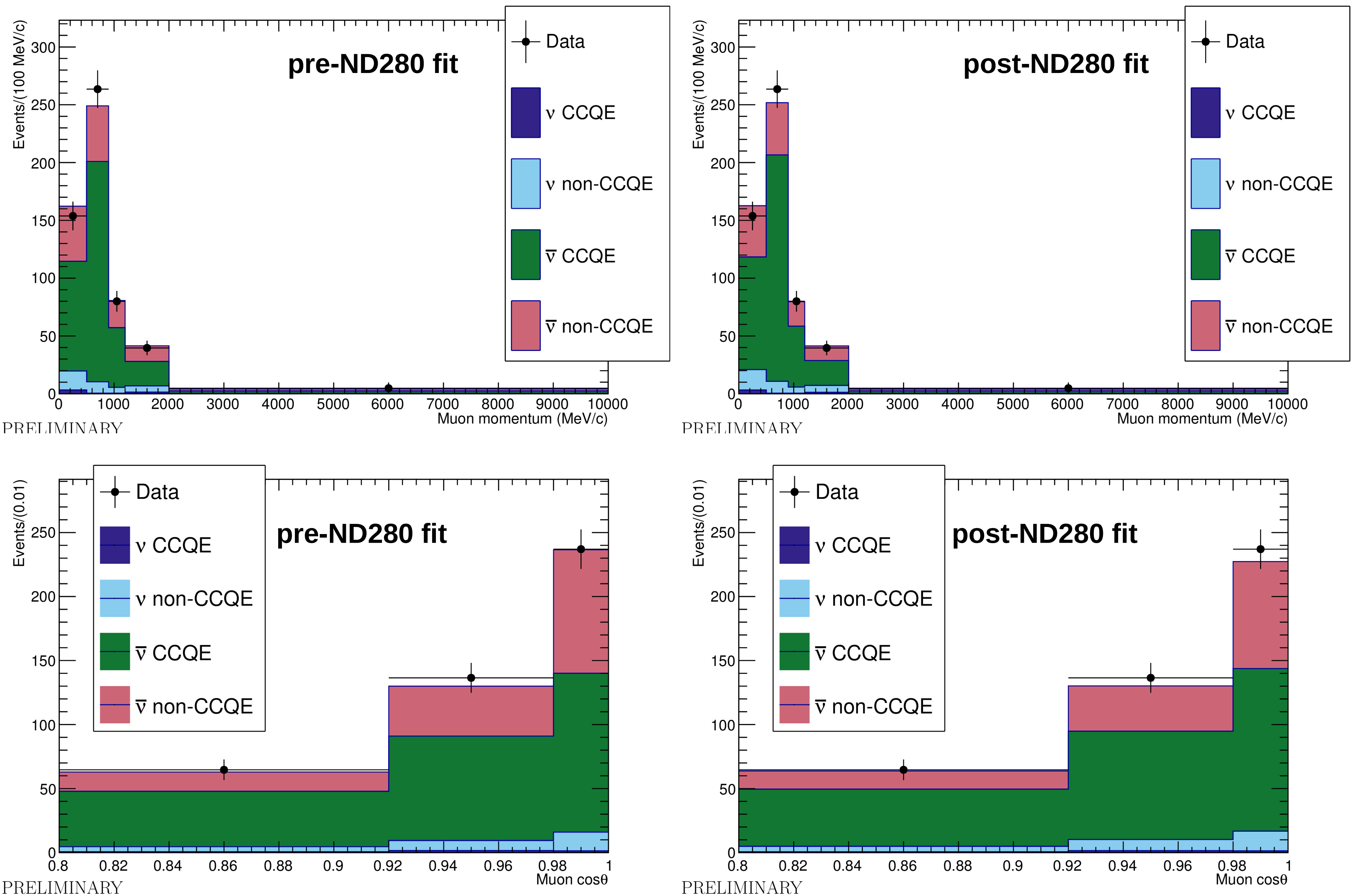

FGD2 selection distributions: $\bar{\nu}$ in $\bar{\nu}$ mode CC-1π+oth

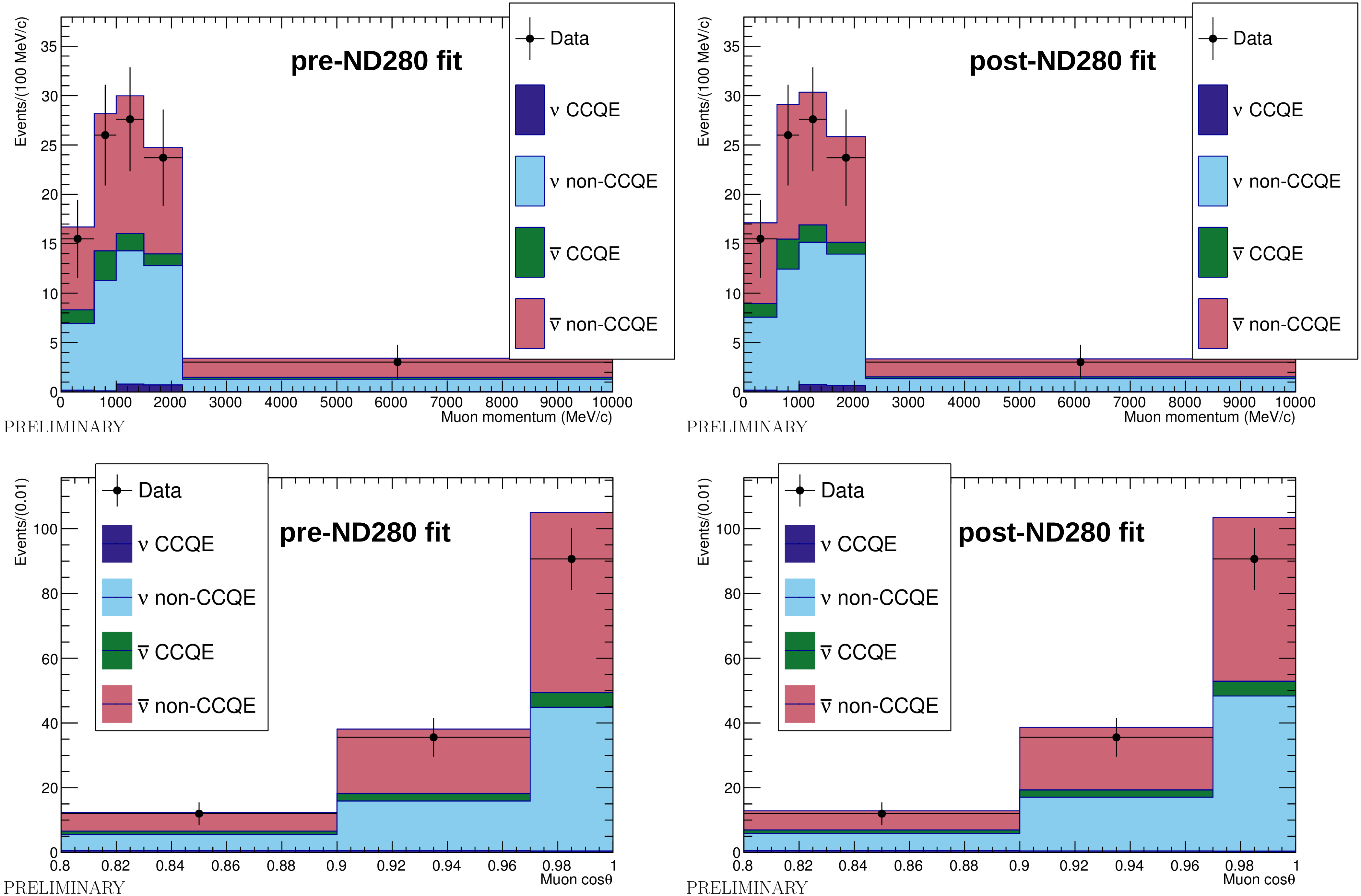

Super-K spectra comparison

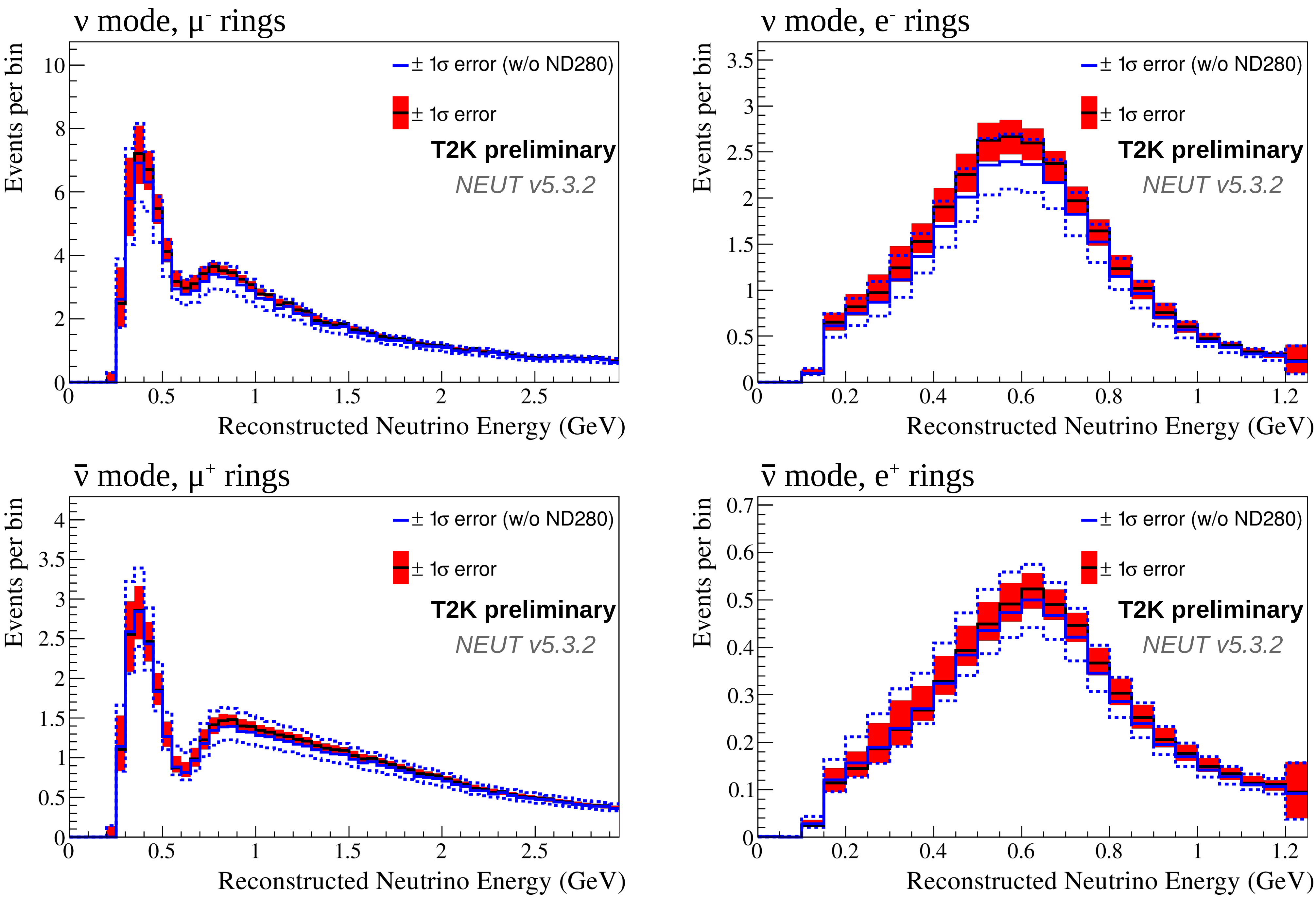

ND280 fit : goodness of fit

The fitted $\Delta\chi^2$ for the data at the minimum is 1448.05.
This corresponds to a p-value 0.086 when compared to the $\Delta\chi^2$ distribution from toy experiments, the observed value of 1448.05 is situated at the upper tail of the distribution.

FGD 1 selection, ν mode

	Number of entries Data	Number of entries MC (scaled to data)	data/MC
CC-0-pion	17399	17751.1	0.98

	Number of entries data	Number of entries MC (scaled to the data)	data/MC
CC-1-pion	3998	4752.8	0.84

	Number of entries data	Number of entries MC (scaled to the data)	data/MC
CC-other	4260	3789.8	1.12

FGD 2 selection, ν mode

	Number of entries Data	Number of entries MC (scaled to data)	data/MC
CC-0-pion	18284	18816.71	0.97

	Number of entries data	Number of entries MC (scaled to the data)	data/MC
CC-1-pion	3474	4064.84	0.85

	Number of entries data	Number of entries MC (scaled to the data)	data/MC
CC-other	4252	3760.46	1.13

ND280 fit : goodness of fit

The fitted $\Delta\chi^2$ for the data at the minimum is 1448.05.
This corresponds to a p-value 0.086 when compared to the $\Delta\chi^2$ distribution from toy experiments, the observed value of 1448.05 is situated at the upper tail of the distribution.

FGD 1 selection, $\bar{\nu}$ in $\bar{\nu}$ mode

Run 5c			Run 6b			Run 6c			Run 6d		
Data	MC	ratio	Data	MC	ratio	Data	MC	ratio	Data	MC	ratio
CC-1track											
437	380.41	1.15	1198	1127.41	1.06	444	444.36	1.00	604	566.35	1.07
CC-Ntracks											
134	126.08	1.06	344	373.66	0.92	137	147.27	0.93	184	187.70	0.98

FGD 2 selection, $\bar{\nu}$ in $\bar{\nu}$ mode

Run 5c			Run 6b			Run 6c			Run 6d		
Data	MC	ratio	Data	MC	ratio	Data	MC	ratio	Data	MC	ratio
CC-1track											
406	391.44	1.04	1292	1160.13	1.11	477	457.26	1.04	609	582.78	1.04
CC-Ntracks											
92	129.58	0.71	349	384.05	0.91	139	151.37	0.92	181	192.92	0.94

ND280 fit : goodness of fit

The fitted $\Delta\chi^2$ for the data at the minimum is 1448.05.
This corresponds to a p-value 0.086 when compared to the $\Delta\chi^2$ distribution from toy experiments, the observed value of 1448.05 is situated at the upper tail of the distribution.

FGD 1 selection, ν in $\bar{\nu}$ mode

Sample	MC Events	Data Events	Topology	MC Events	MC Composition
CC-1Track	1043.6	1017±32	CC-0π	527.2	50.5%
			CC-Nπ	289.4	27.7%
			BKG	98.5	9.5%
			External	128.5	12.3%
CC-NTracks	1033.9	1054±32	CC-0π	157.8	15.3%
			CC-Nπ	683.7	66.1%
			BKG	129.0	12.5%
			External	63.3	6.1%

FGD 2 selection, ν in $\bar{\nu}$ mode

CC-1Track	1080.3	1059±32	CC-0π	530.1	49.1%
			CC-Nπ	282.9	26.2%
			BKG	109.5	10.1%
			External	157.8	14.6%
CC-NTracks	1002.2	998±32	CC-0π	143.3	14.3%
			CC-Nπ	671.9	67.0%
			BKG	132.9	13.3%
			External	54.1	5.4%

Interaction models : nuclear matter environment

New J.Phys. 16 (2014) 075015

global Relativistic Fermi gas (RFG):

The relativistic Fermi gas model is a common simple model across Fermionic physical systems. The assumption is that all particles are in a potential, and form plane-wave states, leading to all states being filled up to a Fermi-level, above which no states are filled. In this model, the nuclear ground state is a Fermi gas of non-interacting nucleons characterized by a global Fermi momentum and a constant binding energy.

local Relativistic Fermi gas (LFG):

An improvement over the global RFG is the so called relativistic local Fermi Gas where the Fermi momentum is fixed according to the local density of protons and neutron. The binding energy is often neglected but a minimal excitation energy required for the transition to the ground state of the final nucleus has been taken into account in the CCQE model

Spectral Functions (SF):

"Spectral function" is a generic term for a function that describes the momentum and energy distributions of initial nucleons in a nucleus (the RFG can be described by a spectral function very easily). For medium-size nuclei, such as carbon and oxygen, various approximations need to be made, but spectral functions can still be built by combining information from electron scattering data with the theoretical calculations from uniform nuclear matter of different densities. The spectral functions used in NEUT were provided by O.Benhar [1]. The spectral function is made up of two different terms, a mean-field term for single particles, and a term from correlated pairs of nucleons.

[1] O.Benhar, A. Fabrocini, S. Fantoni, I. Sick. Spectral function of finite nuclei and scattering of GeV electrons. Nucl. Phys. A. 579, 493-517 (1994).

Interaction models : Random Phase Approximation

The medium polarization effect is given by Random phase approximation in Many Body formalism. RPA computes the propagation of ph pair through the dense medium, mediated by residual ph excitation and accounts for long range correlation. [1] shows irreducible diagrams responsible for the polarization effects in the 1p1h contribution to the W-self-energy. When the electroweak interaction takes place in the nucleus, 1p1h medium polarization leads to change in strength of the electroweak coupling altering the CCQE free nucleon prediction. The update in NEUT uses Nieves Model [1]. The calculation for RPA is based on Local Fermi gas model (LFG), using standard axial mass, M_A^{QE} of 1.0 GeV. RPA alters the CCQE cross-section mainly as a function of Q^2 , predominantly suppressing the CCQE cross-section at low Q^2 . The RPA effect is large at low energy where the momentum transfer is comparable to or less than nucleon mass.

[1] J. Nieves, J. E. Amaro, and M. Valverde. Inclusive quasielastic charged-current neutrino-nucleus reactions. Phys. Rev. C, 70:055503, 2004.

Interaction models : 2p2h

Predictions for the multi-nucleon–neutrino contribution to the total charged-current cross-section are computed by a multi-body expansion of the weak propagator in the medium. The first-order expansion gives a prediction for the standard CCQE interaction, where the hadronic vertex involves a single nucleon-hole pair. The second-order terms in the expansion predict interactions involving additional nucleons or Δ resonances in the hadronic current. This process is often called a multinucleon interaction, a 'two particle, two hole' interaction, or 2p2h, indicating the presence of two particles ejected from the nucleus, and two holes in the nucleus. The process considered in these models is distinct from that considered in spectral function models of nuclear dynamics: in the correlation term of the spectral function, the two nucleons have some momentum correlation but the hadronic current has only one nucleon, whereas in 2p2h interactions, two nucleons contribute to the hadronic current.

J. Nieves, I. Ruiz Simo, and M. J. Vicente Vacas. Inclusive charged-current neutrino-nucleus reactions. Phys. Rev. C, 83:045501, Apr 2011.

M. Martini, M. Ericson, G. Chanfray, and J. Marteau. A Unied approach for nucleon knock-out, coherent and incoherent pion production in neutrino interactions with nuclei. Phys. Rev. C, C80:065501, 2009.

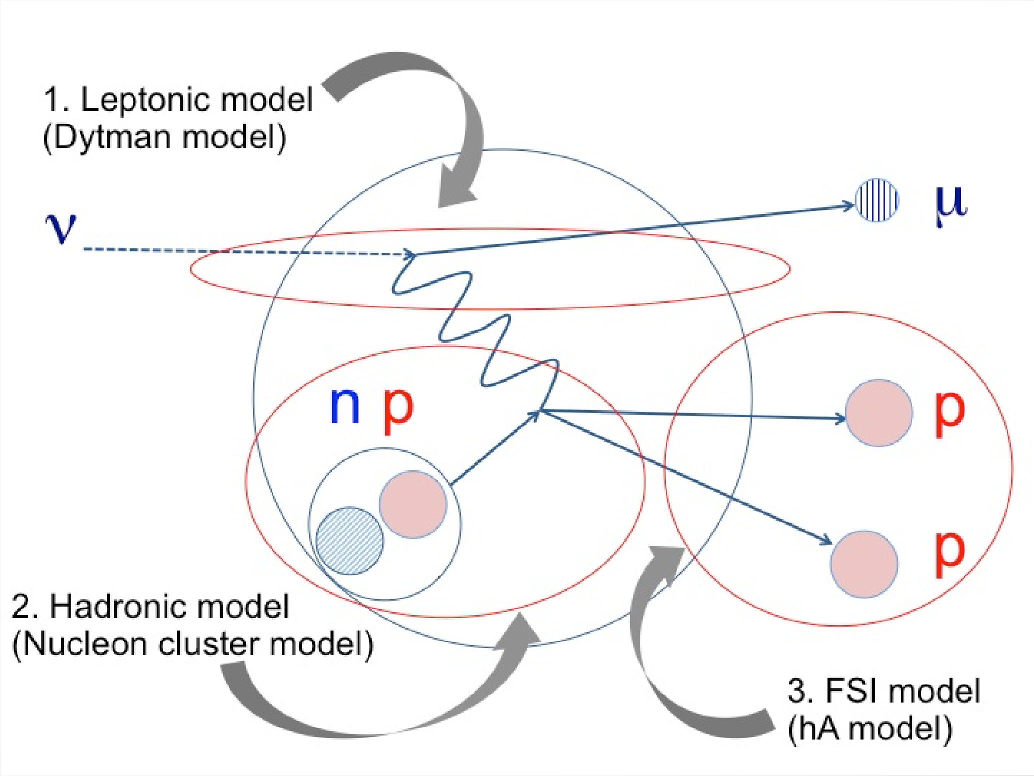

Interaction models : 2p2h effect on oscillations

INT-PUB-14-059, FERMILAB-CONF-14-484-E

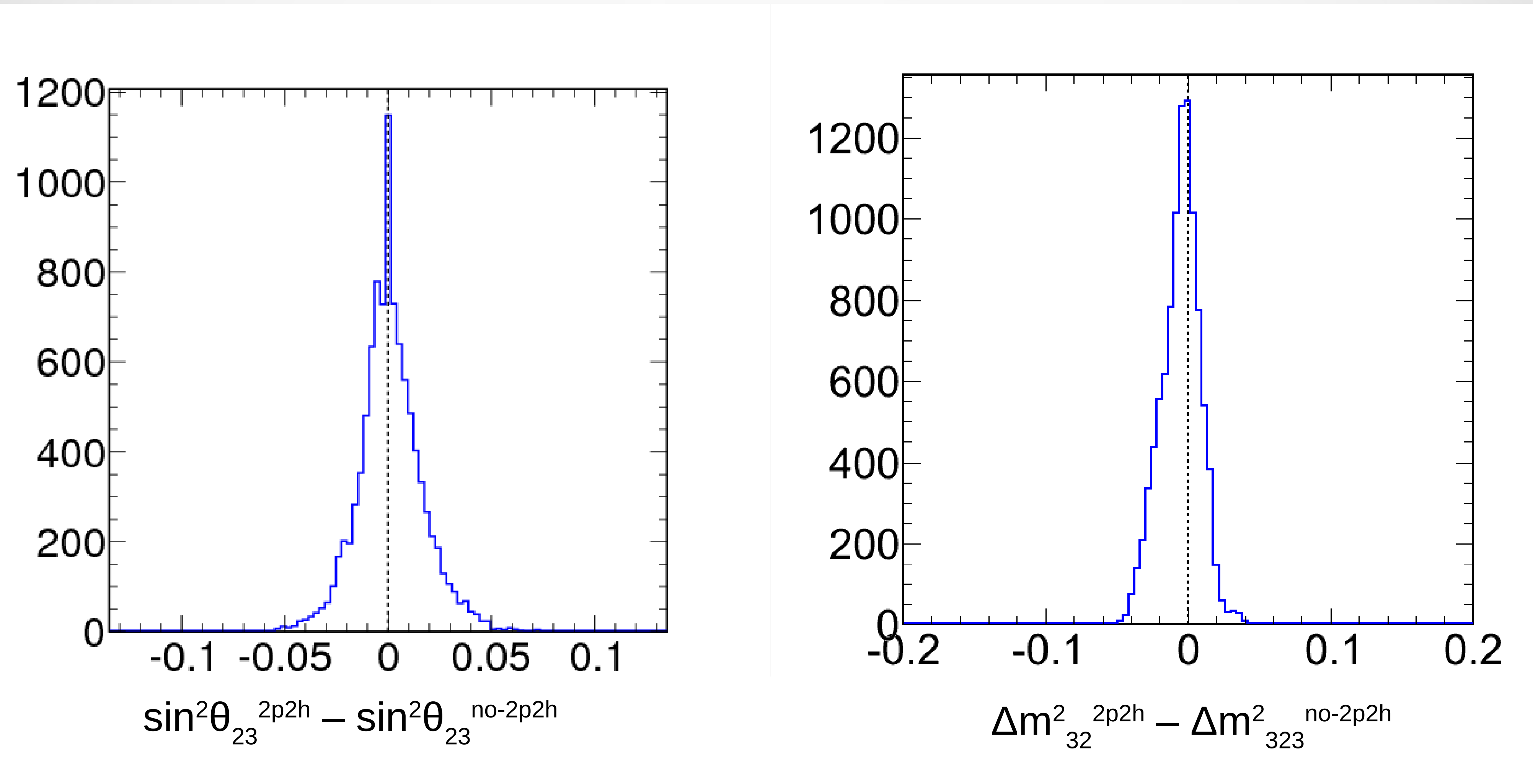

Interaction models: fit to eternal data

Phys. Rev. D 93, 072010 (2016)

Fit type	$\chi^2/N_{\rm DOF}$	$M_{\rm A}$ (GeV/c^2)	2p2h norm. (%)	$p_{\rm F}$ (MeV/c)	$\lambda_{\nu}^{\rm MB}$	$\lambda_{\bar{\nu}}^{\rm MB}$
RFG+rel.RPA+2p2h	97.8/228	1.15±0.03	27±12	223±5	0.79±0.03	0.78±0.03
RFG+non-rel.RPA+2p2h	117.9/228	1.07±0.03	34±12	225±5	0.80±0.04	0.75±0.03
SF+2p2h	97.5/228	1.33±0.02	0 (at limit)	234±4	0.81±0.02	0.86±0.02

TABLE IV: Best fit parameter values for the fits to all datasets simultaneously.

Interaction models : Pion production

New J.Phys. 16 (2014) 075015

Rein-Sehgal model : D. Rein and L. M. Sehgal, Annals Phys. 133, 79 (1981). was an attempt to describe all data available in 1980 on neutrino production of single pions in the resonance region up to πN invariant masses W N π of around 2 GeV. The basic assumption is that single pion production is mediated by all interfering resonances below 2 GeV, supplemented with a simple non-interfering, non-resonant phenomenological background of isospin 1/2. The needed transition matrix elements are calculated using the relativistic quark model of Feynman-Kislinger-Ravndal [192] (formulated in 1970) with SU(6) spin-flavor symmetry, and a total of 18 baryon resonances considered.

Vector and axial form factors from Graczyk and Sobczyk : Krzysztof M. Graczyk and Jan T. Sobczyk. Form factors in the quark resonance model. Phys. Rev. D, 77:053001, Mar 2008.